

A Contribution to the Understanding of Percolation Phenomena in Binary Liquids

INAUGURALDISSERTATION

zur

Erlangung der Würde eines Doktors der Philosophie
vorgelegt der
Philosophisch-Naturwissenschaftlichen Fakultät
der Universität Basel

von

Maria Engracia Hernandez Perni
aus Valencia, Spanien

Basel, 2004

Genehmigt von der Philosophisch-Naturwissenschaftlichen Fakultät
auf Antrag von

Herrn Prof. Dr. H. Leuenberger

und

Herrn PD Dr. P. van Hoogevest

Basel, den 6. Juli 2004

Prof. Dr. M. Tanner
Dekan

to my parents

Acknowledgements

This work was carried out at the Department of Pharmaceutical Technology, University of Basel.

I would like to express my profound gratitude to my supervisor Prof. Dr. H. Leuenberger for his invaluable support, encouragement, supervision and useful suggestions throughout this research work.

I wish to express my gratitude to the co-referee of the present dissertation PD Dr. P. van Hoogevest.

For the financial support of my PhD I want to acknowledge the University of Basel.

I warmly thank Mr. Stephan Winzap and Ms. Christina Erb for their kindness and help.

Mi eterno agradecimiento a mis padres, Alejandro y Manuela y también a mi hermana Reme, por su amor, comprensión y apoyo a lo largo de mi vida. Por estar siempre ahí en los buenos y en los malos momentos y por su absoluta confianza en mí (I am as ever, especially indebted to my parents, Alejandro and Manuela and also to my sister Reme for their love, understanding and support throughout my life. Thanks for being there not only in the good but also in the bad moments and for trusting absolutely on me)

During the course of working on this thesis, I was fortunate enough to meet and start living with my love and partner, Andreas Wild. For his patiently standing beside me during this time, for his love, support, encouragement and help I want to express by deepest thanks.

My special acknowledgement is expressed to Darren Dixon for his big support when I needed him.

My sincere thanks go to my friends especially to Silvia Arnold, with whom I have shared my experiences since I arrived in Basel, for her friendship: Many Thanks. To

Philippe Haas and Nathalia Haas for sharing laughs together and to Kevin Short for the good moments in the theater and his fabulous voice.

Many thanks also to my colleagues at the Pharmacenter.

Last but not least, I would also thank that work to the rest of my family.

Besides, I would like to thank: the producers of “Espresso Croquant” Mövenpick ice cream for “making my work sweater” and Radio Basilisk for the good music they always broadcast.

Summary

Water properties are the subject of investigations in physics, chemistry, biology and different applied fields of natural science.

Liquid dosage forms, generally based on aqueous solutions, take an important role in drug administration e.g. as parenteral preparations, ophthalmic formulations or as oral solutions for children and elderly patients. A sufficient drug solubility in water is a prerequisite for orally administered solid dosage forms such as tablets, capsules, etc. to show a sufficient bioavailability. The solubility of a drug is determined by intermolecular forces. While these can be reasonably well characterized in gaseous and solid material, no satisfying description has yet been found for liquids systems, especially for nonideal solutions. The presence of several types of intermolecular interactions let the water show rather a complex associated structure due to which it has a number of its abnormal properties.

In this work, the intermolecular forces in pure solvents and binary mixtures at 298.2K are investigated, using quasistatic low-frequency and AC high-frequency broadband (0.2-20 GHz) dielectric spectroscopy.

The results of this thesis are presented in two papers that have been accepted for publication in the International Journal of Pharmaceutics and a third one that has been submitted to the European Journal of Pharmaceutics and Biopharmaceutics. The results of the two first were presented at the 5th Central European Symposium on Pharmaceutical Technology and Biotechnology, Ljubljana 2003, and the results of the third paper will be presented at the 3rd International conference on Broadband Dielectric Spectroscopy and its Applications. Delft, August 2004, (see list of publications page iv).

The data were interpreted using for the low frequency measurements the modified Clausius-Mossotti-Debye equation according to Leuenberger and the Kirkwood-

Fröhlich equation. For the description of the dielectric relaxation in the high frequency range there are different mathematical models available which describe the relaxation behavior of a polar liquid. The most simple equation is the Debye equation, which will be described in the theory chapter. To fit the ϵ' , ϵ'' -data in a best way it is also possible to use the Cole-Davidson distribution function or superposition of two Debye equations or superposition of the Debye function with the Cole-Davidson distribution function. It has to be kept in mind that the resulting relaxation times (τ) depend on the mathematical model applied. If the mean corrected R^2 coefficient does not differ significantly for the mathematical models used, it is not possible to make an unambiguous choice of model.

In the two previous papers (Stengele et al., 2001; Stengele et al., 2002) it was shown, that the Clausius-Mossotti-Debye equation for the quasi-static dielectric constant (ϵ) can be extended to liquids if the parameter E_i/E is introduced. E_i corresponds to the local mean field due to close molecule-molecule interactions after the application of an external electric field E . The present study is a continuation of the previous publications.

In the first paper a detailed study of the E_i/E parameter in the characterization process of polar liquids is performed. The relationship between the values of E_i/E and the total Hildebrand solubility parameter (δ_t) at room temperature, as well as the study of the correlation of E_i/E value with the partial Hansen solubility parameters (δ_h , δ_p) for polar liquids is analyzed.

In the second paper the percolation phenomena is detected in water/1,4-dioxane, methanol/1,4-dioxane and benzylalcohol/1,4-dioxane binary polar liquid mixtures by using broadband (0.2-20 GHz) dielectric spectroscopy and analyzing the modified Clausius-Mossotti-Debye equation and the relaxation behavior. As 1,4-dioxane has no intrinsic dipole moment but can form hydrogen bonds and is completely miscible with water, methanol and benzylalcohol, percolation phenomena can be observed which can be related to the relaxation behavior of the dipole moment of its polar co-solvent.

The third paper collects a wide study of percolation phenomena in DMSO-water binary mixtures.

List of publications

- (1) Hernandez-Perni G., Stengele and Leuenberger H. 2004a. Towards a better understanding of the parameter E_i/E in the characterization of polar liquids. Proceedings of the 5th Central European Symposium on Pharmaceutical Technology and Biotechnology, Ljubljana 2003. Int. J. Pharm. (Accepted for publication)
- (2) Hernandez-Perni G., Stengele and Leuenberger H. 2004b. Detection of percolation phenomena in binary polar liquids by broadband dielectric spectroscopy. Proceedings of the 5th Central European Symposium on Pharmaceutical Technology and Biotechnology, Ljubljana 2003. Int. J. Pharm. (Accepted for publication)
- (3) Hernandez-Perni G., and Leuenberger H. 2004. The characterization of aprotic polar liquids and percolation phenomena in DMSO-water mixtures. Proceedings of the 3rd International conference on Broadband Dielectric Spectroscopy and its Applications. Delft, The Netherlands. Eur. J. Pharm. Biopharm. (Submitted)

Contents

Symbols and Abbreviations	viii
Chapter 1	1
1 Introduction	1
1.1 References	3
Chapter 2	4
2 Theory	4
2.1 Water	4
2.1.1 Liquid and solid water	6
2.1.2 The anomalous properties of water	7
2.1.3 Water clusters, structured water and biowater	9
2.1.3.1 So-called "structured water"	9
2.1.3.2 Biowater	10
2.2 Dielectric spectroscopy as an analytical technique	12
2.3 Properties of isolating material in electric fields	13
2.3.1 Permanent and induced electric dipole moments	13
2.3.2 Dielectric constant	14
2.3.3 Background of dielectric response: The Clausius-Mossotti and Debye equations	17
2.3.4 The modified Clausius-Mossotti and Debye equation according to Leuenberger	20
2.3.5 g-values obtained from the Kirkwood-Fröhlich Equation (Stengele et al., 2001)	22
2.3.6 Broadband dielectric spectroscopy	23
2.3.6.1 The Debye equation for the complex dielectric permittivity (ϵ^*)	24
2.3.6.2 The Cole-Davidson relaxation behavior and its superposition with the Debye equation	26
2.4 Solubility parameters: Theory and Application	27
2.4.1 The Hildebrand Solubility Parameter	27
2.4.2 Hansen parameter	30
2.5 Application of percolation theory to liquid binary mixtures	32
2.6 References	39
Chapter 3	42
3 Materials and Methods	42
3.1 Materials	42
3.1.1 Solvents	42
3.1.2 Apparatus	48
3.1.3 Computer Software	50
3.2 Methods	50
3.2.1 Sample preparation	51
3.2.2 Measurement of static permittivity and conductivity	51
3.2.2.1 Measuring principle	51
3.2.2.2 Apparatus and Measuring Procedure	54

3.2.2.3	Accuracy and reproducibility of the measurement	55
3.2.3	Measurement of complex permittivity	56
3.2.3.1	Measuring principle	56
3.2.3.2	Apparatus and Measuring Procedure	59
3.2.3.3	Accuracy and reproducibility of measurement	60
3.2.4.	Measurement of density	62
3.2.4.1	Measuring principle	62
3.2.4.2	Apparatus and measuring procedure	63
3.2.4.3	Accuracy and reproducibility of the measurement	63
3.2.5.	Measurement of refractive index	64
3.2.5.1	Measuring principle	64
3.2.5.2	Apparatus and measuring procedure	65
3.2.5.3	Accuracy and reproducibility of measurement	66
3.2.6.	Data analysis	66
3.2.6.1	Determination of additional physical properties	66
3.2.6.2	Nonlinear regression of dielectric raw data	67
3.2.6.3	Subdivision of curves into segments by means of nonlinear regression	69
3.2.6.4	Software	69
3.3	References	70
Chapter 4		73
4	Results and discussion	73
4.1.	Introduction	73
4.2.	E_i/E of the modified Clausius-Mossotti equation for water liquid binary mixtures	74
4.3.	g -values according to the Kirkwood-Fröhlich equation for water liquid binary mixtures	82
4.4	Towards a better understanding of the parameter E_i/E in the characterization of polar liquids	84
4.4.1	Abstract	84
4.4.2	Introduction	85
4.4.3	Theoretical	85
4.4.3.1	The Clausius-Mossotti-Debye equation modified according to Leuenberger for the quasi-static dielectric constant (Stengele et al., 2001)	85
4.4.3.2	Dimroth-Reichardt E_T parameter: an empirical solvent polarity parameter	87
4.4.4	Materials and methods	88
4.4.4.1	Data analysis	88
4.4.5	Results	91
4.4.5.1	The correlation of E_i/E with the total Hildebrand solubility parameter (δ_t) and the partial Hansen solubility parameters (δ_p , δ_h) at room temperature.	91
4.4.5.2	The correlation of E_i/E with D_{OH}	93
4.4.5.3	The correlation of E_i/E with $D_{\mu\mu}$ at room temperature	94
4.4.5.4	The correlation between the D_{OH} and $D_{\mu\mu}$ at room temperature	95
4.4.5.5	The correlation of E_i/E with the Dimroth-Reichardt $E_T(30)$ at room temperature	95

4.4.6	Conclusions	97
4.4.7	References	97
4.5	Detection of percolation phenomena in binary polar liquids by broadband dielectric spectroscopy	100
4.5.1	Abstract	100
4.5.2	Introduction	101
4.5.2.1	Broadband dielectric spectroscopy	101
4.5.2.1.1	General remarks	102
4.5.2.1.2	The Clausius-Mossotti-Debye equation modified according to Leuenberger for the quasi-static dielectric constant (Stengele et al., 2001)	102
4.5.2.1.3	The Debye equation for the complex dielectric permittivity (ϵ^*)	104
4.5.2.1.4	The Cole-Davidson relaxation behavior and its superposition with the Debye equation	106
4.5.2.1.5	Application of percolation theory	107
4.5.3	Materials and methods	109
4.5.3.1	Solvents	109
4.5.3.2	Experimental setup and data analysis	109
4.5.3.2.1	Measurement of the static permittivity and conductivity	110
4.5.3.2.1.1	Data analysis: Calculation of the E_i/E parameter for binary polar liquid mixtures	111
4.5.3.2.2	Measurement of the complex permittivity	112
4.5.3.2.2.1	Data analysis: Calculation of the relaxation time (τ)	113
4.5.3.2.2.2	Subdivision of curves into segments by means of nonlinear regression: detection of percolation thresholds	115
4.5.3.2.3	Other measurements	117
4.5.4	Results and discussion	117
4.5.4.1	Percolation phenomena observed in binary mixtures based in the results of the modified Clausius-Mossotti-Debye equation (Eq. 17)	118
4.5.4.1.1	Water/1,4-dioxane binary mixtures	118
4.5.4.1.2	Methanol/1,4-dioxane binary mixtures	119
4.5.4.1.3	Benzylalcohol/1,4-dioxane binary mixtures	120
4.5.4.2	Percolation phenomena observed in binary mixtures based in the results of broadband dielectric spectroscopy of binary mixtures at 298.2 K	121
4.5.4.2.1	Water/1,4-dioxane binary mixtures	121
4.5.4.2.2	Methanol/1,4-dioxane binary mixtures	124
4.5.4.2.3	Benzylalcohol/1,4-dioxane binary mixtures	125
4.5.5	Conclusions	128
4.5.6	References	128
4.6	The characterization of aprotic polar liquids and percolation phenomena in DMSO-water binary mixtures	130
4.6.1	Abstract	130
4.6.2	Introduction	131
4.6.3	Theoretical background	
4.6.3.1	The Clausius-Mossotti-Debye equation modified according to Leuenberger for the quasi-static dielectric constant (Stengele et al., 2001)	133

4.6.3.2	g-values obtained form the Kirkwood-Fröhlich Equation (Stengele et al., 2001)	134
4.6.3.3	The Debye equation for the complex dielectric permittivity ϵ^*	135
4.6.3.4	Application of percolation theory	136
4.6.3.5	Structural differences between a solid, liquid and a gas	138
4.6.4	Materials and methods	140
4.6.4.1	Solvents	140
4.6.4.2	Experimental setup and data analysis	140
4.6.4.2.1	Measurement of the static permitivity and conductivity: The use of the E_i/E parameter in the characterization of aprotic liquids at room temperature: Data analysis	140
4.6.4.2.2	Measurement of the complex permittivity: Calculation of the relaxation time τ	144
4.6.4.2.3	Subdivision of curves into segments by means of nonlinear regression: detection of percolation thresholds	144
4.6.5	Results and discussion	145
4.6.5.1	The use of the E_i/E parameter in the characterization of aprotic liquids at room temperature	145
4.6.5.2	Percolation phenomena observed in DMSO-water binary mixtures based in the results of the modified Clausius-Mossotti-Debye equation	150
4.6.5.3	Percolation phenomena observed in DMSO-water binary mixtures based in the results of g-values according to the Kirkwood-Fröhlich equation	153
4.6.5.4	Relaxation time according to the Debye equation for the complex dielectric permittivity ϵ^*	154
4.6.5.5	Other physical properties explaining the phenomenon of percolation in DMSO-water binary mixtures.	155
4.6.6	Conclusions	157
4.6.7	References	159
	Outlook	163
	Appendix A	165
	Appendix B	169
	Appendix C	173
	Curriculum Vitae	175

Symbols and Abbreviations

Latin symbols

A	area [m^2]
A^*	apparatus specific constant of density meter
B^*	apparatus specific constant of density meter
B	susceptance, imaginary part of admittance [S]
C	capacitance [F]
c	cohesive energy density [Jmol^{-1}]
C_0, C_{vacuum}	capacitance of the condenser in vacuum [F]
C_{mut}	capacitance of material under test [F]
D_{OH}	density of OH-groups per volume [cm^{-3}]
$D_{\mu\mu}$	density of the square of the dipole moment per molar volume [$\text{D}^2\text{molcm}^{-3}$]
E	electric field [Vm^{-1}]
E_e	external electric field [Vm^{-1}]
E_i	internal electric field [Vm^{-1}]
E_L	Lorenz-field
E_{local}	local electric field [Vm^{-1}]
E_{sph}	electric field caused by induced dipoles outside the sphere, causing charges on the surface
$E_T, E_T(30)$	Dirmroth-Reichardt parameter [Kcalmol^{-1}]
E_T^N	normalized values of the Dirmroth-Reichardt parameter
G	conductance [$\text{S} = \Omega^{-1}$]
g	Kirkwood-Fröhlich correlation factor
ΔH	molar vaporization enthalpy [Jmol^{-1}]
i	imaginary unit $(-1)^{1/2}$
l	weight factor of the relaxation time
k	Boltzmann constant = $1.38 \cdot 10^{-23}$ [JK^{-1}]
K	cell constant [m^{-1}]
L	inductance [H]

$ m $	slope of the linear regression $(E_i/E) = f(1/T)$
b	intercept of the linear regression $(E_i/E) = f(1/T)$
M_r	molecular weight [gmol^{-1}]
$M_{r,m}$	molecular weight of the mixture [gmol^{-1}]
N	number of molecules per volume [m^{-3}]
n	refractive index
N_A	Avogadro constant = $6.02 \cdot 10^{23}$ [mol^{-1}]
P_{atm}	atmospheric pressure [Torr]
P	occupation probability
p_c	percolation threshold
P	polarization [Cm^{-2}]
P_M	molar polarization [Cmol^{-1}]
Q	total electric charge
q	critical exponent
q	charge
R	resistance [Ω]
R	gas constant [$8.314 \text{ Jmol}^{-1}\text{K}^{-1}$]
R^*	resistance of the standard [Ω]
r	distance
S	scale/ proportionality factor
STDEV	standard deviation
T	temperature [K]
T^*	oscillation period of the sample-filled U-tube [s]
T	transmittance
V_1	volume fraction of liquid 1
V_2	volume fraction of liquid 2
V_A/V	volume fraction of A in A+B
V_m	molar volume [$\text{m}^3\text{mol}^{-1}$]
V	potential difference between the plates
X	reactance, imaginary part of impedance [Ω]
Y	admittance, $Y = G + iB$ [s]
Z	impedance, $Z = R + iX$ [Ω]

Greek symbols

α	angle of incidence
α	polarizability [$\text{C m}^2\text{V}^{-1}$]
β	Cole-Davidson parameter for asymmetric distribution of relaxation times
β	angle of refraction
Γ	reflection coefficient
δ or δ_t	Hildebrand solubility parameter or total solubility parameter [$(\text{Jm}^{-3})^{1/2}$] [$1 \text{ cal}^{1/2}\text{cm}^{-3/2} = 2.0455 \text{ J}^{1/2}\text{cm}^{-3/2}$]
δ_h	hydrogen bonding contribution to the solubility parameter
δ_p	polar contribution to the solubility parameter
δ_d	dispersion contribution to the solubility parameter
δ	phase of admittance, dielectric loss angle; $\tan \delta = \frac{\epsilon''}{\epsilon'}$
$\delta+$, $\delta-$	charges of the dipole
ϵ_{exp}	experimentally obtained permittivity values
ϵ_{lit}	permittivity values in literature
ϵ_m	measured quasi-static dielectric constant for the mixtures
ϵ , ϵ_{stat} , ϵ_{rel}	static permittivity; relative permittivity or dielectric constant
ϵ_0	electric field constant in vacuo = $8.85410 \cdot 10^{-12} [\text{C}^2\text{J}^{-1}\text{m}^{-1}]$
ϵ_∞	dielectric constant characteristic for induced polarisation, measured at a frequency low enough that both atomic and electronic polarisation are the same as in static electric field and high enough so that the permanent dipoles can no longer follow the field
ϵ^*	complex permittivity
ϵ'	real part of complex permittivity
ϵ''	imaginary part of complex permittivity, loss factor
μ	permanent dipole moment [Cm]
μ_g	permanent dipole moment in the gas phase [Cm] 1 Debye = $3.33564 \cdot 10^{-30} \text{ Cm}$
μ_i	induced dipole moment [Cm]
μ^*	complex permeability
ν	frequency [s^{-1}]

ρ	density [kgm^{-3}]
ρ_m	density of the mixture [kgm^{-3}]
σ	specific conductivity [Sm^{-1}]
τ	dielectric relaxation time [s]
τ_0	main dielectric relaxation time [s]
θ	phase of impedance
ω	angular frequency [s^{-1}]
ω_{res}	resonance frequency [s^{-1}]

Chapter 1

1. Introduction

Water properties are the subject of investigations in physics, chemistry, biology and different applied fields of natural science.

Liquid dosage forms, generally based on aqueous solutions, take an important role in drug administration e.g. as parenteral preparations, ophthalmic formulations or as oral solutions for children and elderly patients. Intermolecular forces determine the solubility of a drug. While these can be reasonably well characterized in gaseous and solid material, no satisfying description has yet been found for liquids systems, especially for nonideal solutions. The presence of several types of intermolecular interactions let the water show rather a complex associated structure due to which it has a number of its abnormal properties.

In this work, the intermolecular forces in pure solvents and binary mixtures at 298.2K are investigated, using quasi-static low-frequency and AC high-frequency broadband (0.2-20 GHz) dielectric spectroscopy. Dielectric spectroscopy is an old experimental tool, which has vastly developed during the last two decades. It covers nowadays the extraordinary spectral range from 10^{-06} to 10^{12} Hz. This enables researchers to make sound contributions to contemporary problems in modern physics.

The data in this work were interpreted using for the low frequency measurements the modified Clausius-Mossotti-Debye equation according to Leuenberger and the Kirkwood-Fröhlich equation. For the description of the dielectric relaxation in the high frequency range there are different mathematical models available which describe the relaxation behaviour of a polar liquid. The most simple equation is the Debye equation

(see Fig. 1), which will be described in the chapter of theory. To fit the ϵ' , ϵ'' - data in a best way it is also possible to use the Cole-Davidson distribution function or superposition of the Debye function with the Cole-Davidson function. It has to be kept in mind that the resulting relaxation times (τ) depend on the mathematical model applied. If the mean corrected R^2 coefficient does not differ significantly for the mathematical models used, it is not possible to make an unambiguous choice of model. The goal is to use the model with an adequate corrected R^2 and with the lower number of parameters to be adjusted.

In the two previous papers (Stengele et al., 2001; Stengele et al., 2002) it was shown, that the Clausius-Mossotti-Debye equation for the quasi-static dielectric constant (ϵ) can be extended to liquids if the parameter E_i/E is introduced. E_i corresponds to the local mean field due to close molecule-molecule interactions after the application of an external electric field E . The present study is a continuation of the previous publications.



Figure 1. Portrait of P. Debye during the time when he was professor of experimental physics at the University of Leipzig (1927-1935). He is the founder of the dielectric relaxation function. Debye was awarded with the Nobel Prize in Chemistry 1936.

In the first part a detailed study of the E_i/E parameter in the characterization process of polar liquids is performed. The relationship between the values of E_i/E and the total Hildebrand solubility parameter (δ_t) at room temperature, as well as the study of the correlation of E_i/E value with the partial Hansen solubility parameters (δ_h , δ_p) for polar liquids is analyzed.

In a second part the percolation phenomena is detected in water/1,4-dioxane, methanol/1,4-dioxane and benzylalcohol/1,4-dioxane binary polar liquid mixtures by

using broadband (0.2-20 GHz) dielectric spectroscopy and analyzing the modified Clausius-Mossotti-Debye equation and the relaxation behavior. As 1,4-dioxane has no intrinsic dipole moment but can form hydrogen bonds and is completely miscible with water, methanol and benzylalcohol, percolation phenomena can be observed which can be related to the relaxation behavior of the dipole moment of its polar co-solvent.

The third part collects a wide study of percolation phenomena in DMSO-water binary mixtures. It is demonstrated the important role of the E_i/E parameter in the characterization of not only polar liquids able to form hydrogen bonds but also aprotic liquids being an easier measurable alternative parameter to describe the polarity of liquids. It is also demonstrated that the values of E_i/E as a function of the components in the binary mixtures can be related to the viscosity changes, which are also related to percolation theory. Therefore, it is demonstrated that the E_i/E parameter can be used to characterize aprotic liquids.

The results of this thesis are presented in three papers (see Sections 4.4, 4.5, and 4.6) that are printed in order of their chronological development. The two first papers have been accepted for publication in the International Journal of Pharmaceutics and the third paper has been submitted to the European Journal of Pharmaceutics and Biopharmaceutics. The results of the two first were presented at the 5th Central European Symposium on Pharmaceutical Technology and Biotechnology, Ljubljana 2003, and the results of the third paper will be presented at the 3rd International conference on Broadband Dielectric Spectroscopy and its Applications. Delft, August 2004, (see list of publications page iv). The articles were originally formatted in line with the preferences of the individual journals and then few changes were made to fit the papers in the concept of this basis.

1.1 References

Stengele, A., Rey, St., Leuenberger, H., 2001. A novel approach to the characterization of polar liquids. Part 1: pure liquids. *Int. J. Pharm.* 225, 123-134.

Stengele, A., Rey, St., Leuenberger, H., 2002. A novel approach to the characterization of polar liquids. Part 2: binary mixtures. *Int. J. Pharm.* 241, 231-240.

Chapter 2

2. Theory

2.1 Water

If a single molecule were to be selected as the most important chemical entity of life, most people would agree that this is water.

Water has long been known to exhibit many physical properties that distinguish it from other small molecules of comparable mass. Chemists refer to these as the "anomalous" properties of water, but they are by no means mysterious; all are entirely predictable consequences of the way the size and nuclear charge of the oxygen atom conspire to distort the electronic charge clouds of the atoms of other elements when these are chemically bonded to the oxygen.

A covalent chemical bond consists of two atoms that share a pair of electrons between them. In the water molecule H_2O , the single electron of each H is shared with one of the six outer-shell electrons of the oxygen, leaving four electrons, which are organized into two non-bonding pairs. Thus, the oxygen atom is surrounded by four electron pairs that would ordinarily tend to arrange themselves as far from each other as possible in order to minimize repulsions between these clouds of negative charge. This would ordinarily result in a tetrahedral geometry in which the angle between electron pairs (and therefore the H-O-H bond angle) is 109° . However, because the two non-bonding pairs remain closer to the oxygen atom, these exert a stronger repulsion against the two covalent bonding pairs, effectively pushing the two hydrogen atoms closer together. The result is a distorted tetrahedral arrangement in which the H—O—H angle is 104.5° .

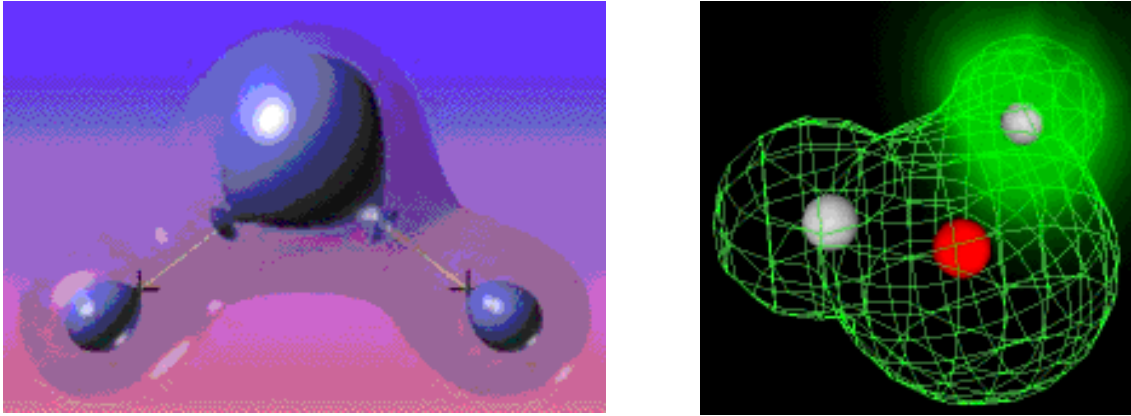


Figure 2. 1 These two computer-generated images of the H₂O molecule come from calculations that model the electron distribution in molecules. The outer envelopes show the effective "surface" of the molecule (Lower, 2001).

The H₂O molecule is electrically neutral, but the positive and negative charges are not distributed uniformly. This is shown clearly in the two images above, and in Fig. 2.2. The electronic (negative) charge is concentrated at the oxygen end of the molecule, owing partly to the nonbonding electrons (solid blue circles), and to oxygen's high nuclear charge. This charge displacement constitutes an *electric dipole*, represented by the arrow at the bottom in Fig. 2.2 (A).

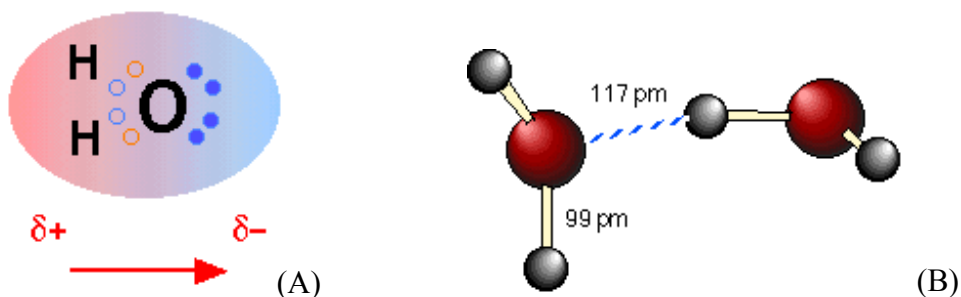


Figure 2. 2 A) Electric dipole of water B) hydrogen bond between two water molecules (Lower, 2001).

Hydrogen bonds appear in substances where there is a hydrogen united covalently to very electronegative elements (e.g., F, Cl, O and N), which is the case with water. The hydrogen bond can be either intermolecular (e.g., H₂O) or intramolecular (e.g., DNA). The leading role of hydrogen is due to its small size and its tendency to become positively polarized, specifically to the elevated density of the charge, which

accumulates on the mentioned compounds. In this way, hydrogen is capable, such as in the case of water, of being doubly bonded: on the one hand it is united covalently to an atom of oxygen belonging to its molecule and, on the other, it electrostatically attracts another atom of oxygen belonging to another molecule, so strengthening the attractions between molecules. In this way, each atom of oxygen of a molecule of water can take part in four links with four more molecules of water, two of these links being through the hydrogen atoms covalently united to it and the other two links through hydrogen bonds thanks to the two pairs of solitary electrons which it possesses.

Those solvents, which are capable of forming hydrogen bonds have a well known affinity for the solvents with a similar characteristic, which is the case of water. The formation of hydrogen bonds between solute molecules and those of solvents explains, for example, the good solubility in water of ammonia and of the short chain organic acids. Notice that the hydrogen bond (shown by the dashed blue line) is somewhat longer (117 pm) than the covalent O—H bond (99 pm) (see Fig. 2.2 (B)).

The hydrogen bonding is considerably weaker than the corresponding water bonds; it is so weak, that a given hydrogen bond cannot survive for more than a tiny fraction of a second.

2.1.1 Liquid and solid water

If we examine ice, we see that there are ten modifications of ice known (I_h ; I_{II} , ..., I_{IX} ; I_c), but cooling water down to 273 K and below at atmospheric pressure, only the hexagonal form I_h is received. All polymorphic forms have in common that each oxygen atom is hydrogen bonding to four other oxygens. At absolute zero, the distance between neighbouring oxygen atoms in I_h is 2.74 Å and the angle O...H-O-H...O is the tetrahedral 109.47°.

This basic assembly repeats itself in three dimensions to build the ice crystal (see Fig. 2.3).

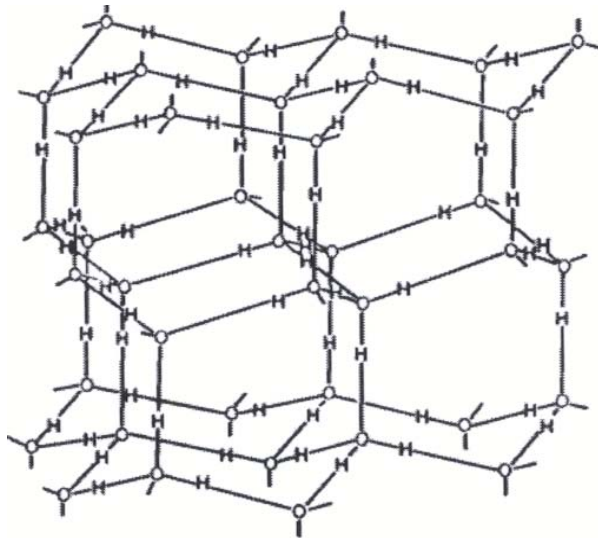


Figure 2. 3 The structure of ice I_h (Stillinger, 1982)

When ice melts to form **liquid water**, the uniform three-dimensional tetrahedral organization of the solid breaks down as thermal motions disrupt, distort, and occasionally break hydrogen bonds. The methods used to determine the positions of molecules in a solid do not work with liquids, so there is no unambiguous way of determining the detailed structure of water (see Fig. 2.4).

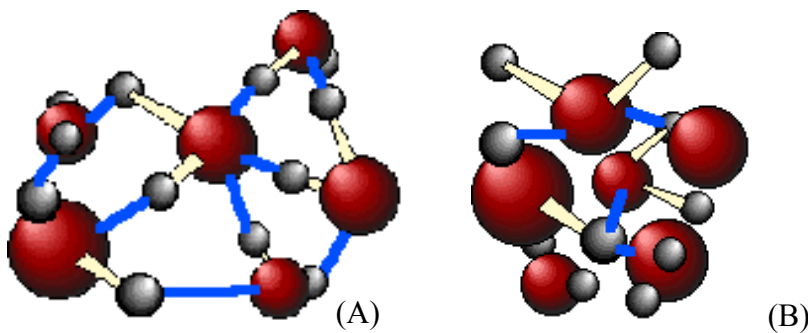


Figure 2. 4 Here are three-dimensional views of a typical local structure of liquid water (A) and of ice (B). Notice how the greater openness of the ice structure which is necessary to ensure the strongest degree of hydrogen bonding in a uniform, extended crystal lattice (Lower, 2001).

2.1.2 The anomalous properties of water

The presence of hydrogen bonds together with the tetrahedral coordination of the molecule of water constitutes the key to explain its unusual properties.

Water is almost unique among the more than 15 million known chemical substances in that its solid form is less dense than the liquid. Fig. 2.5 shows how the volume of water varies with the temperature; the large increase (about 9%) on freezing shows why ice floats on water and why pipes burst when they freeze. The expansion between 4°C and 0°C is due to the formation of larger clusters. Above 4°C, thermal expansion sets in as thermal vibrations of the O—H bonds becomes more vigorous, tending to shove the molecules apart more.

The other widely-cited anomalous property of water is its high boiling point. As Fig. 2.6 shows, a molecule as light as H₂O " should " boil at around -90°C; that is, it should exist in the world as a gas rather than a liquid, if H-bonding were not present. Notice that H-bonding is also observed with fluorine and nitrogen (see Fig. 2.6).

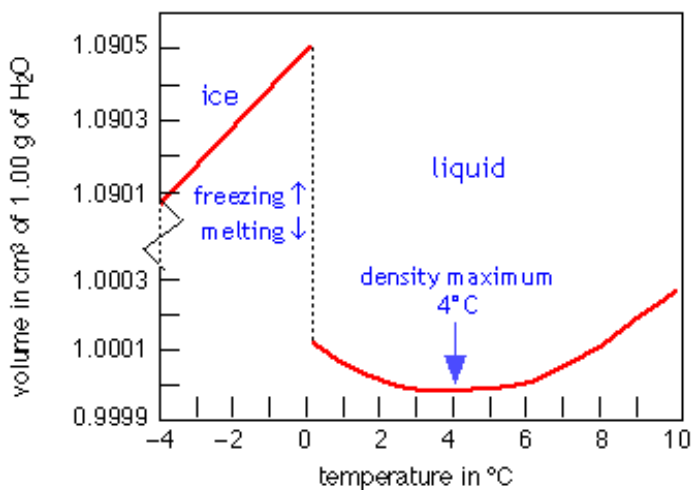


Figure 2. 5 Volume of water as a function of the temperature (Lower, 2001).

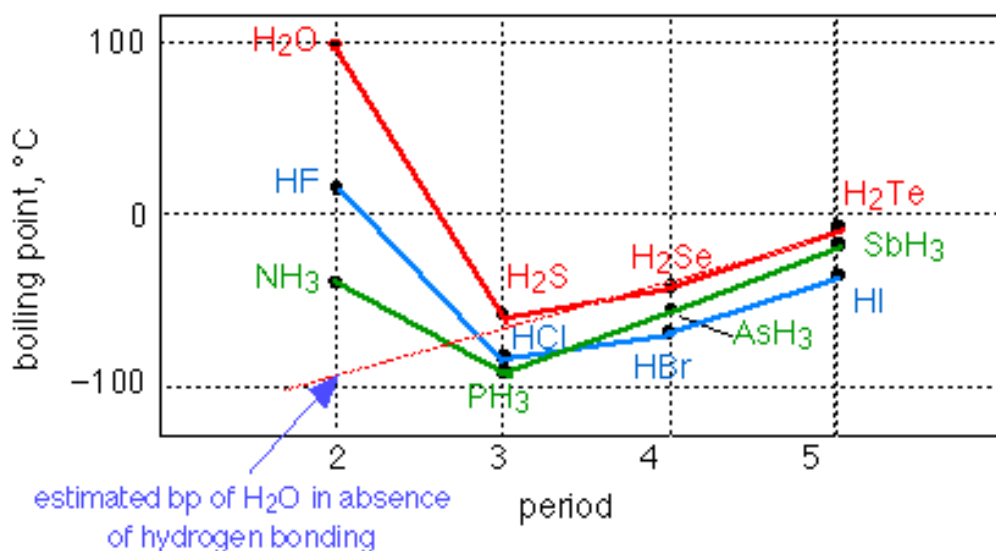


Figure 2. 6 Influence of H-bonding on the boiling point of H₂O, HF and NH₃ (Lower, 2001).

2.1.3 Water clusters, structured water and biowater

Since the 1930s, chemists have described water as an "associated" liquid, meaning that hydrogen-bonding attractions between H₂O create loosely-linked aggregates. Because the strength of a hydrogen bond is comparable to the average thermal energy at ordinary temperatures, these bonds are disrupted by thermal motions almost as quickly as they form. Theoretical studies have shown that certain specific cyclic arrangements ("**clusters**") of 3, 4, and 5 H₂O molecules are especially stable, as is a three-dimensional hexamer (6 molecules) that has a cage-like form. But even the most stable of these clusters will flicker out of existence after only about 10 picoseconds. It must be emphasized that no clustered unit or arrangement has ever been isolated or identified in pure liquid water (see Fig. 2.7).

2.1.3.1 So-called "structured water"

Water molecules interact strongly with non-hydrogen bonding species as well. A particularly strong interaction occurs when an ionic substance such as sodium chloride (ordinary salt) dissolves in water. Owing to its high polarity, the H₂O molecules closest to the dissolved ion are strongly attached to it, forming what is known as the primary

hydration shell. Positively-charged ions such as Na^+ attract the negative (oxygen) ends of the H_2O molecules, as shown in Fig. 2.8. The ordered structure within the primary shell creates, through hydrogen-bonding, a region in which the surrounding waters are also somewhat ordered; this is the outer hydration shell, or cybotactic region.

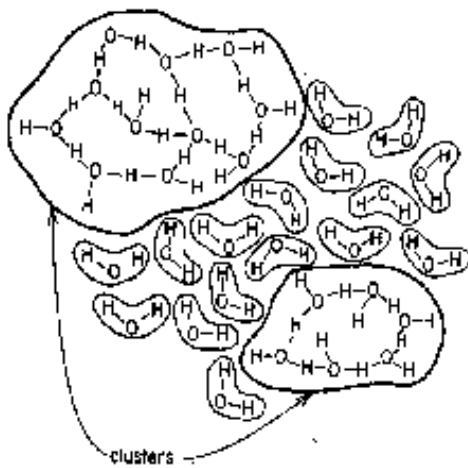


Figure 2. 7 Liquid water can be thought of as a seething mass of water molecules in which hydrogen-bonded clusters are continually forming, breaking apart, and re-forming. Theoretical models suggest that the average cluster may encompass as many as 90 H_2O molecules at 0°C , so that very cold water can be thought of as a collection of ever-changing ice-like structures. At 70°C , the average cluster size is probably no greater than about 25 (Lower, 2001).

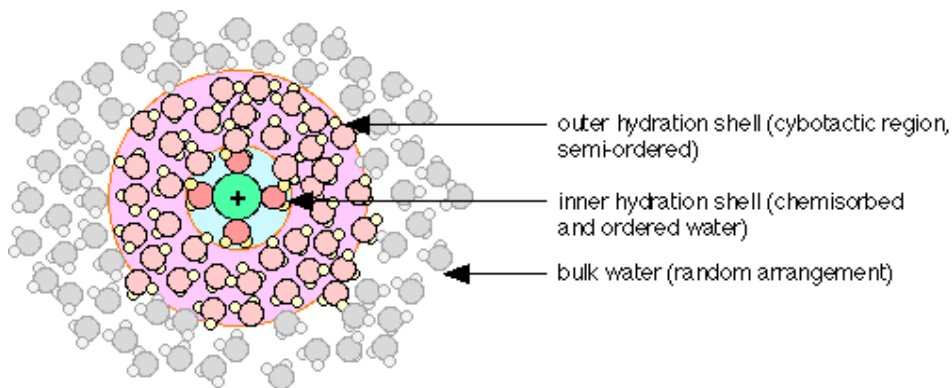


Figure 2. 8 Organization of water molecules when an ionic substance such as sodium chloride (ordinary salt) is dissolved (Lower, 2001).

2.1.3.2 Biowater

Water can hydrogen-bond not only to itself, but also to any other molecules that have -OH or $-\text{NH}_2$ units hanging off of them. This includes simple molecules such as alcohols, surfaces such as glass, and macromolecules such as proteins. The biological activity of proteins (of which enzymes are an important subset) is critically dependent not only on their composition but also on the way these huge molecules are folded; this

folding involves hydrogen-bonded interactions with water, and also between different parts of the molecule itself. Anything that disrupts these intramolecular hydrogen bonds will denature the protein and destroy its biological activity. This is essentially what happens when you boil an egg; the bonds that hold the egg white protein in its compact folded arrangement break apart so that the molecules unfold into a tangled, insoluble mass which, be cannot be restored to their original forms. Note that hydrogen-bonding need not always involve water; thus the two parts of the DNA double helix are held together by H—N—H hydrogen bonds.

It is now known that the intracellular water very close to any membrane or organelle (sometimes called *vicinal water*) is organized very differently from bulk water, and that this structured water plays a significant role in governing the shape (and thus biological activity) of large folded biopolymers. It is important to bear in mind, however, that the structure of the water in these regions is imposed solely by the geometry of the surrounding hydrogen bonding sites.

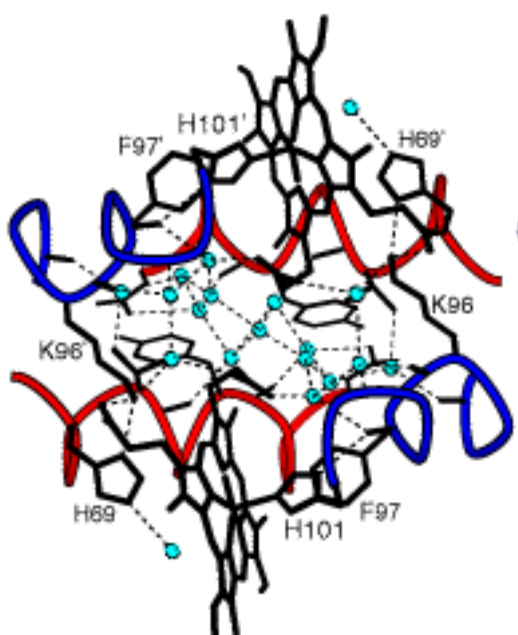


Figure 2. 9 This picture, taken from the work of William Royer Jr. of the U. Mass. Medical School, shows the water structure (small green circles) that exists in the space between the two halves of a kind of dimeric hemoglobin. The thin dotted lines represent hydrogen bonds. Owing to the geometry of the hydrogen-bonding sites on the heme protein backbones, the H₂O molecules within this region are highly ordered; the local water structure is stabilized by these hydrogen bonds, and the resulting water cluster in turn stabilizes this particular geometric form of the hemoglobin dimer.

[Lower, 2001]

2.2 Dielectric spectroscopy as an analytical technique

Dielectric spectroscopy involves the study of response of material to an applied electric field. By appropriate interpretation of the data, it is possible to obtain structural information on a range of samples using this technique. While the use of dielectric

spectroscopy technique has previously been largely confined to the field of physics, the generality of dielectric behavior has led to the technique being used in more diverse fields such as colloid science, polymer science and, more recently, the pharmaceutical sciences.

Most pharmaceutical systems may be described as dielectrics, which for present purposes may be defined as materials, which contain dipoles. In principle, therefore, the majority of such materials may be studied using the technique. The use of the information obtained may be broadly divided into two categories. Firstly, dielectric data may be used as fingerprint with which to compare samples prepared under different conditions; this therefore has implications for the use of dielectric spectroscopy as a quality control. Secondly, each spectrum may be interpreted in terms of the structure and behavior of the sample, therefore leading to more specific information in the sample under study. Both approaches are useful and obviously require different levels of understanding regarding the theory behind the technique.

It is also useful to consider the type of information that may be obtained from the spectra. Techniques can be very broadly divided into those which examine molecular structure (e.g. IR, NMR) and those, which examine the physical arrangement and behavior of molecules within structures (e.g. rheological measurements, DSC). Dielectric spectroscopy tends towards the latter category, although information on molecular structure may also be gained.

As with any technique, there are associated advantages and disadvantages. One of the advantages is that the sample preparation is generally very simple. For example, low frequency measurements may be made via the application of two electrodes to the sample, either by attachment or immersion. Samples with a range of sizes and shapes may therefore be studied; solid compacts, powders, gels or liquids may be easily measured. In the present work pure liquids and binary liquid mixtures will be the object of our study. Further more, in most cases the technique is non-invasive, as the voltages used are small. Finally, the method and conditions of measurement may be varied. For example, the sample may be examined under a range of temperatures, humidities, pressures etc. The principal disadvantages of the technique with respect to pharmaceutical uses are firstly that not all samples may be usefully analyzed, a fault

which is common to all analytical methods. The second disadvantage lies with the general inaccessibility of the dielectrics literature to pharmaceutical sciences. This has arisen largely for historical reasons, as most of the dielectric literature has been written on the (hitherto) reasonable assumption that any reader interested in the subject will already have a prior knowledge of dielectrics (or at least physics)

[Craig, 1995]

2.3 Properties of isolating material in electric fields

2.3.1 Permanent and induced electric dipole moments

A polar molecule is a molecule with a permanent electric dipole moment that arises from the partial charge on atoms linked by polar bonds. Non-polar molecules may acquire a dipole moment in an electric field on account of the distortion the field causes in their electronic distributions and nuclear positions. Similarly, polar molecules may have their existing dipole moments modified by the applied field.

Permanent and induced dipole moments are important in chemistry through their role in intermolecular forces and in their contribution to the ability of a substance to act as a solvent for ionic solids. The latter ability stems from the fact that one end of a dipole may be coulombically attracted to an ion of opposite charge and hence contribute an exothermic to the enthalpy of solution.

The average electric dipole moment per unit volume of a sample is called its polarization (P).

The polarization of a fluid sample is zero in the absence of an applied field because the molecules adopt random orientations and the average dipole moment is zero. In the presence of a field the dipoles are partially aligned and there is an additional contribution from the dipole moment induced by the field. Hence, the polarization of a medium in the presence of an applied field is non-zero (see Fig. 2.10).

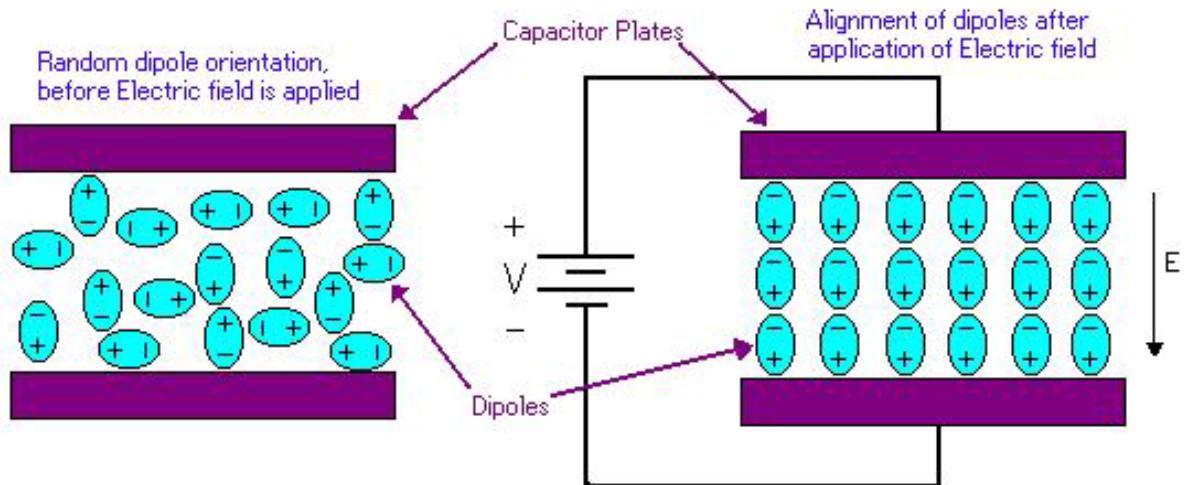


Figure 2. 10 Orientation of dipole moments

<http://www.mse.vt.edu/faculty/hendricks/mse4206/projects97/group01/solidstate/dielect.htm>

In the following we refer to the sample as a dielectric, by which we mean a polarizable, non-conducting medium.

2.3.2 Dielectric constant

The dielectric constant or permittivity of a material is a measure of the extent to which the electric charge distribution in the material can be distorted or “polarized” by the application of an electric field. The individual charges do not travel continuously for relatively large distances, as in the case in electrical conduction by transport. But there is nevertheless a flow of charge in the polarization process, for example, by the rotation of polar molecules, which tend to line up in the direction of the field.

The total electric charge (Q) of two parallel plates of a condenser at equilibrium is proportional to the potential difference (V) between the plates. The capacitance (C) is the proportionality factor between these values.

$$Q = C \times V \tag{2.1}$$

The capacitance of a condenser depends on its geometry and the medium between the plates.

As a standard, the capacitance of a condenser in vacuum is used.

$$C_0 = \frac{\varepsilon_0 \cdot A}{r} \quad (2.2)$$

C_0 = capacitance of the condenser in vacuum

ε_0 = electric field constant in vacuum = $8.854 \cdot 10^{-12}$ [C²/Jm]

A = surface area of each plate

r = distance between parallel plates

The relationship between capacitance (C) in the dielectric to capacitance in vacuum (C_0) is described as dielectric constant (ε_{rel}).

$$\varepsilon_{rel} = \frac{C}{C_0} \quad (2.3)$$

The dielectric constant (ε_{rel}) is dimensionless, substance-specific and equals to one for vacuum according to its definition.

The electric charge of a dielectric in a condenser is polarized by the electric field. The electric field causes the charges to shift in the direction of the field. When the applied field changes direction periodically, the permanent dipole moments reorientate and follow the field. The electric field can also induce dipole in a system, which is actually dipole-free.

The dielectric constant is dependent on the polarizability of the dielectric. As the polarizability increases, the dielectric constant increases with it.

The dielectric constant is also frequency dependent. Dielectric constant measured at low frequencies is called static permittivity, at high frequencies complex permittivity. Depending on the frequency, different polarization types of the dielectric can be observed.

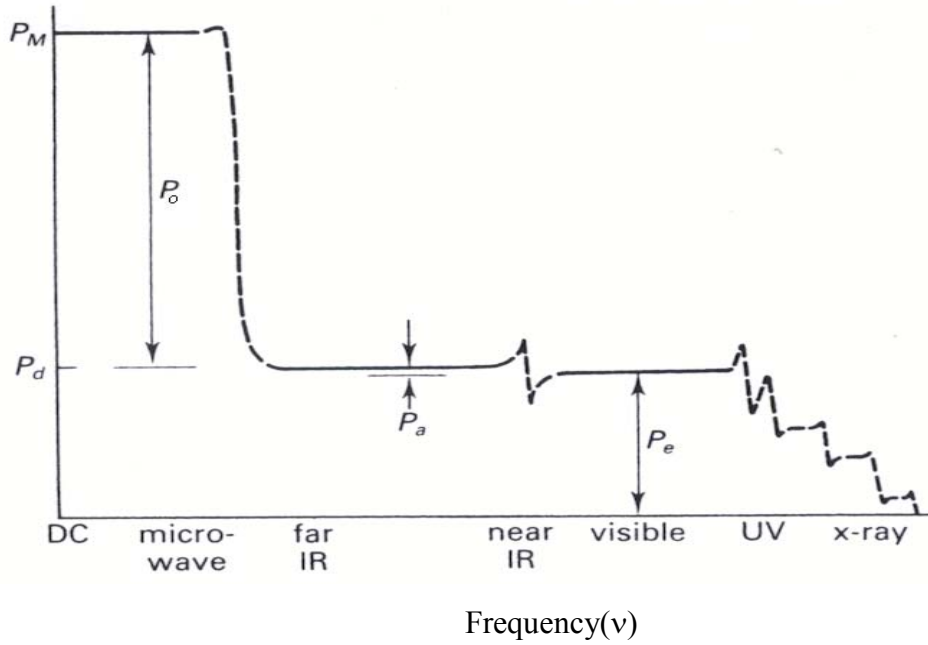


Figure 2. 11 Frequency dependence of the molar polarisation of permanent dipoles. (Shoemaker et al., 1989) where P_M = molar polarization; P_o = orientational polarization; P_a = atomic polarization; P_e = electronic polarization; P_d = distortion polarization.

The total polarization is measured on static conditions (alternating current at low frequencies). The static electric constant is also called static permittivity (ϵ_{stat}) or relative permittivity (ϵ_{rel}).

$$\epsilon = \epsilon_{rel} = \epsilon_{stat} = \frac{C}{C_0} \quad (2.4)$$

In this work, static dielectric constant (ϵ_{stat}) will be abbreviated as (ϵ).

[Alonso et al., 1992], [Shoemaker et al., 1989]

2.3.3 Background of dielectric response: The Clausius-Mossotti and Debye equations.

Pure pharmaceutical solvents, for example water and ethanol, are dielectrics, i.e. insulating materials. Every kind of insulation material consists at an atomic level of negative and positive charges balancing each other in microscopic as well as in more macroscopic scales. Macroscopically, some localized space charge may be present, but even then an overall charge neutrality exists.

As soon as the material is exposed to an electric field (as generated by a voltage across electrodes between which the dielectric is embedded), very different kinds of dipoles become excited even within atomic scales. A local charge imbalance is thus “induced” within the neutral species (atoms or molecules) as the “centers of gravity” for the equal amount of positive and negative charges, $\pm q$, become separated by a small distance (d), thus creating a dipole with a dipole moment, $\mu = q \cdot d$, which is related to the “local” or “microscopic” electric field (E_{Local}) acting in close vicinity of the species. Thus, the dipole moment can also be written as:

$$\mu = \alpha \cdot E_{Local} \quad (2.5)$$

where α = polarizability [Cm^2V^{-1}] of the species or material under consideration.

It is necessary to point out that E_{Local} refers to the local field rather than the applied field. This distinction is drawn because the local field will be the vectorial sum of the applied field and the fields generated by the presence of the surrounding charges (i.e. the other dipoles). The question then arises as to how the local field may be related to the applied electric field. One of the earliest approaches involves the general relationship between polarization and the applied electric field strength:

$$P = (\varepsilon - 1) \cdot \varepsilon_0 \cdot E_e \quad (2.6)$$

where P = polarization, dipole density [Cm^{-2}], ϵ = relative permittivity or dielectric constant and ϵ_0 = electric field constant in vacuum = $8.85410 \cdot 10^{-12}$ [$\text{C}^2\text{J}^{-1}\text{m}^{-1}$]; E_e = external electric field, produced by the applied voltage

[Craig, 1995]

The local field was first calculated by Lorenz (1909) by considering all the electric fields influencing the molecule in the cavity:

$$E_{\text{Local}} = E_i + E_e - E_{\text{sph}} \quad (2.7)$$

E_{Local} = local electric field

E_i = internal electric field, caused by interactions with other induced dipole in the sphere.

E_e = external electric field, produced by the applied voltage.

E_{sph} = electric field caused by the induced dipoles outside the sphere, causing charges on the surface.

In an ideal gas, E_{sph} and E_i are zero. In liquids, neighboring molecules show a polarising effect leading to charges on the sphere's boundary, resulting in

$$E_{\text{sph}} = -\frac{P}{3 \cdot \epsilon_0} \quad (2.8)$$

By combining Eqs. (2.6), (2.7), and (2.8) we obtain for the local field:

$$E_{\text{Local}} = E_i + E_e \cdot \left(\frac{\epsilon + 2}{3} \right) \quad (2.9)$$

If $E_i = 0$, E_{Local} is reduced to the Lorenz field (E_L):

$$E_{Local} = E_L = \frac{\varepsilon + 2}{3} E_e \quad (2.10)$$

According to Clausius and Mossotti we obtain for nonpolar molecules of constant polarizability the following relation:

$$P = N \cdot \mu_i \quad (2.11)$$

Where P = polarization, dipole density [Cm^{-2}]; N = number of molecules per volume and μ_i = induced dipole moment.

By combining Eq. (2.5) with (2.11) we get:

$$P = N \cdot \mu_i = N \cdot \alpha \cdot E_{Local} \quad (2.12)$$

Combination of Eq. (2.6), (2.10) and (2.12) lead to the **Clausius-Mossotti equation for nonpolar molecules** (Eq. (2.13) and (2.14))

$$\frac{(\varepsilon - 1)}{(\varepsilon + 2)} = \frac{N \cdot \alpha}{3 \cdot \varepsilon_0} \quad (2.13)$$

where $N = \frac{N_A}{V_M} = \frac{N_A \cdot \rho}{M_r}$ is the number of polarisable molecules per unit volume.

Therefore, the Eq. (2.13) can be defined as molar polarization P_M (Eq. (2.14))

$$P_M = \frac{\varepsilon - 1}{\varepsilon + 2} \cdot \frac{M_r}{\rho} = \frac{N_A}{3 \cdot \varepsilon_0} \cdot \alpha \quad (2.14)$$

where P_M = molar polarization [$\text{m}^3 \text{mol}^{-1}$] and N_A = Avogadro's constant = 6.023×10^{23} [mol^{-1}]

[Clausius, 1879] [Lorenz, 1909] [Mossotti, 1847]

The Clausius-Mossotti equation was extended by Debye to polar molecules:

$$\frac{\varepsilon - 1}{\varepsilon + 2} \cdot \frac{M_r}{\rho} = \frac{N_A}{3 \cdot \varepsilon_0} \cdot \left(\alpha + \frac{\mu_g^2}{3 \cdot k \cdot T} \right) \quad (2.15)$$

With ε = quasi-static relative dielectric constant; M_r = molecular weight; ρ = density; N_A = Avogadro number, 6.023×10^{23} (mol⁻¹); ε_0 = electric field constant in the vacuum, 8.854×10^{-12} (C² J⁻¹ m⁻¹); α = polarizability of the molecule (Cm²V⁻¹); μ_g = dipole moment in the state of an ideal gas (C m); k = Boltzmann's constant, 1.38×10^{-23} (J K⁻¹); T = temperature (K).

The Debye equation (Eq. (2.15)) is only valid for gas under low pressure and highly diluted solutions of polar molecules in nonpolar solvents, as dipole-dipole interactions are neglected. Therefore, it is not valid for polar liquids but can be used to estimate quite accurately the dipole moment μ_g of water in a highly diluted solution of water in 1,4-dioxane simulating an ideal gas state condition (Hedestrand, 1929).

[Debye, 1912][Böttcher, 1973]

2.3.4 The modified Clausius-Mossotti and Debye equation according to Leuenberger

The essential point of the original derivation of the Clausius-Mossotti-Debye equation consisted in the fact that the local mean field E_i being the result of short range Van der Waals interactions and of hydrogen bonding of neighbouring molecules was neglected. The introduction of the term E_i/E with E = applied external electric field leads to the following modification:

$$\frac{\varepsilon - 1}{3 \frac{E_i}{E} + (\varepsilon + 2)} \cdot \frac{M_r}{\rho} = \frac{N_A}{3 \cdot \varepsilon_0} \cdot \left(\alpha + \frac{\mu_g^2}{3 \cdot k \cdot T} \right) \quad (2.16)$$

E_i/E for binary mixtures was calculated according to the following Eq. (2.17).

$$\frac{E_i}{E} = \frac{M_{r,m}}{3 \cdot \rho_m} \cdot \frac{\varepsilon_m - 1}{\frac{N_A}{3 \cdot \varepsilon_0} \left[V_1 \left(\alpha_1 + \frac{\mu_{g,1}^2}{3 \cdot k \cdot T} \right) + V_2 \left(\alpha_2 + \frac{\mu_{g,2}^2}{3 \cdot k \cdot T} \right) \right]} - \frac{\varepsilon_m + 2}{3} \quad (2.17)$$

where ρ_m = density of mixture; $M_{r,m}$ = molecular weight of the mixture; ε_m = measured quasi-static relative dielectric constant for the mixture; V_1 = volume fraction of liquid 1; V_2 = volume fraction of liquid 2.

For calculating the respective contributions of the liquids, their volume contributions are considered. For the description of binary mixtures by means of percolation theory, the volume fractions are used, as they are more meaningful for the characterization of three-dimensional networks than molar fractions.

The **Clausius-Mossotti-Debye equation modified according to Leuenberger** (Stengele et al., 2001) (Eq. (2.16)) can be used to characterize polar liquids. In case of a highly polar liquid such as water the value of E_i/E is -21.0 at room temperature. The parameter E_i/E is temperature dependent and can be modeled as follows:

$$\frac{E_i}{E} = -|m| \cdot \left(\frac{1}{T} \right) + b \quad (2.18)$$

Interestingly an empirical relationship between $|m|$ and the Hildebrand solubility parameter (δ) could be established (Stengele et al., 2001). This relationship has to be judged with caution as it is often neglected that δ is temperature dependent. The values of δ which are listed in tables such as in the book of Barton (Barton, 1991) are estimated values valid at room temperature. The slope $|m|$ on the other hand is a temperature independent parameter. If the temperature T is kept constant, the parameter $(|m|/T)$ is a constant, too, and the correlation between the Hildebrand solubility parameter (δ) and $(|m|/T)$ is still valid. One can expect that as a consequence the value

E_i/E at room temperature may directly yield a good correlation with the total Hildebrand solubility parameter (δ_t). Thus it should be possible to find an empirical relationship between the values of E_i/E and the total Hildebrand solubility parameter (δ_t) at room temperature. This evaluation will be part of the first publication as well as the study of the correlation of E_i/E value with the partial Hansen solubility parameters and structural properties of the polar liquid.

[Stengele et al., 2001]

2.3.5 g -values obtained from the Kirkwood-Fröhlich Equation (Stengele et al., 2001)

Short-range interactions between dipoles are considered by the Kirkwood–Fröhlich Equation (Eq. (2.19)), which was introduced by Kirkwood (Kirkwood, 1939) and further developed by Fröhlich (Fröhlich, 1958).

$$\frac{(\varepsilon - \varepsilon_\infty) \cdot (2 \cdot \varepsilon + \varepsilon_\infty)}{\varepsilon \cdot (\varepsilon_\infty + 2)^2} = \frac{N_A}{9 \cdot \varepsilon_0 \cdot k \cdot T} \cdot \frac{\rho}{M} \cdot \mu_g^2 \cdot g \quad (2.19)$$

Where ε , respectively ε_∞ correspond to the is dielectric constant characteristic for induced polarization, measured at a frequency low enough that both atomic and electronic polarization are the same as in the static field respectively high enough so that the permanent dipoles can no longer follow the field; g is the correlation factor.

The correlation factor g was calculated following the Kirkwood-Fröhlich equation for binary mixtures (Hasted, 1973), using the volume fractions for calculations instead of molar fractions, so that the results are comparable to the values for E_i/E (Section 2.3.4):

$$\frac{(\varepsilon_m - \varepsilon_{\infty,m}) \cdot (2 \cdot \varepsilon_m + \varepsilon_{\infty,m})}{\varepsilon_m (\varepsilon_{\infty,m} + 2)^2} = \frac{N_A}{9 \cdot \varepsilon_0 \cdot k \cdot T} \cdot \frac{\rho_m}{M_{r,m}} \cdot (V_1 \mu_{g,1}^2 + V_2 \mu_{g,2}^2) \cdot g \quad (2.20)$$

The correlation factor g is a measure of intermolecular correlations, considering one dipole surrounded by its z next neighbours:

$$g = 1 + z \langle \cos \phi_{ij} \rangle \quad (2.21)$$

$\langle \cos \phi_{ij} \rangle$ is the average of the cosine of the angle between the two neighboring molecules i and j .

So we find for a parallel alignment of molecules, i.e. $\langle \cos \phi_{ij} \rangle = 1$, $g > 1$, and for an antiparallel alignment, i.e. $\langle \cos \phi_{ij} \rangle = -1$, $g < 1$.

Values for the induced polarization ϵ_∞ are not easily gained through experiment. It may be replaced by the square of the refractive index n , usually measured at $\lambda=598.3$ nm (n_D^2), making use of the Maxwell relation: $\epsilon_\infty = n^2$.

[Fröhlich, 1958] [Kirkwood, 1939]

The Kirkwood–Fröhlich Equation (Eq. (2.19)) is only valid for polar molecules. The value of g is ambiguous, as $g=1$ stands either for an ideal disorder or equal amounts of parallel and antiparallel aligned molecules outweighing each other.

2.3.6 Broadband dielectric spectroscopy

The broad-band dielectric spectroscopy measures as direct data the complex dielectric permittivity (ϵ^*) consisting of the real part (ϵ') and the imaginary part (ϵ''). There are different mathematical models available which describe the relaxation behaviour of a polar liquid. The most simple equation is the Debye equation, which will be described in the next section. To fit the ϵ' , ϵ'' -data in a best way it is also possible to use the Cole-Davidson distribution function or superposition of the Debye function with the Cole-Davidson function.

It is evident to check first whether the application of the Debye equation may be sufficient in order to avoid a distribution with the additional parameter β . Thus, before

using a more complex distribution, which is just “descriptive” it is favorable to analyze 1) the superposition of two Debye-equations 2) to model the relaxation behavior with the Cole-Davidson distribution function and 3) whether a superposition of the Debye-equation with the Cole-Davidson distribution function describes satisfactory the relaxation behavior for the binary mixtures.

It has to be kept in mind that the resulting relaxation times (τ) depend on the mathematical model applied. If the mean corrected R^2 coefficient does not differ significantly for the mathematical models used, it is not possible to make an unambiguous choice of model.

2.3.6.1 The Debye equation for the complex dielectric permittivity (ϵ^*).

The Debye equation describes the behavior of the frequency (ω) dependence of the complex dielectric permittivity $\epsilon^* = \epsilon', \epsilon''$:

$$\epsilon^*(\omega) = \epsilon_\infty + \frac{\epsilon - \epsilon_\infty}{1 + i\omega\tau} \quad (2.22)$$

With ϵ^* = complex permittivity, ϵ = quasi-static dielectric permittivity (dielectric constant at ca. zero frequency) and ϵ_∞ = dielectric permittivity for induced polarization, measured at a frequency low enough that both atomic and electronic polarization are the same as in the static field and high enough so that the permanent dipoles can no longer follow the field ($\omega \rightarrow \infty$), τ = characteristic relaxation time [s^{-1}]. ω = angular frequency [s^{-1}] and i = imaginary unit = $(-1)^{1/2}$.

Eq. (2.22) can be split for the real (ϵ') and imaginary part (ϵ'') of the complex permittivity:

$$\varepsilon'(\omega) = \varepsilon_{\infty} + (\varepsilon - \varepsilon_{\infty}) \frac{1}{1 + \omega^2 \tau^2}, \quad (2.23)$$

and

$$\varepsilon''(\omega) = (\varepsilon - \varepsilon_{\infty}) \frac{\omega \tau}{1 + \omega^2 \tau^2}. \quad (2.24)$$

Eqs. (2.23) and (2.24) can be interpreted as follows: At low frequencies the dipole moment of the polar molecules, i.e. the molecule, orients in the applied electric field. Thus the real part (ε') is approximately constant and the imaginary part (ε'') is close to zero. At a specific ω_{res} the imaginary part (ε'') assumes a maximum value which corresponds to a maximal energy absorption. At higher frequencies the dipole can no longer follow the directions of the external applied field. Thus ε' and ε'' assume rather low values (see Fig. 2.12).

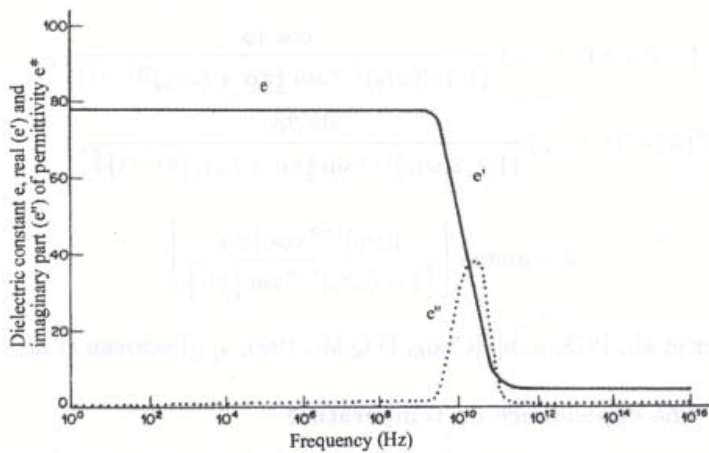


Figure 2. 12 Dielectric permittivity of a polar substance as a function of frequency (after Decareau et al., 1985)

A single relaxation time (τ) is an exception. One has to imagine that all dipoles relax “in phase”, i.e. in a cooperative way i.e. highly synchronized. In fact one has to assume that long- range forces must exist to achieve a high order of its dynamical behavior. In a less organized system more than one relaxation time exists. It may be assumed that the addition of a certain volume percentage of 1,4-dioxane to water may only slightly

modify the water structure, giving rise to more than one single relaxation time. Thus, the case for two relaxation times can be modeled as follows:

$$\varepsilon^*(\omega) = \varepsilon_\infty + (\varepsilon - \varepsilon_\infty) \left\{ \frac{l_1}{1+i\omega\tau_1} + \frac{l_2}{1+i\omega\tau_2} \right\} \quad (2.25)$$

with relaxation times τ_1 , τ_2 and corresponding weights l_1 , l_2 being $l_1 + l_2 = 1$. The following equations and the Cole-Davidson equation represent distribution functions describing a more chaotic behavior of the relaxation process.

2.3.6.2 The Cole-Davidson relaxation behavior and its superposition with the Debye equation

The Cole-Davidson relaxation behavior can be described as follows, taking into account the real and imaginary part:

$$\varepsilon'(\omega) = \varepsilon_\infty + (\varepsilon - \varepsilon_\infty) (\cos \phi)^\beta \cos \beta\phi, \quad (2.26)$$

$$\varepsilon''(\omega) = (\varepsilon - \varepsilon_\infty) (\cos \phi)^\beta \sin \beta\phi, \quad (2.27)$$

$$\text{with } \phi = \arctan(\omega\tau_0). \quad (2.28)$$

In case of $\beta=1$ the Cole-Davidson equation is identical with the Debye-equation (Eq. (2.22)).

It is evident to check first whether the application of the Debye equation may be sufficient in order to avoid a distribution with the additional parameter β . Thus before using a more complex distribution, which is just “descriptive” it is favorable to analyze

1) the superposition of two Debye-equations 2) to model the relaxation behavior with the Cole-Davidson distribution function and 3) whether a superposition of the Debye-equation with the Cole-Davidson distribution function (Eqs. (2.29), (2.30)) describes satisfactory the relaxation behavior for the binary mixtures:

$$\varepsilon'(\omega) = \varepsilon_{\infty} + (\varepsilon - \varepsilon_{\infty}) \left[l_1 \left(\frac{1}{1 + \omega^2 \tau_1^2} \right) + l_2 ((\cos \phi)^{\beta} \cos \beta \phi) \right] \quad (2.29)$$

$$\varepsilon''(\omega) = (\varepsilon - \varepsilon_{\infty}) \left[l_1 \left(\frac{\omega \tau_1}{1 + \omega^2 \tau_1^2} \right) + l_2 ((\cos \phi)^{\beta} \sin \beta \phi) \right] \quad (2.30)$$

With with $\phi = \arctan(\omega \tau_0)$, and $l_1 + l_2 = 1$.

2.4 Solubility parameters: Theory and Application

Solubility parameters provide an easy numerical method of rapidly predicting the extent of interaction between materials, particularly liquids and polymers. They are useful in ensuring the suitability of polymers for practical applications and in formulating blends of solvents for particular purposes.

2.4.1 The Hildebrand Solubility Parameter

The solubility parameter is a numerical value that indicates the relative solvency behavior of a specific solvent. It is derived from the **cohesive energy density** of the solvent, which in turn is derived from the **heat of vaporization**. What this means will be clarified when we understand the relationship between vaporization, Van der Waals forces, and solubility.

VAPORIZATION

When a liquid is heated to its boiling point, energy (in the form of heat) is added to the liquid, resulting in an increase in the temperature of the liquid. Once the liquid reaches its boiling point, however, the further addition of heat does not cause a further increase in temperature. The energy that is added is entirely used to separate the molecules of the liquid and boil them away into a gas. Only when the liquid has been completely vaporized will the temperature of the system again begin to rise. If we measure the *amount* of energy (in calories) that was added from the onset of boiling to the point when all the liquid has boiled away, we will have a direct indication of the amount of energy required to separate the liquid into a gas, and thus the amount of Van der Waals forces that held the molecules of the liquid together.

It is important to note that we are not interested here with the *temperature* at which the liquid begins to boil, but the *amount of heat* that has to be added to separate the molecules. A liquid with a low boiling point may require considerable energy to vaporize, while a liquid with a higher boiling point may vaporize quite readily, or vice versa. What is important is the energy required to vaporize the liquid, called the **heat of vaporization**. (Regardless of the temperature at which boiling begins, the liquid that vaporizes readily has less intermolecular stickiness than the liquid that requires considerable addition of heat to vaporize.)

COHESIVE ENERGY DENSITY

From the heat of vaporization, in calories per cubic centimetre of liquid, we can derive the cohesive energy density (*c*) by the following expression

$$c = \frac{\Delta H - R \cdot T}{V_m} \quad (2.31)$$

where:

c = cohesive energy density, ΔH = heat of vaporization, *R* = gas constant, *T* = temperature, V_m = molar volume

In other words, the cohesive energy density of a liquid is a numerical value that indicates the energy of vaporization in calories per cubic centimetre, and is a direct reflection of the degree of Van der Waals forces holding the molecules of the liquid together.

Interestingly, this correlation between vaporization and Van der Waals forces also translates into a correlation between vaporization and solubility behavior. This is because the same intermolecular attractive forces have to be overcome to vaporize a liquid as to dissolve it. This can be understood by considering what happens when two liquids are mixed: the molecules of each liquid are physically separated by the molecules of the other liquid, similar to the separations that happen during vaporization. The same intermolecular Van der Waals forces must be overcome in both cases.

Since the solubility of two materials is only possible when their intermolecular attractive forces are similar, one might also expect that materials with similar cohesive energy density values would be miscible. This is in fact what happens.

SOLUBILITY PARAMETER

In 1936 **Joel H. Hildebrand** (who laid the foundation for solubility theory in his classic work on the solubility of nonelectrolytes in 1916) proposed the square root of the cohesive energy density as a numerical value indicating the solvency behavior of a specific solvent.

$$\delta = \sqrt{c} = \left[\frac{\Delta H - R \cdot T}{V_m} \right]^{\frac{1}{2}} \quad (2.32)$$

It was not until the third edition of his book in 1950 that the term "**solubility parameter**" was proposed for this value and the quantity represented by a delta (δ).

Subsequent authors have proposed that the term **hildebrands** be adopted for solubility parameter units, in order to recognize the tremendous contribution that Dr. Hildebrand has made to solubility theory.

The SI unit for expressing pressure is the pascal, and SI Hildebrand solubility parameters are expressed in square root of mega-pascals (1 mega-pascal or mpa=1 million pascals). Conveniently, SI parameters are about twice the value of standard parameters:

$$\delta/\text{cal}^{1/2}\text{cm}^{-3/2} = 0.48888 \times \delta/\text{MPa}^{1/2} \quad (2.33)$$

$$\delta/\text{MPa}^{1/2} = 2.0455 \times \delta/\text{cal}^{1/2}\text{cm}^{-3/2} \quad (2.34)$$

[Burke, 1984]

2.4.2 Hansen parameter

Many attempts have been made to extend the solubility parameter approach to polar and hydrogen-bonding systems. The more successful approach proposed by **Hansen** (1967) and was the result of acknowledging that the cohesive energy density is the sum of intermolecular forces consisting of dispersion forces, polar forces involving permanent dipoles, and hydrogen bonding (Eq. (2.35)) with the values of each component being determined empirically on the basis of many experimental observations:

$$\delta_t^2 = \delta_d^2 + \delta_p^2 + \delta_h^2 \quad (2.35)$$

Each of these components can be represented in a three-dimensional solubility parameter (Fig. 2.13) where δ_t is the one-dimensional solubility parameter.

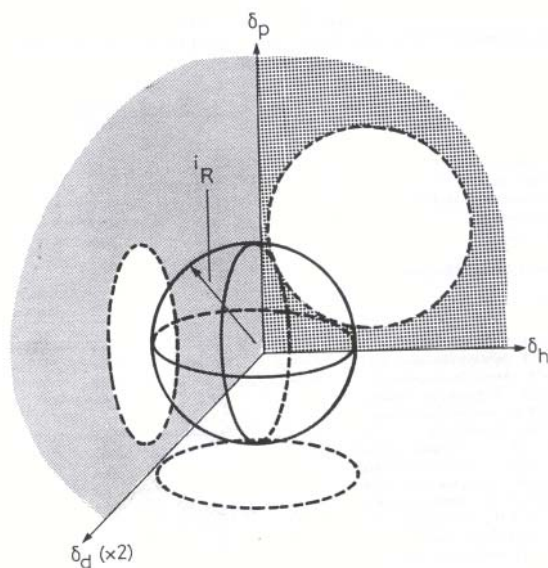


Figure 2. 13 Representation of a Hansen parameter solubility sphere and its projections on three axial planes (Barton, 1991)

Three dimensional solubility parameters have been the subject of much investigation, and tables of these solubility parameters, in particular for common solvents, are available (Beerbower and Dickey 1969; Hansen and Beerbower 1971; Hansen 1972; Barton 1983).

[Barton, 2001]

The parameter E_i/E is temperature dependent and can be modeled as follows:

$\frac{E_i}{E} = -|m| \left(\frac{1}{T} \right) + b$. Interestingly an empirical relationship between $|m|$ and the Hildebrand parameter (δ) could be established $\delta = 2.4|m| + 20348$, $r^2=0.97$. According to Table 2.1, m -values range between 85.20 and -12173.86 (Stengele et al. 2001). This relationship has to be judged with caution as it is often neglected that δ is temperature dependent. The values of δ which are listed in tables such as in the book of Barton (Barton, 1991) are estimated values valid at room temperature. The slope $|m|$ on the other hand is a temperature independent parameter. If the temperature T is kept constant, the parameter $(|m|/T)$ is a constant, too, and the correlation between the Hildebrand solubility parameter (δ) and $(|m|/T)$ is still valid. One can expect that as a

consequence the value E_i/E at room temperature may directly yield a good correlation with the total Hildebrand solubility parameter (δ_t).

Solvent	$(E_i/E) = m(1/T) + b$; squared correlation coefficient R^2		
	m	b	R^2
Benzene	85.2	-0.33	0.783
Benzylalcohol	-620.4	1.52	0.985
Chlorobenzene	-386.6	0.49	0.988
1,4-dioxane	-19.0	0.23	0.759
Ethanol	-2918.9	7.34	0.998
Glycerol	-5606.7	10.28	0.999
1,2-propanediol	-3670.9	7.82	0.999
1-propanol	-1770.5	4.87	0.993
Water	-121 73.86	20.21	0.999

Table 2. 1 The linear regression of (E_i/E) versus ($1/T$) (Stengele et al., 2001)

Thus, it should be possible to find an empirical relationship between the values of E_i/E and the total Hildebrand solubility parameter (δ_t) at room temperature. This evaluation will be part of the first paper as well as the study of the correlation of E_i/E value with the partial Hansen solubility parameters and the Dimroth-Reichardt $E_T(30)$ parameter and structural properties of the polar liquid.

2.5 Application of percolation theory to liquid binary mixtures

Percolation process were first developed by Flory (1941) and Stockmayer (1943) to describe how small branching molecules react and form very large macromolecules in the gelation process, however, the terminology of percolation was presented later by Broadbent and Hammersley (1957). It was not until late eighties that percolation theory found its way to the field of pharmaceuticals (Leuenberger, 1987).

In the framework of this thesis, it is certainly impossible to provide a through introduction to the theory of percolation. For deeper understanding of percolation theory it is therefore recommendable to read basic textbooks on this subject as for example "Introduction of percolation theory" by Stauffer and Aharony (1985) and the PhD Thesis of Kuentz (1999).

It often happens that in order to define a concept, one first presents an example that illuminates the most important features of the problem at hand and then uses the insights gained in this way, to obtain a more formal definition.

This is the path we are going to follow in order to introduce percolation theory. The example we are going to present is inspired from (Stauffer, 1985). The first step is to consider a square lattice, like the one presented in Fig. 2.14. Intuitively it is clear what the meaning of the word lattice. More formally one would say that we consider is a point lattice. Its definition is presented below.

A **point lattice** is an infinite array of discrete points with an arrangement and orientation that appears exactly the same, from whichever of the points the array is viewed.

One can see that the lattice we considered in Fig. 2.14 fulfils this condition. If we imagine the lattice to be infinitely extended in all directions, then all points are equivalent. In this case there is a certain freedom connected to what one could call the points or sites in the lattice. They could be either the squares determined by the gridlines or the points where these lines intersect. For this example we are going to assume the squares to be the relevant entities.

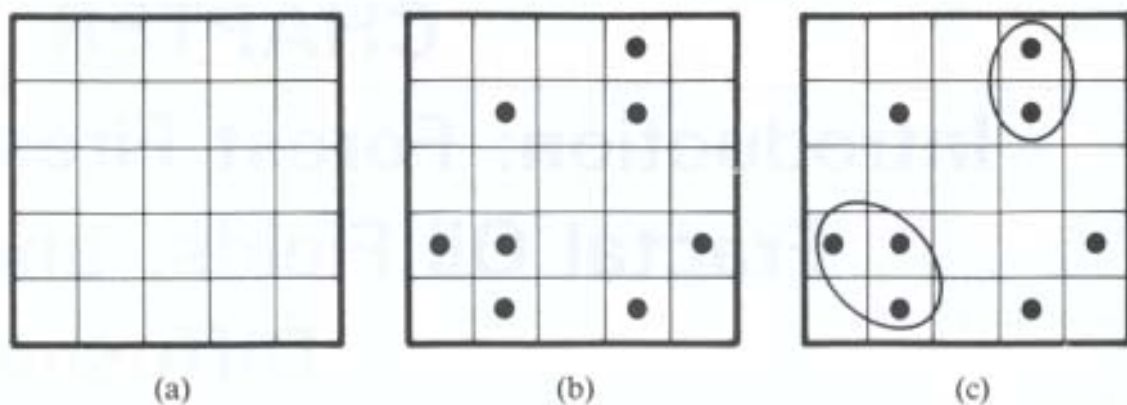


Figure 2. 14 Definition of percolation and its clusters: a) shows parts if a square lattice; in b) some squares are occupied with big dots; in c) the ‘clusters’, groups of neighbouring occupied squares, are encircled except when the ‘cluster’ consists of a single square (Stauffer, 1985).

Let us assume that one places a mark in each of the squares determined by the grid lines with probability p . One possible outcome of such an experiment is presented in Fig. 2.14 (C). One can observe the formation of clusters, which in the present situation are defined as groups of neighboring squares occupied by a dot. Therefore, a **cluster** can be defined as a group of nearest neighboring occupied sites. In the lattice above (Fig. 2.14 c), we have one cluster of size 3 and a cluster of size 2.

One can also observe that the result of the percolation depends on the probability with which each site is occupied. For a low probability a small number of the squares will be occupied. The result might look like the lattice in Fig. 2.15 (A). On the other hand if the probability to occupy one square is high then a big number of squares will be occupied. The result might look like the lattice in Fig. 2.15 (B). An important feature of the second case is the existence of a cluster that connects the top and bottom, left and right sides of the lattice. Such a cluster is called a percolating cluster and its presence represents a qualitative change in the structure of the lattice from a disconnected state to a connected one. As we will see later, such a transition usually suggests an important transformation in the system that is modeled. Moreover, one could ask what is the smallest probability for which a percolating cluster appears and what is its structure?

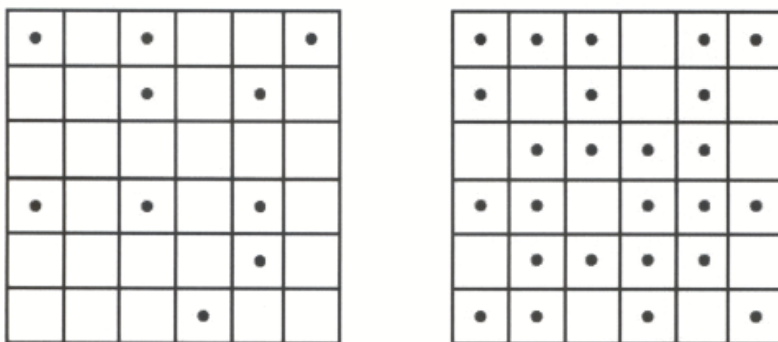


Figure 2. 15 Percolation on a square lattice for two percolation probabilities: a) low probability; b) high probability.

These are typical questions that one can investigate and answer in the framework of percolation theory. It is now an appropriate moment to give the definition that this example prepared.

Percolation theory studies the formation and structure of clusters in a large lattice whose sites or bonds are present with a certain probability.

The example we considered above has an important number of the characteristics of problems approached by percolation theory, but of course it is not the most general situation. The ultimate goal is to restate real life problems in the language of percolation theory, but in order to do such an analysis one needs to expand the model described above. One can easily imagine that percolation on a square lattice will prove fast enough its limitations. Thus the next step we will take is going to expand our model, by considering more general cases of percolation.

In the first place we are going to expand on a feature that we already noticed above. Given a lattice, the relevant entities for the percolation problem can be either the sites or the bonds between the sites. Thus the first distinction we can make is between **site and bond percolation**. As the name suggests the former considers the sites to be the relevant entities, which can be present with probability p , while for the latter the same role is played by the bonds between the sites. Fig. 2.16 presents an example for both site and bond percolation on a square lattice.

In the **bond percolation problem**, the bonds of the network are either *occupied* (i.e., they are open to flow, diffusion and reaction, they are microscopic conducting elements of a composite, etc.), randomly and independently of each other with probability p , or are *vacant* (i.e., they are closed to flow or current, or have been plugged, they are insulating elements of composite, etc.) with probability $1-p$. For a large network, this assignment is equivalent to removing a fraction $1-p$ of all bonds at random. Two sites are called *connected* if there exists at least one path between them consisting solely of occupied bonds. As we defined, A set of connected sites bounded by vacant bonds is called *cluster*. If the network is of very large extent and if p is sufficiently small, the size of any connected cluster is small. But if p is close to 1, the network should be entirely connected, apart from occasional small holes. At some well-defined value of p , there is a transition in the topological structure of the random network from a macroscopically disconnected structure to a connected one; this value is called the **bond percolation threshold**, p_{cb} . This is the *largest* fraction of occupied bonds below which there is no sample-spanning cluster of occupied bonds.

Similarly, in the **site percolation problem** sites of network are occupied with probability p and vacant with probability $1-p$. Two nearest-neighbor sites are called connected if they are both occupied, and connected clusters on the network are again defined in the obvious way. There is a **site percolation threshold** p_{cs} above which an infinite (sample-spanning) cluster of occupied sites spans the network.

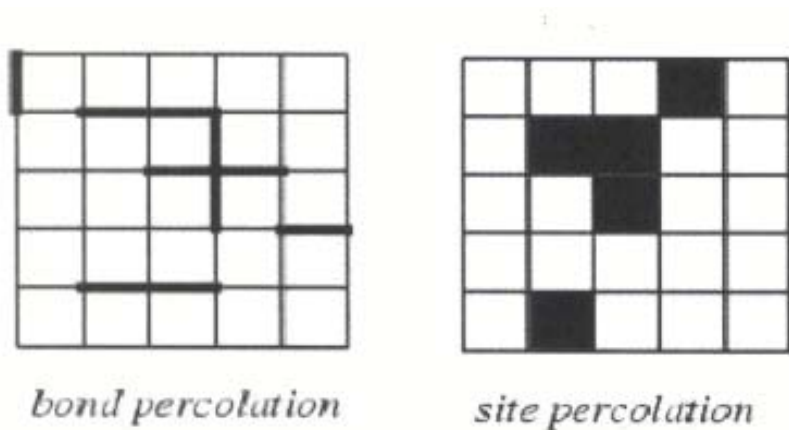


Figure 2. 16 Site and bond percolation on a square lattice Credit for the picture: <http://mathworld.wolfram.com/PercolationTheory.html>, May22, 2003

One can also consider the combined situation in which the sites are occupied with probability p and the bonds between neighboring sites are open with probability x . This corresponds to site-bond percolation, for which an example is presented in Fig. 2.17. In this case we are interested in cluster of occupied sites connected by open bonds.

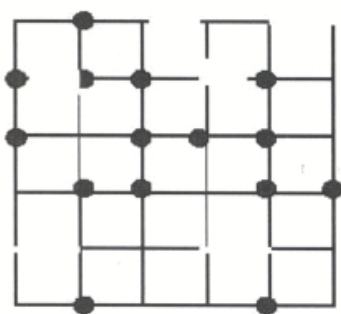


Figure 2. 17 Site-bond percolation on a square lattice

[Stauffer, 1985]

Lattice	Site	Bond	Coordination number z
Honeycomb	0.6962	0.65271	3
Square	0.592746	0.50000	4
Triangular	0.500000	0.34729	6
Diamond	0.43	0.388	4
Simple cubic	0.3116	0.2488	6
BCC	0.246	0.1803	8
FCC	0.198	0.119	12
Bethe	$1/(z - 1)$	$1/(z - 1)$	z

Table 2.2 Site and bond percolation thresholds for different lattices (Sahimi, 1994)

It is also conceivable that percolation thresholds of an ideal system occupied by isometric particles depends on the lattice type, the type of percolation (bond or site) and on the dimension of the lattice (see Table 2.2). In an ideal system the lattice size is extremely large, i.e. infinite compared to the size of a unit lattice cell. Unfortunately, for most of the lattices the percolation thresholds (p_c) cannot be calculated in a straightforward way, but have to be estimated experimentally by computer simulation of such a lattice and its random occupation.

Close to the percolation threshold a property X of the system follows the scaling law of the percolation theory. The following relationship expresses the scaling law:

$$X = S * |p - p_c|^q \quad \text{where } 0 \leq p \leq 1 \quad (2.36)$$

- X = property studied
- p = occupation probability
- p_c = the percolation threshold
- q = the critical exponent
- S = scaling factor

The percolation threshold at $p = p_c$ gives the position of a phase transition where the system changes its behavior qualitatively for one peculiar value of a continuously varying parameter. In the percolation case, if p increases smoothly from zero to unity,

then we have no percolating cluster for $p < p_c$ and (at least) one percolating cluster for $p > p_c$. Thus at $p = p_c$, and only there, for the first time an infinite cluster is formed.

[Stauffer, 1985], [Siegmund et al., 1999], [Sahimi, 1994], [Kirkpatrick, 1973]

Finally, one can leave the two dimensional world of plane lattices and consider lattices in three or even, in general, in d dimensions.

Percolation theory is used in many fields. It can be applied to model forest fires or in the case of the oil industry it can be used as a key issue to predict the amount of oil that a well will produce. Percolation theory can be used in this case as a simple idealized model for the distribution of the oil or gas inside porous rocks or oil reservoirs.

Percolation theory has produced an important number of significant results and continues to be an active area of research. Even though it may not present the final solution to some of the problems it addresses, in conjunction with other techniques, it can offer at least a valid point from which further ideas can be advanced.

[Stauffer, 1985]

In case of a binary mixture between a polar and a nonpolar liquid it is of interest to apply the concepts of percolation theory (Stengele et al., 2002; Stauffer and Aharony, 1998). The binary mixtures of the polar liquids water, methanol and benzylalcohol with 1,4-dioxane are systems of choice in the second publication, as there is a full miscibility due to the formation of hydrogen bonds, despite the fact that the pure components have very different properties. Thus it should be possible to detect percolation phenomena, i.e. percolation thresholds (p_c).

Peyrelasse et al., 1988 studied the conductivity and permittivity of various water/AOT/oil systems (AOT = surfactant active agent = sodium bis(2-ethylhexyl) sulfosuccinate) being able to interpret the results according to the phenomenon of percolation. In a second step they studied the viscosity of those systems and they concluded that the shape of viscosity curves could also be interpreted, at least

qualitatively, in the framework of percolation theory. They also suggested that the phenomenon of percolation must be involved in other physical properties.

The aim of this thesis is to study the phenomenon of percolation in binary solvent mixtures trying to find a connection between different physical properties.

2.6 References

Alonso, M., Finn, E.J., 1992. *Physics*, Addison-Wesley, Reading.

Barton, A.F.M., 1991. *CRC Handbook of Solubility Parameters and Other Cohesion Parameters*, 2nd Ed., CRC Press, Boca Raton.

Böttcher, C.J.F., 1973. *Theory of Electric Polarization, Volumen I: Dielectrics in static fields*, 2nd Ed., Elsevier, Amsterdam.

Burke, J., 1984. *Solubility Parameters: Theory and Application*. AIC Book and Paper Group Annual, Ed. Jensen C., Vol.3, 13-58.

Clausius, R.J.E., 1879. *Die mechanische Wärmethorie*, Volume 2, Vieweg, Braunschweig.

Craig, D.Q.M., 1995. *Dielectric analysis of pharmaceutical systems*, Taylor & Francis, London.

Debye, P., 1912. *Einige Resultate einer kinetischen Theorie der Isolatoren*. *Phys. Z.*, 13, 97-100.

Decareau, R.V., Mudgett, R.E., 1985. *Microwaves in the Food Processing Industry*, Academic Press, Orlando.

Fröhlich, H., 1958. *Theory of dielectrics*, Oxford University Press, Oxford.

- Hasted, J.B., 1973. Aqueous dielectrics, Chapman and Hall, London, pp. 176-203.
- Kirkpatrick, S., 1973. Percolation and conduction, Rev. Mod. Phys., 45, pp. 574-588.
- Kirkwood, J.G., 1939. The dielectric polarization of polar liquids. J. Chem. Phys., 7, 911-919.
- Kuentz, M.T., 1999. Mechanical properties of pharmaceutical polymer tablets: modelling by taking into account the theory of percolation. PhD thesis, University of Basel, Switzerland.
- Leuenberger, H., Rohera, B.D., Hass, C., 1987. percolation theory: a novel approach to solid dosage form design. Int. J. Pharm. 38, 109-115.
- Lorentz, H.A., 1909. Theory of electrons, Teubner, Leipzig.
- Lower, St., 2001.
URL: <http://www.chem1.com/acad/sci/aboutwater.html>
- Mossotti, O.F., 1847. Recherches théoriques sur l'induction électrostatique, envisagée d'après les idées de Faraday. Bibl. Univ. Modena, 6, 193-198.
- Sahimi, M., 1994. Applications of percolation theory, Taylor & Francis, London.
- Schoemaker, D.P., Garland, C.W., Nibler, J.W., 1989. Experiments in physical Chemistry, 5th Ed., McGraw-Hill, New York, pp. 402-418.
- Siegmund, C., Leuenberger, H., 1999. Percolation theory, conductivity and dissolution of hydrophilic suppository bases (PEG-Systems), Int. J. Pharm., 189, 187-196.
- Stauffer, D., Aharony, A., 1985. Introduction to percolation theory, 2nd Ed., Taylor & Francis, London.

Stengele, A., Rey, St., Leuenberger, H., 2001. A novel approach to the characterization of polar liquids. Part 1: pure liquids. *Int. J. Pharm.* 225, 123-134.



Stillinger, F.H., 1982. Low Frequency Dielectric Properties of Liquid and Solid Water. In: Montroll, E.W., Lebowitz, J.L. (Ed.): *Studies in Statistical Mechanics, Volume VIII: The liquid State of Matter: Fluids, Simple and Complex*, North-Holland, Amsterdam, pp. 341-432.

Chapter 3

3. Materials and Methods

3.1 Materials

3.1.1 Solvents

For investigation the following solvents and solvent mixtures were chosen:

Water/1,4-dioxane: the measurement of these two very different substances allows us to investigate a nonpolar/polar mixture. 1,4-dioxane, a cyclic flexible diether, possesses through its symmetry no overall dipole moment, but it is miscible with water due to hydrogen bonding to the exposed oxygen atoms.

Methanol/1,4-dioxane: the measurement of these two very different substances allows us to investigate a nonpolar/polar mixture. 1,4-dioxane, a cyclic flexible diether, possesses through its symmetry no overall dipole moment, but it is miscible with methanol due to hydrogen bonding to the exposed oxygen atoms.

Benzylalcohol/1,4-dioxane: the measurement of these two very different substances allows us to investigate a nonpolar/apolar (but able to form hydrogen bonds due to the OH-group) mixture. 1,4-dioxane, a cyclic flexible diether, possesses through its symmetry no overall dipole moment, but it is miscible with benzylalcohol which possesses due to hydrogen bonding to the exposed oxygen atoms.

In order to know more about the influence of aprotic substances on water structure we investigated **DMSO/water, NMP/water, and acetone/water** binary mixtures. The pure

aprotic liquids: **Sulpholane, acetonitrile, dimethylformamide, dimethylacetamide, methyl ethyl ketone, tetrahydrofuran and ethyl acetate** were also investigated.

In order to know more about the influence of side chains and OH-groups, **methanol/water**, (compared with ethanol/water), **diglycerol/water** (compared with glycerol/water), and **PEG200/water** were investigated. **PEG 300, PEG 400 and PEG 600** were also investigated.

All mixtures and pure liquids were investigated at room temperature.

The physical properties of these compounds are described below.

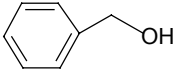
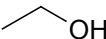
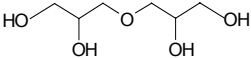
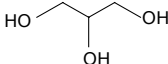
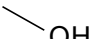
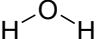
Substance	Benzylalcohol	Ethanol	Diglycerol	Glycerol	Methanol	PEG200	Water
						$\text{HO}-\left[\text{CH}_2-\text{CH}_2-\text{O}\right]_n-\text{H}$ n=4	
CA registry number	100-51-6	64-17-5	59113-36-9	56-81-5	67-56-1	25322-68-3	7732-18-5
Molecular formula	C ₇ H ₈ O	C ₂ H ₆ O	C ₆ H ₁₄ O ₅	C ₃ H ₈ O ₃	CH ₄ O	—	H ₂ O
Molecular weight mw [g/mol]	108.10	46.07	166.20	92.10	32.04	190-210	18.02
Density ρ [kg/m ³]	1.04127	0.78504	1.28000	1.25829	0.78664	1.12088	0.99705
Static permittivity ε	13.10	24.30	34.20	42.50	32.63	19.89	78.54
Dipole moment μ _{Gas} [D]	1.71	1.69	3.18	2.60 ¹	1.70	3.28	1.85
Molecular polarizability α' [-10 ⁻³⁰ m ³]	0.13	5.13	0.15	8.13	3.28	0.20	1.47
Hildebrand parameter δ / MPa ^{0.5}	23.80	26.50	—	36.10	29.60	—	47.80

Figure 3. 1 Literature values of some physical properties of the measured solvents at 298.2 K [Barton, 1991], [CRC Handbook of Chemistry and Physics, 1997], [ChemDAT, 2001], [Fluka, 2001], [Merck Index, 1983], [Purohit et al., 1991].

¹ This value was reportedly gained through measurement on the pure liquid or in solution, it is therefore less reliable.

Substance	Acetone	Acetonitile	Dimethylacetamide	Dimethylformamide	DMSO
		$\text{CH}_3\text{-C}\equiv\text{N}$			
CA registry number	67-64-1	75-05-8	127-19-5	68-12-2	67-68-5
Molecular formula	$\text{C}_3\text{H}_6\text{O}$	$\text{C}_2\text{H}_3\text{N}$	$\text{C}_4\text{H}_9\text{NO}$	$\text{C}_3\text{H}_7\text{NO}$	$\text{C}_2\text{H}_6\text{OS}$
Molecular weight mw [g/mol]	58.08	41.05	87.12	73.20	78.13
Density ρ [kg/m ³]	0.791	0.782	0.942	0.94800	1.10000
Static permittivity ϵ	21.01	36.64	38.85	38.25	47.24
Dipole moment μ_{Gas} [D]	2.88	3.93	3.70	3.73	3.96
Molecular polarizability α' [$\cdot 10^{-30} \text{m}^3$]	6.40	4.41	9.62	7.90	7.99
Hildebrand parameter $\delta / \text{MPa}^{0.5}$	20.00	24.40	22.70	24.80	26.70

Figure 3. 2 (continued) Literature values of some physical properties of the measured aprotic solvents at 298.2 K [Barton, 1991], [CRC Handbook of Chemistry and Physics, 1997], [ChemDAT, 2001], [Fluka, 2001], [Merck Index, 1983].

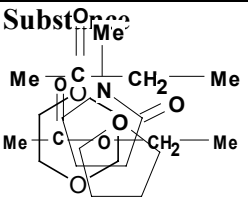
Subst	1,4-dioxane	Ethyl acetate	Methyl ethyl ketone	Methylpyrrolidone	Tetrahydrofuran
					
CA registry number	123-91-1	141-78-6	78-93-3	51013-18-4	109-99-9
Molecular formula	C ₄ H ₈ O ₂	C ₄ H ₈ O ₂	C ₄ H ₈ O	C ₅ H ₉ NO	C ₄ H ₈ O
Molecular weight mw [g/mol]	88.11	88.00	72.11	99.13	72.11
Density ρ [kg/m³]	1.02797	0.90100	0.80490	1.03200	0.88700
Static permittivity ε	2.21	6.08	18.56	32.55	7.52
Dipole moment μ_{Gas} [D]	0.00	1.78	2.78	4.10	1.75
Molecular polarizability α' [$\cdot 10^{-30} \text{m}^3$]	8.60	8.82	8.20	0.11	7.93
Hildebrand parameter δ / MPa^{0.5}	20.50	18.10	19.00	22.90	19.40

Figure 3. 3 (continued) Literature values of some physical properties of the measured aprotic solvents at 298.2 K [Barton, 1991], [CRC Handbook of Chemistry and Physics, 1997], [ChemDAT, 2001], [Fluka, 2001], [Merck Index, 1983].

The described substances were used of the following qualities:

Dioxane puriss. p.a.

Fluka Chemie GmbH CH-9471 Buchs

Article number 42512

Benzylalcohol puriss. p.a.

Fluka Chemie GmbH CH-9471 Buchs

Article number 13160

Dimethyl sulfoxide puriss. p.a.

Fluka Chemie GmbH CH-9471 Buchs

Article number 41644



Methanol pur

Synopharm. Chemische Fabrik Schweizerhall. CH-4013 Basel

Article number 0171960



1-Methyl-2-pyrrolidone puriss. p.a.

Fluka Chemie GmbH CH-9471 Buchs

Article number 69118



Diglycerol

Solvay. Elektrolysespezialitäten GmbH. D-47495 Rheinberg

Article number 211-013-8



Aceton PH.EUR.III

Synopharm. Chemische Fabrik Schweizerhall. CH-4013 Basel

Article number 010 0095



Polyethylenglykol 200

Fluka Chemie GmbH CH-9471 Buchs

Article number 81150

Macrogolum 300 = Pheur.Polyethylenglykol 300

Hänseler A.G. 9101 Herisau

Article number 26-5640-0



Macrogolum 400 = Pheur.Polyethylenglykol 300

Hänseler A.G. 9101 Herisau

Article number 26-5700-2



Polyethylenglykol 600

Fluka Chemie GmbH CH-9471 Buchs

Article number 81180

Water, bidistilled

Freshly prepared by means of Büchi Fontavapor 285

3.1.2 Apparatus

The following apparatus were used for sample preparation and analysis:

Abbé Refractometer

A. Krüss Optronic GmbH D-22297 Hamburg

AR8; 30098

Analytic Balance

Mettler-Toledo AG CH-8606 Greifensee

AT 460 Delta Range; 1115330561

Bidistilling Apparatus

Büchi AG CH-9230 Flawil

Fontavapor 285; 499982

Cylinder Condensator

By courtesy of Ramsden PhD (Mechanische Werkstatt Biozentrum, Universität Basel)

Density Meter

Anton Paar AG A-8054 Graz

DMA 58;8

Digital Thermometer

Haake GmbH D-76227 Karlsruhe

DT 10; -

Pt. 100 platinum resistance thermometer

High-Temperature Dielectric Probe Kit

Agilent Technologies Inc. USA-Palo Alto CA 94304-1185

HP 85070B OPT 002;-

Network Analyser

Agilent Technologies Inc. USA-Palo Alto CA 94304-1185

HP 8720D; US38111202

Precision LCR Meter

Agilent Technologies Inc. USA-Palo Alto CA 94304-1185

HP 4284A; 2940J01533

Thermostat

B. Braun Biotech International GmbH D-34209 Melsungen

Thermomix UB; 852 042/ 9; 9012 498

Frigomix U-1; 852 042/ 0; 8836 004

Test Fixture

Agilent Technologies Inc. USA-Palo Alto CA 94304-1185

HP 16047C;-

Ultrasound Bath

Retsch GmbH & Co. D-42781 Haan

UR 1; 306072082

Vortex Mixer

Scientific Industries Inc. USA-Bohemia NY 11716

G 560-E; 2-48666

Water Bath

Salvis AG CH-6015 Reussbühl

WBR-4; 333127

3.1.3 Computer Software

The following software were used for sample analysis:

HP VEE

Agilent Technologies Inc. USA-Palo Alto CA 94304-1185

Version 5.01

HP 85070B Software Program

Agilent Technologies Inc. USA-Palo Alto CA 94304-1185

Version B.01.05

The following software were used for data analysis:

Excel

Microsoft corp. USA-Redmond WA 98052-6399

Version 97 SR-2

SYSTAT for Windows

SPSS Inc. USA-Chicago IL 60606-6307

Version 7.0

3.2 Methods

3.2.1. Sample preparation

Apparatus Analytic Balance

Mettler-Toledo AG CH-8606 Greifensee
AT 460 Delta Range; 1115330561

Vortex Mixer

Scientific Industries Inc. USA-Bohemia NY 11716
G 560-E; 2-48666

Preparation Samples were prepared by weighing the necessary amounts of solvents/solutes into glass flasks.

The samples were then shaken vigorously for 15 seconds and then stirred for 1 minute using a Vortex mixer.

3.2.2. Measurement of static permittivity and conductivity

3.2.2.1. Measuring principle

The static permittivity and conductivity in this work are measured via the impedance and conductance, respectively, by means of a LCR Meter at a low ac frequency (ν), so the measured permittivity corresponds to the dielectric constant measured in direct current (dc).

LCR meters (inductance (L), capacitance (C), and resistance (R)) measure the impedance of a material at specific frequencies. The impedance (Z) is defined as the total opposition a device or circuit offers to the flow of an alternating current at a given frequency (ν). It is a complex expression

$$Z = R + iX = |Z| e^{i\theta}, \quad (3.1)$$

$$X = 2\pi\nu L \quad (3.2)$$

Z = impedance [Ω]

R = resistance [Ω]

X = reactance [Ω]

θ = phase of impedance

L = inductance [H]

ν = frequency

The reciprocal of impedance is the admittance (Y)

$$Y = G + iB = |G| e^{i\delta} = \frac{1}{Z} = \frac{1}{R + iX} \quad (3.3)$$

$$B = 2\pi\nu C_{MUT}. \quad (3.4)$$

Y = admittance [S]

G = conductance [S]

B = susceptance [S]

δ = phase of admittance, dielectric loss angle

C = capacitance [F]

The static permittivity ε - for $\nu \ll \nu_{rel}$ - equals the real part of the permittivity

$$\varepsilon' = \frac{C_{MUT}}{C_{vacuum}}. \quad (3.5)$$

ε' = real part of permittivity ε^*

C_{MUT} = capacitance of material under test [F]

C_{vacuum} = capacitance of vacuum [F]

In the present work, the measured C_{air} is substituted for C_{vacuum} , the calculated values for ϵ are corrected via a calibration curve (equation 3.10).

The tangent of δ is called the dielectric dissipation factor,

$$\tan \delta = \frac{G}{|B|} = \frac{G}{2\pi\nu C_{MUT}}. \quad (3.6)$$

In a parallel circuit, the conductance (G) is reciprocal of the parallel resistance (R_p)

$$G = \frac{1}{R_p}, \quad (3.7)$$

and the specific conductivity (σ)

$$\sigma = K \times G \quad (3.8)$$

K = cell constant [cm^{-1}]

For materials relaxing in the frequency range of the LCR meter (20 Hz – 1 MHz), the imaginary part ϵ'' of the permittivity ϵ^* can be calculated as following:

$$\epsilon'' = \epsilon' \cdot \tan \delta = \frac{1}{R_p \omega C_{vacuum}}. \quad (3.9)$$

$$\omega = 2\pi\nu \quad (3.10)$$

[Agilent Technologies Inc., 1988], [Agilent Technologies Inc., 1994]

3.2.2.2. Apparatus and Measuring Procedure

Apparatus Precision LCR Meter (Agilent Technologies Inc. HP 4284A; 2940J01533), Test Fixture (Agilent Technologies Inc. USA-Palo Alto CA 94304-1185 HP 16047C).

To the test fixture connected:

Cylinder Condensator (by courtesy of Ramsden PhD (Mechanische Werkstatt Biozentrum, Universität Basel)

inner electrode: diameter 12.92mm, height 9.85 mm

outer electrode: diameter 18.74 mm

To the cylinder condensator connected:

Thermostat (B. Braun Biotech International GmbH D-34209 Melsungen: Thermomix UB; 852 042/ 9; 9012 498/ Frigomix U-1; 852 042/ 0; 8836 004), allowing temperature control of ± 0.1 K

The temperature of the cylinder condensator was checked by means of:

Digital Thermometer (Haake GmbH D-76227 Karlsruhe DT 10; -), Pt. 100 platinum resistance thermometer (± 0.1 K)

For the measurement set-up used in this work the capacitance C and the conductance G are measured in a parallel circuit mode [Lehnert, 1992]. As test frequency 100 kHz was chosen, giving stable results and being $10^3 - 10^5$ lower than the relaxation frequencies of the liquids measured in this work.

The measurements were made by means of a personal computer connected to the LCR Meter, using the software HP VEE 5.01 (Agilent Technologies Inc. USA-Palo Alto CA 94304-1185).

Measuring procedure The cylinder condensator is brought to the measuring temperature and filled with sample. 5 minutes after the required temperature is reached, the sample is measured 5 times, waiting for 1 minute after each measurement. Using the

before determined capacitance of the empty condensator and the calibration curve (equation 3.10), the static permittivity is calculated.

3.2.2.3. Accuracy and reproducibility of the measurement

Accuracy Due to the effects of boundary fields, the cylinder condensator is to be calibrated. The calibration is performed by measuring pure solvents of known static permittivities at 298.2 K.

Taking the geometry of the condensator into consideration, the calibration curve is

$$\epsilon_{\text{lit}} = 2.7394 \cdot \epsilon_{\text{exp}} - 1.8031 \quad r^2=1.000. \quad (3.11)$$

Solvent	ϵ_{exp}	ϵ_{lit}^1
n-pentane	1.324	1.836
cyclohexane	1.379	2.015
tetrachlormethane	1.471	2.228
1,2-dichlorethane	4.438	10.360
1-propanol	8.093	20.100
methanol	12.482	32.630
water bidest.	29.340	78.540

Table 3. 1: Literature and experimental static permittivities of pure solvents at 298.2 K

The correction of measured values by means of equation (3.11) leads to values for the dielectric constant of good accuracy (see Table 3.2) compared to literature values. In this work, ϵ will stand for experimental values corrected with equation (3.11).

Reproducibility The values for the static permittivity used in this work are based on three measurements per sample. The standard deviations are of the same order of magnitude as those for the nonpolar 1,4 dioxane and for the highly polar, hydrogen-

¹ [Riddick et al., 1972], [CRC Handbook of Chemistry and Physics, 1997]

bonding water listed in Table 3.3. Therefore no further listing of standard deviations for the measured static permittivities is made.

Solvent	$\epsilon_{\text{exp,corr}}$	ϵ_{lit}^1	accuracy
			$\frac{ \epsilon_{\text{lit}} - \epsilon_{\text{exp,corr}} \cdot 100}{\epsilon_{\text{exp}}} [\%]$
benzene	2.30	2.27	1.21
n-butanol	17.82	17.51	1.74
glycerol	42.80	42.50	0.60

Table 3. 2 Accuracy of the corrected values for the static permittivities of pure solvents at 298.2 K.

Temperature[K]	1,4 Dioxane		Water, bidistilled	
	ϵ	rel. STDEV [%]	ϵ	rel. STDEV [%]
290.7	2.260	1.21	82.203	0.35
298.2	2.255	0.62	78.994	0.23
305.7	2.243	0.43	75.904	0.13
313.2	2.226	0.38	72.431	0.50
320.7	2.209	0.34	69.583	0.21
328.2	2.169	1.11	66.327	0.45
335.7	2.145	0.97	63.403	0.34
343.2	2.116	1.33	60.829	0.95

Table 3. 3 Reproducibility of measurements of static permittivity (n=3)

3.2.3. Measurement of complex permittivity

3.2.3.1. Measuring principle

The measuring system consists of a dielectric probe connected to a network analyzer by means of a semi-rigid coaxial cable. An electromagnetic signal is generated by the network analyzer and transmitted into the material under test (MUT) via cable and probe. The signal is reflected by the MUT and its phase and amplitude are compared by the network analyzer to those of the incident e.m. wave.

Both phase and amplitude of the reflected e.m. wave are determined by the intrinsic impedance Z :

$$Z = \sqrt{\frac{\mu^*}{\varepsilon^*}} \quad (3.12)$$

Z = intrinsic impedance [Ω]

μ^* = complex permeability
interaction of a material with a magnetic field

ε^* = complex permittivity
interaction of a material with an electric field

The reflection coefficient Γ of MUT and line is defined as:

$$\Gamma = \frac{Z_{MUT} - Z_{line}}{Z_{MUT} + Z_{line}} \quad (3.13)$$

Γ = reflection coefficient

Z_{MUT} = impedance of sample [Ω]

Z_{line} = impedance of line [Ω]

For calculating ε' and ε'' the S_{11} -parameter is used, the scattering parameter, comparing incident and reflected signal at port 1.

$$S_{11} = \frac{(1 - T^2) \cdot \Gamma}{1 - T^2 \cdot \Gamma} \quad (3.14)$$

T = transmission coefficient

Assuming the sample to be infinite size, we receive for Γ :

$$\Gamma = \frac{Z_{MUT} - Z_{line}}{Z_{MUT} + Z_{line}} = \frac{\sqrt{\frac{\mu^*}{\epsilon^*}} - 1}{\sqrt{\frac{\mu^*}{\epsilon^*}} + 1} \quad (3.15)$$

Assuming the MUT to be non-magnetic ($\mu^* = 1$) we receive:

$$\Gamma = \frac{\sqrt{\frac{1}{\epsilon^*}} - 1}{\sqrt{\frac{1}{\epsilon^*}} + 1} \quad (3.16)$$

In dielectrics the energy absorption is very high, so $T \approx 0$:

$$S_{11} = \frac{(1 - T^2) \cdot \Gamma}{1 - T^2 \cdot \Gamma} = \frac{\Gamma}{1} = \frac{\sqrt{\frac{1}{\epsilon^*}} - 1}{\sqrt{\frac{1}{\epsilon^*}} + 1} \quad (3.17)$$

For calculation of ϵ' and ϵ'' the following relationships are used:

$$|\epsilon^*| = \sqrt{\epsilon'^2 + \epsilon''^2} \quad (3.18)$$

$$\tan \delta = \frac{\epsilon''}{\epsilon'} \quad (3.19)$$

δ = loss angle, phase difference between dielectric displacement and dielectric field

[Agilent Technologies Inc., 1985], [Agilent Technologies Inc., 1993], [Rauxel-Dornik, 1991]

3.2.3.2. Apparatus and Measuring Procedure

Apparatus Network Analyzer

Agilent Technologies Inc. USA-Palo Alto CA 94304-1185

HP 8720D; US38111202

To the Network Analyzer connected:

High-Temperature Dielectric Probe Kit

Agilent Technologies Inc. USA-Palo Alto CA 94304-1185

HP 85070B OPT 002;-

The sample was kept at the required temperature through immersion in:

Thermostat (B. Braun Biotech International GmbH D-34209 Melsungen: Thermomix UB; 852 042/ 9; 9012 498 / Frigomix U-1; 852 042/ 0; 8836 004), allowing temperature control of ± 0.1 K.

The temperature was checked by means of:

Digital Thermometer (Haake GmbH D-76227 Karlsruhe DT 10; -), Pt. 100 platinum resistance thermometer (± 0.1 K)

The measurements were made by means of a personal computer connected to the Network Analyzer, using software HP 85070B Probe Software Program (Agilent Technologies Inc. USA-Palo Alto CA 94304-1185).

Measuring procedure Measurements were made between 0.2 and 20 GHz at 401 frequencies.

The dielectric probe was calibrated at the measurement temperature T_{meas} by air, a metal block, and bidistilled water. The computer software requires a fast performance of these calibration steps which does not allow for an exact temperature adjustment. Therefore, this operation was followed by a calibration refresh procedure, using bidistilled water at

$T_{\text{meas}} \pm 0.1$ K. Calibration and refresh calibration were made before starting measurements at T_{meas} and after every fifth sample.

For measurement, the probe was immersed in the sample, which was brought to T_{meas} by means of a water bath/refrigerator. Special attention has to be paid to avoid air bubbles in the probe and the stability of the coaxial cable. Using the thermostat as a water bath, the sample was stabilized at $T_{\text{meas}} \pm 0.1$ K before starting the measurement.

3.2.3.3. Accuracy and reproducibility of measurement

In order to check accuracy and reproducibility of measurements, air and water at three temperatures were measured three times after the calibration procedure, and compared to literature values. As only few data of high frequency measurements are available in literature, it was decided to use water at 278.2, 298.2, and 283.2 K, as these have only recently been closely reinvestigated by Kaatze (1989).

Frequency [GHz]	Literature		Experimental		Accuracy $\frac{ lit - exp \cdot 100}{exp} [\%]$	
	ϵ'	ϵ''	ϵ'	ϵ''	ϵ'	ϵ''
1.150	85.1	8.56	85.0	9.3	0.12	7.78
1.800	83.7	13.2	83.5	14.1	0.23	6.26
2.786	80.8	19.5	80.2	20.7	0.75	5.68
3.723	76.0	24.6	76.3	26.0	0.35	5.51
5.345	69.8	31.8	68.4	33.0	2.03	3.77
7.762	58.6	37.8	56.4	38.7	3.88	2.20
12.82	38.9	39.2	36.9	39.3	5.38	0.24
15.06	33.6	37.1	31.0	37.6	8.31	1.35
17.35	28.1	35.8	26.4	35.5	6.49	0.80

Table 3. 4 Experimental values of water at 278.2 K compared to those given by Kaatze (1989).

For air, ϵ' should be 1 and ϵ'' 0, invariant of frequency. The measured values were $\epsilon' = 1.02 \pm 0.02$ and $\epsilon'' = 0.03 \pm 0.02$. This shows that while the measurements are well comparable to the theoretical values for air, ϵ'' is more hampered by noise than ϵ' .

The average relative standard deviation for water at 278.2 K is 0.10 % for ϵ' (2.78 % for ϵ''), at 298.2 K is 0.08 % and 2.71 %, and at 283.2 K 0.13 % and 2.74 %. This means that the measurements lead to an excellent reproducibility for ϵ' and to an acceptable reproducibility for ϵ'' , in accordance with the data for typical reproducibility of 1-2.5 % given by Agilent Technologies Inc. (1993).

The accuracy of measurements (see Table 3.4, 3.5, 3.6) lies in general very well in the range given by Agilent Technologies Inc. (1993) of $\epsilon' \pm 5\%$ and $\tan\delta \pm 0.05\%$. Nevertheless, it must be noticed that best accuracy is obtained at room temperature and that in many cases measurements of ϵ' are more accurate than those of ϵ'' .

Frequency [GHz]	Literature		Experimental		Accuracy $\frac{ lit - exp \cdot 100}{exp} [\%]$	
	ϵ'	ϵ''	ϵ'	ϵ''	ϵ'	ϵ''
2.000	77.9	7.57	77.6	7.79	0.40	2.83
2.628	77.1	9.86	77.0	10.11	0.16	2.51
3.773	75.3	14.5	75.6	14.0	0.37	3.55
5.433	73.1	19.3	72.6	19.4	0.62	0.75
6.300	71.2	21.6	70.9	21.9	0.40	1.45
6.958	69.7	23.3	69.5	23.7	0.28	1.48
7.850	67.9	25.6	67.5	25.8	0.62	0.72
8.579	66.8	27.2	65.8	27.4	1.57	0.64
11.73	58.5	32.3	58.1	32.5	0.75	0.71
13.38	54.0	34.0	54.1	34.2	0.19	0.70
16.60	47.0	35.9	46.8	36.0	0.38	0.39
19.02	41.7	36.2	42.0	36.5	0.68	0.70

Table 3. 5 Selection of experimental values of water at 298.2 K compared to those given by Kaatz (1989).

Frequency [GHz]	Literature		Experimental		Accuracy	
	ϵ'	ϵ''	ϵ'	ϵ''	$\frac{ lit - exp \cdot 100}{exp} [\%]$	
7.707	67.2	14.5	66.2	14.7	1.47	1.26
12.47	61.5	21.4	61.3	21.7	0.33	1.37
17.46	56.3	27.2	55.1	26.9	2.13	1.04

Table 3. 6: Experimental values of water at 323.2 K compared to those given by Kaatze (1989).

3.2.4. Measurement of density

3.2.4.1. Measuring principle

The densities are measured by means of a vibrating-tube densimeter (VTB).

A U-shaped tube, both stationary ends anchored, is filled with the sample and brought to out-of-plane oscillations. The resonant frequency of the tube depends on its total mass m_{total} . As the volume V of the vibrating part is fixed through clamping, m_{total} depends on the known mass of the tube m_{tube} and of the density ρ of the sample:

$$m_{total} = m_{tube} + V \cdot \rho \quad (3. 20)$$

The resonance frequency of this measuring system, which can be viewed to consist of an undamped spring with the mass m attached, is described as following:

$$f = \frac{1}{2\pi} \sqrt{\frac{k}{m_{tube} + V \cdot \rho}} = \frac{1}{T^*} \quad (3. 21)$$

k = spring constant

T^* = period of oscillation

The density can be calculated from (3.20):

$$\rho = T^{*2} \cdot \frac{k}{4\pi^2 V} - \frac{m_{tube}}{V} = A^* \cdot T^{*2} - B^* \quad (3.22)$$

Calibration using air and bidistilled water determines the instrument constants A^* and B^* .

[Davis et al., 1992]

3.2.4.2. Apparatus and measuring procedure

Apparatus Density Meter (Anton Paar AG A-8054 Graz: DMA 58; 8)

Measuring procedure We calibrated the apparatus for each measuring temperature every 100 days, as standards are air and bidistilled water used.

The sample is de-gassed in an ultrasound-bath and brought to measurement temperature (water bath/refrigerator).

2ml sample is filled into the tube using a disposable syringe. After stabilization, the indicated period of oscillation is recorded.

3.2.4.3. Accuracy and reproducibility of the measurement

In order to examine the accuracy and reproducibility of density measurements pure solvents were measured three times and the results were compared to literature data.

Accuracy The measurements showed an excellent agreement with literature data [Riddick et al., 1972] (see Table 3.7).

Reproducibility The densities of solvents were measured three times at different temperatures. The reproducibility proved to be independent of the measuring temperature [Rey, 1998]. The values for the density used in this work are based on three measurements per sample and temperature. The standard deviations are of the same order of magnitude as those listed in Table 3.7. Therefore, no further listing of standard deviations for the measured densities are made.

solvent	density _{lit} [kg/cm ³]	density _{exp} [kg/cm ³]	reproducibility Rel. STDEV [%]	accuracy $\frac{ \rho_{lit} - \rho_{exp} \cdot 100}{\rho_{exp}}$ [%]
benzylalcohol	1.04127	1.04135	0.004	0.008
1,4-dioxane	1.02797	1.02829	0.011	0.031
ethanol	0.78504	0.78535	0.007	0.039
toluene	0.86231	0.86193	0.100	0.044
water, bidistilled	0.99705	0.99705	0.002	0.000

Table 3. 7 Experimental values of some pure solvents 323.2 K compared to those given by Riddick (1972).

3.2.5. Measurement of refractive index

3.2.5.1. Measuring principle

When light passes the interface of two substances of different optical densities both its velocity and direction are changed.

The refractive index n of a transparent medium is defined as the relation of the velocity of the light in vacuum c to that in the medium c_M :

$$n = \frac{c}{c_M} \quad (3.23)$$

For practical reasons, the refractive index is determined, using the velocity of light in air instead of in vacuum as reference system. Thus, the absolute refractive index 1.0000.

On condition of medium 1 being the optical less dense material, viz air, the following relationship can be applied:

$$n_2 = \frac{n_1 \sin \alpha}{\sin \beta} \quad (3.24)$$

α = angle of incidence

β = angle of refraction,

the reference system being the normal to the two media's interface.

The refractive index depends on the wave length of the light source, usually it is referred to the D-line of sodium ($\lambda = 589.3 \text{ nm}$) measured at $20.0 \pm 0.5^\circ\text{C}$ (n_D^{20}).

The Abbé Refractometer determines the critical angle of total reflection α_{crit} , i.e. the incident light is fully reflected. The optical denser medium is a glass prism of a known refractive index n_{glass} and α is set at 90° , so (3.23) can be written as:

$$\frac{n_{\text{glass}}}{n_{\text{medium}}} = \frac{\sin 90^\circ}{\sin \beta} = \frac{1}{\sin \beta}, \quad (3.25)$$

$$n_{\text{medium}} = n_{\text{glass}} \cdot \sin \beta \quad (3.26)$$

[Rücker et al., 1992]

3.2.5.2. Apparatus and measuring procedure

Apparatus Abbé Refractometer (A.Krüss Optronic GmbH D-22297 Hamburg; AR8, 30098)

Thermostat (B.Braun Biotech International GmbH D-34209 Melsungen: Thermomix UB; 852 042/9; 9012 498 / Frigomix U-1; 852 212/0; 8836 004)

Measuring procedure

The refractometer was brought to the measurement temperature of $298.2 \text{ K} \pm 0.1 \text{ K}$ by means of the thermostat. 15 minutes after reaching stable temperature, we calibrated the refractometer using freshly bidistilled water. In order to achieve correct values over a broad range of refractive indices, water, tetrachloromethane and toluene were measured before the start of a measurement series; this allowed a correction of the determined values. For measuring, a drop of liquid was brought onto the prism of the refractometer. After 5 seconds, the refractive index was taken three times through bringing a dark bar to the crosshair in the reading field.

3.2.5.3. Accuracy and reproducibility of measurement

The measured refractive indices show excellent reproducibility and accuracy compared to literature values (Table 3.8).

solvent	$n_{\text{D}_{\text{lit}}}$	$n_{\text{D}_{\text{exp}}}$	reproducibility Rel. STDEV [%]	accuracy
				$\frac{ n_{\text{lit}} - n_{\text{exp, corr}} \cdot 100}{n_{\text{exp}}} [\%]$
Methanol	1.3265	1.3267	0.012	0.019
Water, bidistilled	1.3325	1.3325	0.003	0.004
Ethanol	1.3594	1.3594	0.008	0.001
Tetrachloromethane	1.4574	1.4576	0.012	0.015
Toluene	1.4941	1.4939	0.009	0.011

Table 3.8 Accuracy and reproducibility of refractive index measurements (pure liquids at 298.2 K; n=3)

3.2.6. Data analysis

3.2.6.1. Determination of additional physical properties

Physical properties, which were necessary for calculations, such as the dipole moment in the gas phase μ_{g} and the polarizability α of the investigated compounds, were taken from the literature. If they were not reported, they were determined experimentally.

For the dipole moment, highly diluted solutions of the compound in 1,4-dioxane were measured. μ of the pure liquid was approximated through extrapolation of the calculated values of μ for the mixtures to an infinitely diluted solution of the compound, corresponding to $V_{1,4\text{-dioxane}} = 1$ [Rey, 1998].

The polarizability was determined via the Lorentz-Lorenz-equation (2.32) [Rey, 1998].

3.2.6.2. Nonlinear regression of dielectric raw data

Principle In order to find the values for such parameter as the relaxation time τ or distribution parameter α , the raw data $\varepsilon'(\omega)$, $\varepsilon''(\omega)$ of the dielectric relaxation measurements must be fitted to an equation describing the process.

Close attention must be paid to choosing an adequate equation and fitting procedure, and the number of fitting parameters.

Usually a compromise has to be found between a large number of free parameters, offering a most adequate fit of the data, and a small number, providing robust and meaningful results, especially when data of e.g. various water concentrations are to be compared.

Equation	Free parameters
Debye	3 (ε ; ε_∞ ; τ)
Cole-Cole	4 (ε ; ε_∞ ; τ_0 ; α)
Cole-Davidson	4 (ε ; ε_∞ ; τ_0 ; β)
Havrilak-Negami	5 (ε ; ε_∞ ; τ_0 ; β ; α)
2 Debye	5 (ε ; ε_∞ ; τ_1 ; τ_2 ; l_1 ($l_1 + l_2 = 1$))

Table 3. 9 Number of free parameters for equations describing relaxation phenomena [Böttcher et al.,1978; a, b].

The number of free parameter can be reduced through additional measurements (ε at $\nu \ll \nu_{\text{rel}}$) or assumptions made re the values for α , β , ε_∞ . Many pure liquids and binary

mixtures can be adequately described using either the Cole-Cole- or Cole-Davidson-equation [Böttcher et al., 1978].

The choice of equation was based on literature and on the comparison of fit results re correlation coefficient R^2 and overall look.

Two fitting software were compared for evaluation: SYSTAT 7.0 (SPSS Inc., Chicago) and Easy-Fit 2.0 (Prof. Klaus Schittkowski, University of Bayreuth, Germany). The latter allowed a simultaneously fitting of the real and imaginary part of the equation (see equations 2.51, 2.52), but only 100 points (every fourth) could be included. For SYSTAT 7.0, the inclusion of both real and imaginary parts for fitting can be made as the term $(\varepsilon - \varepsilon_\infty)$ occurs in both parts. This allows reformulation of equation (2.50) as:

$$\varepsilon'(\omega) = \varepsilon_\infty + \varepsilon''(\omega) \cdot \cot\beta\varnothing \quad (3.26)$$

$$\varepsilon''(\omega) = (\varepsilon'(\omega) - \varepsilon_\infty) \cdot \tan\beta\varnothing \quad (3.27)$$

The fitting software were compared to each other using a broad selection of data [water (298.2 and 343.2 K), ethanol (298.2 and 343.2 K), glycerol (298.2 K), ethanol/water $V_{H_2O}/V_{total} = 0.07$ (298.2 and 343.2 K), glycerol/water $V_{H_2O}/V = 0.17$ (320.7 K), and dioxane/water $V_{H_2O}/V = 0.30$ (298.2 and 328.2 K)].

Data	r^2	
	SYSTAT 7.0	Easy-Fit 2.0
water, 298.2 K	0.99996	0.99989
water, 343.2 K	0.99997	0.99964
ethanol, 298.2 K	0.99811	0.98801
ethanol, 343.2 K	0.99547	0.99280
glycerol, 298.2 K	0.99860	0.99865
ethanol/water $V_{H_2O}/V_{total} = 0.07$, 298.2 K	0.99811	0.99039
ethanol/water $V_{H_2O}/V_{total} = 0.07$, 343.2 K	0.98697	0.99283
glycerol/water $V_{H_2O}/V_{total} = 0.17$, 320.7 K	0.99860	0.99731

dioxane/water $V_{H_2O}/V_{total} = 0.30$, 298.2 K	0.98805	0.98986
dioxane/water $V_{H_2O}/V_{total} = 0.30$, 328.2 K	0.99104	0.72709

Table 3. 10 Evaluation of fitting software [Stengele, 2002]

Of ten data sets, SYSTAT 7.0 led in 7 cases to better results, both for the values of r^2 and the overall look.

Software Systat for Windows

SPSS Inc. USA-Chicago IL 60606-6307

Version 7.0

Procedure The data, i.e. the mean based on three separate measurements, are fitted to the chosen equation using nonlinear regression (Gauss-Newton with Least Squares estimation).

3.2.6.3. Subdivision of curves into segments by means of nonlinear regression

Principle From theory, we assume that the properties of a binary mixture should behave like the volume-wise addition of the properties if the pure liquids. If deviations from this theoretical assumption occur, the splitting up of the curve onto small number of segments leads to the distinction of percolation thresholds, critical volume fractions, and to a better description of properties of the system. The subdivision of data into a number of segments may be appropriate if the number of segments is small, the mathematical model describing the segments simple, viz straight lines, and if there are sharp transitions between the segments.

[Belman et al., 1969], [Seber et al., 1989]

3.2.6.4. Software

Systat for Windows

SPSS Inc. USA-Chicago IL 60606-6307

Version 7.0

Procedure The data were inspected in order to decide about a suitable number of sub-segments and potential critical concentrations. For the following example (see Table 3.11), three sub-segments seem appropriate with critical values for $x_{crit} \approx 4-6$ and 8-10.

The data were arbitrary split into three straight subsegments around these possible x_{crit} , e.g. the first four points to subsegment A, the next four to subsegment B, the last four to subsegment C. Using nonlinear regression, the data were fitted to the following equation:

$$y = A (m_1x + b_1) + B (m_2x + b_2) + C (m_3x + b_3) \quad (3. 28)$$

The final decision to which segment the data are to be assigned is made considering the correlation coefficient r^2 for the overall fit. For this example, the best fit ($r^2 = 0.9985$) was received for a distribution 5 / 3 / 4 (A: $y = -0.62x + 13.78$; B: $-2.10x + 21.8$; C: $0.35x + 0.25$).

x	y	Data belong to segment		
		A	B	C
1.0	13.0	1	0	0
2.0	12.6	1	0	0
3.0	12.1	1	0	0
4.0	11.4	1	0	0
5.0	10.5	0	1	0
6.0	9.2	0	1	0
7.0	7.1	0	1	0
8.0	5.0	0	1	0
9.0	3.6	0	0	1
10.0	3.5	0	0	1
11.0	4.0	0	0	1
12.0	4.6	0	0	1

Table 3. 11 Subdivision of curves into segments: example

3.3 References

Agilent Technologies Inc., 1985. Materials Measurements: Measuring the dielectric constant of solids with the HP 8510 network analyzer: Product Note 8510-3, Agilent Technologies, Palo Alto. 1985

Agilent Technologies Inc., 1988. HP 4284A Precision LCR Meter Operation Manual, Agilent Technologies, Palo Alto.

Agilent Technologies Inc., 1993. HP 85070M Dielectric Probe Measurement System / HP 85070B High-Temperature Dielectric Probe Kit: Technical Data, Agilent Technologies, Palo Alto.

Agilent Technologies Inc., 1994. The Impedance measurement Handbook: A guide to Measurement Technology and Techniques, Agilent Technologies, Palo Alto.

Barton, A.F.M., 1991. CRC Handbook of Solubility Parameters and Other Cohesion Parameters, 2nd Ed., CRC Press, Boca Raton.

Belman, R., Roth, R., 1969. Curve fitting by segmented straight lines. J. Am. Stat. Assoc., 64, 1079-1084.

ChemDat, 2001. The Merck Chemical Databases, Darmstadt.

URL: <http://www.merck.de/english/services/chemdat/english/index.htm>

CRC Handbook of Chemistry and Physics, 1997. 77th edition, CRC Press Inc. Boca Raton.

Davis, R.S., Koch, W.F., 1992. Mass and Density Determinations. In: Rossiter, B.W., Baetzold, R.C. (Ed.): Physical Methods of Chemistry, Volume VI: Determination of Thermodynamic Properties, New York, pp. 59-62.

Fluka, Laborchemikalien und analytische Reagenzien, 2001/2002. Fluka Chemie GmbH, Buchs.

Merck Index, 1983. 10th edition, Merck & Co. Inc. Rahway.

Purohit, H.D., Sengwa, R.J., 1991. Dipole moment and molecular association in polyethylene glycols. *J. Polym. Mater.* 8, 317-320.

Rauxel-Dornik, M., 1991. Pharmazeutisch - Technologische Untersuchungen über Wechselwirkungen von Arznei Zubereitungen mit Mikrowellen. PhD Thesis, University of Munich, Germany, pp. 15-19.

Rey, St., 1998. Ein Beitrag zur Charakterisierung von polaren binären Lösungsmittelgemischen. PhD Thesis, University of Basel, Switzerland.

Riddick, J.A., Bunger, W.B., 1972. *Techniques of Chemistry, Volume II: Organic Solvents*, 3rd Ed., Wiley, New York.

Rücker, G., Neugebauer, M., Willems, G.G., 1992. *Instrumentelle pharmazeutische Analytik*, 2nd Ed., Wissenschaftliche Verlagsgesellschaft GmbH, Stuttgart, pp. 24-27

Stengele, A., 2002. A contribution to the description of the behavior of polar and hydrogen-bonding liquids. PhD Thesis, University of Basel, Switzerland.

Seber, G.A.F., Wild, C.J., 1989. *Nonlinear Regression*, Wiley, New York, pp. 433-489.

Chapter 4

4 Results and discussion

4.1. Introduction

In this section, we tried to put some light into the structure of liquid mixtures. The following binary mixtures were investigated: diglycerol/water, glycerol/water, methanol/water, ethanol/water, PEG200/water, acetone/water, DMSO/water, NMP/water, water/1,4-dioxane, methanol/1,4-dioxane and benzylalcohol/1,4-dioxane by using parameters such as E_i/E of modified Clausius-Mossotti equation and g -values according to the Kirkwood-Fröhlich equation for low frequency dielectric spectroscopy and relaxation time τ and β distribution parameter for high frequency dielectric spectroscopy. The results and discussion are reported below and data in appendix A, B, C, and D.

In section 4.2 the E_i/E parameter of the modified Clausius-Mossotti equation for the water binary mixtures is analyzed.

In section 4.3 the g -values according to the Kirkwood-Fröhlich equation for the water binary mixtures are analyzed.

The sections 4.4, 4.5, and 4.6 correspond with the three submitted papers. In section 4.4 a detailed study of the E_i/E parameter in the characterization process of polar liquids is performed. The relationship between the values of E_i/E and the total Hildebrand solubility parameter (δ_t) at room temperature, as well as the study of the correlation of

E_i/E value with the partial Hansen solubility parameters for polar liquids is analyzed. In section 4.5 the percolation phenomena is detected in water/1,4-dioxane, methanol/1,4-dioxane and benzylalcohol/1,4-dioxane binary polar liquid mixtures by using broadband dielectric spectroscopy and analyzing the modified Clausius-Mossotti-Debye equation and the relaxation behavior. Finally, section 4.6 collects a wide study of percolation phenomena in DMSO-water binary mixtures. A similar study presented in section 4.4 but for aprotic polar substances is also enclosed.

4.2. E_i/E of the modified Clausius-Mossotti equation for water liquid binary mixtures

The values for E_i/E (Eq. (2.17)) were calculated for the binary mixtures of diglycerol/water, PEG200/water, acetone/water, DMSO/water, NMP/water and methanol/water at 298.2 K and compared with glycerol/water, ethanol/water and 1,4-dioxane/water binary mixtures values obtained from Stengele, 2002. The data are represented in Fig. 4.1 and listed in appendix A.

The data for the investigated pure substances are represented in Table 4.1.

	E_i/E
Diglycerol	-6.16
Glycerol	-8.54
Methanol	-5.26
Ethanol	-2.45
PEG200	-3.11
PEG300	-2.55
PEG400	-2.01
PEG600	-1.62
Acetone	-5.37
DMSO	-13.26
NMP	-8.91
1,4-dioxane	0.22
benzylalcohol	-0.48
water	-20.73

Table 4. 1 Experimental values for E_i/E of the investigated pure solvents at 298.2K.

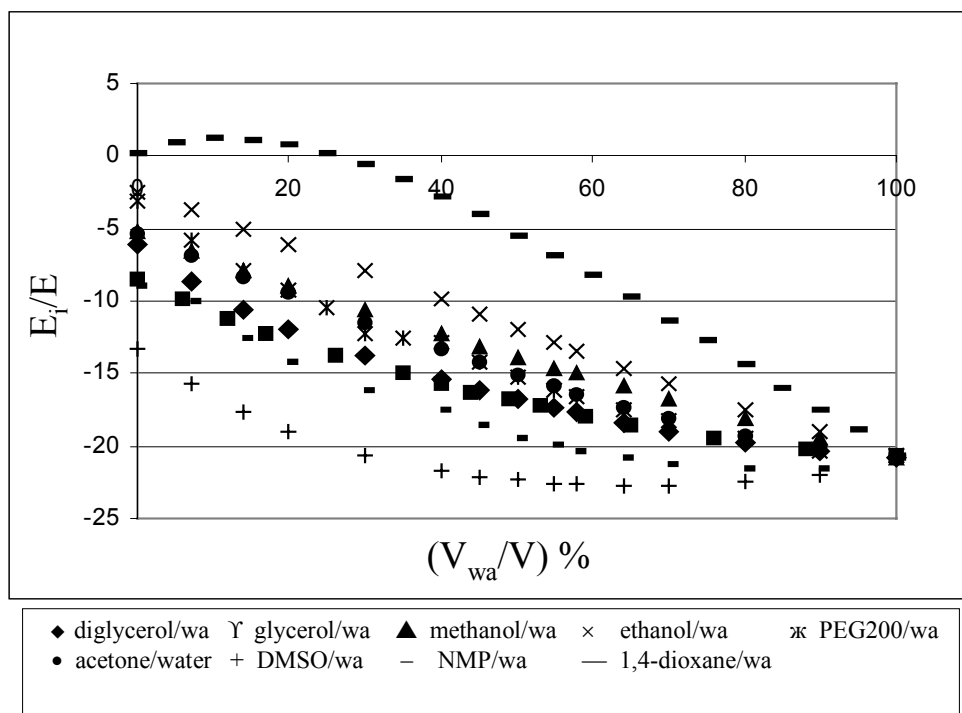


Figure 4. 1 E_i/E -values of the investigated aqueous binary solutions at 298.2 K versus % volume fraction of water (V_{wa}/V).

Pure Liquids:

Water, which possesses $\frac{4}{3}$ ⁱ hydroxy groups, has the highest absolute value for E_i/E of all investigated pure liquids ($E_i/E = -20.73$).

The values for pure **1,4-dioxane** are zero because it is a non-polar solvent with zero dipole moment.

If we compared the two linear alcohols (pure methanol and ethanol), we observe that the E_i/E absolute value for **methanol** is larger ($E_i/E = -5.26$) than the E_i/E absolute value for **ethanol** ($E_i/E = -2.45$) because the size of the non-polar rest in ethanol is larger. Therefore, the intensity of close interaction forces decrease per unit volume.

The value for pure **benzylalcohol** is $E_i/E = -0.48$. Although it has a polar moment similar to methanol the intensity value E_i/E of close interaction forces dominated by dipole-dipole interactions and hydrogen bonds are almost zero due to the fact that here

ⁱ One hydroxy group is able to form 3 hydrogen bonds, two passively and one actively; water is able to build four hydrogen bonds.

the non-polar rest (the benzene ring) is much bigger than in the case of the alcohols investigated.

As a general rule, the value of E_i/E will be larger for liquids forming hydrogen bonds, as the intermolecular interactions between hydrogen bonded groups are stronger than dipole/dipole interactions (Stengele, 2002). After studying the aprotic solvents (see Table 4.1) like for example **DMSO** ($E_i/E = -13.26$) and **N-methylpyrrolidone** ($E_i/E = -8.91$) we see that after water, the highest E_i/E values are found in those solvents, which are not able to form hydrogen bonds in pure state but have a very high dipole moment and dielectric constant. Therefore, the E_i/E values are strongly influenced by the dipole moment. As we will see in Section 4.4 a correlation between the E_i/E parameter and the square of the dipole moment per molar volume $D\mu\mu$ for polar substances in general was found. The same correlation was also found for aprotic substances (see Section 4.6).

We see that the E_i/E absolute value for **glycerol** ($E_i/E = -8.54$) is larger than the E_i/E absolute value for **diglycerol** ($E_i/E = -6.16$) (diglycerol value are less negative) despite having double number of hydroxy groups that could form hydrogen bonding. This can be explained by the fact that the molar volume is much larger in diglycerol so that although it has more OH groups, the molecular interactions will be lower than in glycerol.

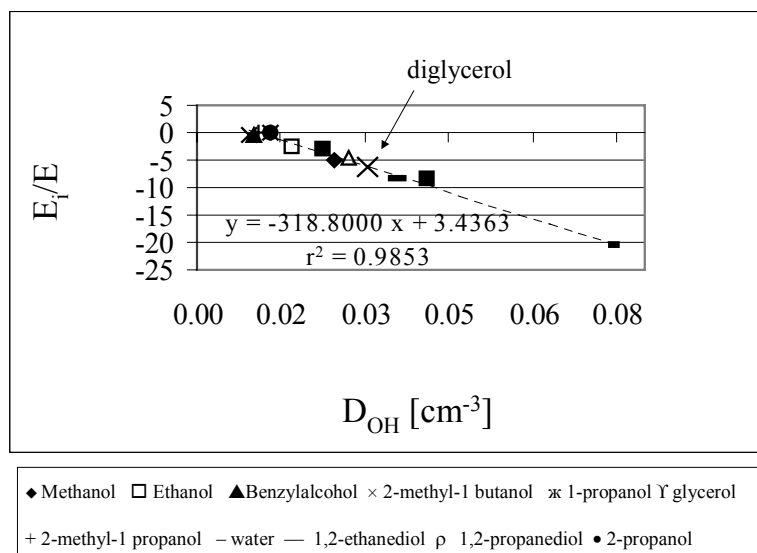


Figure 4. 2 E_i/E values as a function of the density of OH-groups per volume D_{OH} at 298.2 K after including diglycerol.

If we include diglycerol in Fig. 5 (see Section 4.4) we obtain Fig. 4.2. In section 4.4 we observe a correlation between the density of OH-groups per volume (D_{OH}) and E_i/E values. If we include diglycerol inside we can say that diglycerol (4 OH-groups) fits into the straight line but we find it between 1,2-Propanediol (2 OH-groups) and 1,2-Ethandiol (2 OH-groups) following by glycerol with 3 OH-groups. It clearly confirms the correlation between the E_i/E parameter and D_{OH} .

With the polymer **PEG 200** we find not only the OH-groups at the end of the chain, but also oxygen atoms in the chain that can enter into intra -and inter-molecular hydrogen bonding. It has been confirmed by X-ray analysis and theoretical energy calculations that the PEG molecule has a helically coiled chain with wide possibilities of oscillation around the gauche position (Heun and Breitzkreutz, 1994). We were expecting higher E_i/E absolute values for PEG200 but it seems that the E_i/E parameter can better detect the intermolecular association and not the intramolecular interactions.

If we compare PEG200 with other polyethylene glycols of low molecular weight (see Table 4.2 and Figs. 4.3 and 4.4) we see that as we increase the effective degree of polymerization n , the E_i/E values decrease. E_i/E values also decrease when the specific dipole moment μ_{sp} increase. In this context it has to be kept in mind that Purohit et al. 1991 observed that the specific dipole moment μ_{sp} of polyethylene glycols in carbon tetrachloride decreases with the increase of the degree of polymerization and attains a limiting constant value. In this study PEGs with molecular weights between 200 and 9000 were analyzed. Purohit et al. 1991 concluded that this fact can be attributed to the increase in flexibility of the chain due to the coiling as a function of an increased degree of polymerization. The same reasoning could be used to explain the decrease in the E_i/E values. We obtain a good linear relation between E_i/E values and n ($r^2 = 0.93$) as well as for the relation between E_i/E values and μ_{sp} ($r^2 = 0.98$). Further studies are needed to see if E_i/E values reach a constant value when we introduce PEGs with higher molecular weight as it was seen for the relation μ_{sp} with the degree of polymerization.

It can be concluded that whereas E_i/E can be used for describing the close interaction forces, which are dominated by hydrogen bonds and dipole-dipole-interactions, the size

and structure of the nonpolar groups strongly influence the amount and strength of these interactions

	E_i/E values	Effective degree of polymerization n^*	Dielectric constant	Dipole Moment (D)*	Specific dipole moment μ_{sp} (D)*
PEG200	-3.11	4.10	19.89	3.28	1.62
PEG300	-2.55	6.40	16.11	3.91	1.55
PEG400	-2.01	8.70	14.56	4.20	1.42
PEG600	-1.62	13.20	13.88	4.82	1.33

*J.Polym.Mat.8(1991)317-320

Table 4. 2 E_i/E values, effective degree of polymerization, dielectric constant, dipole moment and specific dipole moment ($\mu_{sp}=(\mu^2/n)^{1/2}$) for polyethylene glycols of low molecular weight.

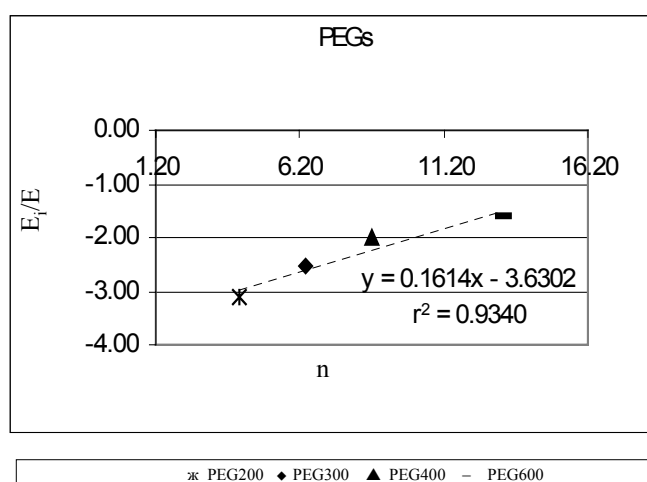


Figure 4. 3 E_i/E values as a function of the effective degree of polymerization n for PEG 200, PEG 300, PEG 400 and PEG 600.

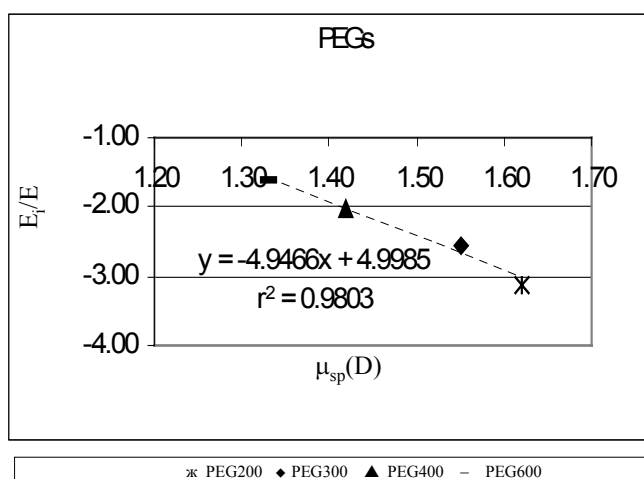


Figure 4. 4 E_i/E values as a function of the specific dipole moment μ_{sp} (D)* for PEG 200, PEG 300, PEG 400 and PEG 600.

Binary mixtures and percolation phenomena:

A splitting of the curves of E_i/E versus the volume fraction of water into segments for diglycerol/water, glycerol/water, methanol/water, ethanol/water, PEG200/water, acetone/water, DMSO/water, NMP/water and 1,4-dioxane/water mixtures is possible:

	diglycerol-water	glycerol-water¹⁾	methanol-water	ethanol-water¹⁾	PEG200-water
R²	1.00	1.00	1.00	1.00	1.00
m₁	-28.66	-19.99	-15.49	-18.54	-28.98
b₁	-6.38	-8.67	-5.80	-2.52	-3.49
m₂	-13.12	-11.59	-	-	-17.48
b₂	-10.04	-11.05	-	-	-6.33
m₃	-4.95	-5.17	-	-	-5.70
b₃	-15.81	-15.53	-	-	-15.06
p % (V_{wa}/V)	24/71	28/70	-	-	25/74
	acetone-water	DMSO-water	NMP-water	1,4dioxane-water¹⁾	
R²	1.00	0.99	1.00	1.00	
m₁	-20.36	-24.37	-25.35	9.60	
b₁	-5.41	-13.79	-8.76	0.30	
m₂	-16.77	-3.22	-12.01	-13.84	
b₂	-6.59	-20.67	-13.10	3.44	
m₃	-7.25	8.61	4.42	-29.93	
b₃	-13.52	-29.45	-25.25	9.52	
p % (V_{wa}/V)	33/73	32/74	35/69	13/38	

Table 4. 3: Parameter of the regression lines $E_i/E = f \% (V_{wa}/V)$ and critical volume fraction of water p % (V_{wa}/V) including data ¹⁾ obtained by Stengele 2002.

In **methanol/water** mixtures the absolute E_i/E values increase linearly as the volume fraction of water increases.

In **ethanol/water** mixtures, the E_i/E values increase linearly as the volume fraction of water increases.

In **diglycerol/water** mixtures the curve can be approximated by divided into three straight lines. The intersections are located at % (V_{wa}/V) = 24 and 71 (over-all R²= 1.00).

In **glycerol/water** mixtures, the curve can be approximated divided into three straight lines. The intersections are located at % (V_{wa}/V) = 28 and 62 (over-all R²= 1.00).

In **PEG200/water** mixtures, the curve can be approximated divided into three straight lines. The intersections are located at % (V_{wa}/V) = 25 and 74 (over-all $R^2= 1.00$).

In **acetone/water** mixtures, the curve can be approximated by divided into three straight lines. The intersections are located at % (V_{wa}/V) = 33 and 73 (over-all $R^2= 1.00$).

In **NMP/water** mixtures, the curve can be approximated by divided into three straight lines. The intersections are located at % (V_{wa}/V) = 35 and 69 (over-all $R^2= 1.00$).

In **DMSO/water** mixtures, the curve can be approximated by divided into three straight lines. The intersections are located at % (V_{wa}/V) = 32 and 74 (over-all $R^2= 1.00$).

In **1,4-dioxane/water** mixtures the E_i/E values increase with increasing slopes as the volume fraction of water increases. In the first segment % (V_{wa}/V) 0 - 13, the increase is very weak, but gets stronger at % (V_{wa}/V) 15 – 38, and increases very sharply at % (V_{wa}/V) 38 – 100.

In the following discussion the results are explained on the basis of percolation theory and on the basis of a structural change of the water structure, which include a change in the coordination number of bonds (“polymorphic effect”). It can be assumed that if the percolation threshold is visible, i.e. that a geometric phase transition occurs, then the coordination number of the structured liquid changes.

In **DMSO/water** mixtures both percolation thresholds can be detected: The lower one at ca. 32% (V_{wa}/V) and the upper one at 74% (V_{wa}/V). It indicates that DMSO can disrupt already at low concentration the normal water structure. DMSO/water mixtures are analyzed in detail in Section 4.6.

In **acetone/water and NMP/water** both percolation thresholds can also be detected. Like with pure liquids, we find higher E_i/E values for the liquids with higher dipole moment and dielectric constant.

In **1,4-dioxane/water** mixtures it was not possible to detect percolation threshold between 38% (V_{wa}/V) and 100% (V_{wa}/V) (see Section 4.4). It was assumed that water

starts to percolate at ca 14% (V_{wa}/V), which is the lower percolation threshold. The upper percolation is not visible, which indicates that 1,4-dioxane fits well into the water, i.e. that there is no structural change. It can be assumed that the volume of a single water cluster with 5 water units has a similar molar weight [$mw = 90.10 \text{ gmol}^{-1}$], and a similar volume as one 1,4-dioxane molecule [$mw = 88.11 \text{ gmol}^{-1}$].

In **methanol/water** binary mixtures we find a linear behavior as it was found for **ethanol/water**, 1-propanol / water and 2-propanol / water binary mixtures. (It can be said that the linearity increase with the size) (Stengele, 2002). If we compare the two slopes we see that for ethanol = -18.54 and for methanol = -15.49. It shows that both lines are almost parallel. We find the difference in the starting values, i.e. in the methanol and ethanol rich region. We start with larger values for methanol than for ethanol. When we arrive to the water rich region we observe that the E_i/E values are almost the same when we compare methanol/water and ethanol/water mixtures. It could be expected that changes of composition and thus changes of structure of the liquid should also be recognizable in nonlinearity of the parameter for close interaction forces E_i/E . This even more so as alcohols with one OH-group are believed to form only two-dimensional chains (Minami et al., 1980), compared to the three dimensional structure of water. A comparable situation can be found for the water rich mixtures of 1,4-dioxane/water, where a linear behavior was detected despite the probability very strong rearrangements taking place. This leads to the interpretation that E_i/E is an indicator for close molecular-molecular interactions, but a differentiation between a structural change of the liquid, and a change of the close interaction may be difficult.

In **glycerol/water and diglycerol/water**, a concave curve is received, suggesting stronger close range interactions in the mixtures than expected. This could mean that in mixtures, a macrostructure might be favored where the nonpolar backbones of glycerol are closely packed together exposing the hydroxy groups. If we compared the binary mixtures of the two polyols we see that the E_i/E values for glycerol/water binary mixtures are larger than the E_i/E values for diglycerol/water binary mixtures (diglycerol values are less negative). One reason could be that the molar volume is much larger in diglycerol so that although it has more OH-groups, the molecular interactions will be lower than in glycerol. Thus, the values of OH-groups per volume have to be compared (see Section 4.4).

4.3. g-values according to the Kirkwood-Fröhlich equation for water liquid binary mixtures

The g-values according to the Kirkwood-Fröhlich equation give us information about the arrangements of the molecules (see Section 2.2.5). It can only be applied to polar molecules as the calculation of g includes a division by μ_g necessary. Thus, it does not make sense to analyze mixtures containing 1,4-dioxane with $\mu_g = 0$. For that reason water/1,4-dioxane mixtures are not analyzed according to the g-values.

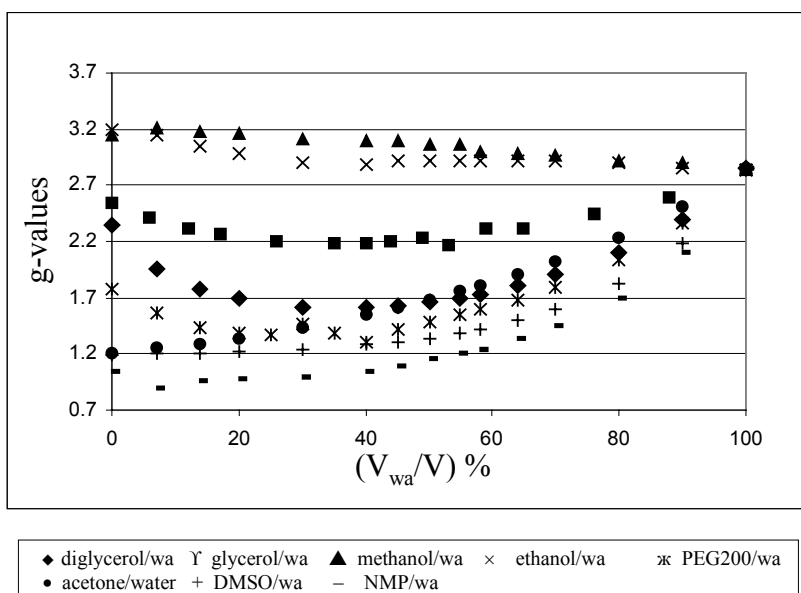


Figure 4. 5 The values of the correlation factor g of the Kirkwood-Fröhlich for the binary mixtures of the investigated liquids. For DMSO/water we find the intersections at ca. 35% and 77% (V_{wa}/V) at 298.2K, and for diglycerol/water binary mixtures at ca. 24% and 75% (V_{wa}/V) at 298.2K.

Unlike polar liquids capable of forming hydrogen bonds (Stengele et al., 2002) such as diglycerol, glycerol and PEG 200 in a mixture with water, the aprotic substances like DMSO and NMP behave differently with respect to the g-values (see Fig. 4.5). In the case of DMSO we find a region nearly constant with g-values close to one till ca. 35% (V_{wa}/V). Thus, there seems to be no structure breaking effect by adding water. Below the lower percolation threshold the water molecules fit well into the aprotic-structure of

the liquid. Due to the value of $g \approx 1$ the water molecules are either randomly distributed in the solvent mixture or in an antiparallel alignment with the dipole moment of the aprotic molecule.

Above the percolation threshold the g -values are increasing i.e. the dipole moments of water and aprotic molecule assume more and more a parallel alignment, a parallel alignment of the dipole moments is being formed due to the increase in the hydrogen bonding formation. From view of percolation theory it could corresponds with the low percolation threshold where water starts to form infinite clusters, both water and the aprotic molecule percolate the system up to ca. 77% (V_{wa}/V) where the second percolation threshold is found. From that point the aprotic molecule starts to form isolated clusters and is no longer percolating the system.

4.4 Towards a better understanding of the parameter E_i/E in the characterization of polar liquids

Graci Hernandez-Perni, Andrea Stengele, Hans Leuenberger*

*Institute of Pharmaceutical Technology, Pharmacenter University of Basel,
Klingelbergstrasse 50, CH-4056 Basel, Switzerland*

4.4.1 Abstract

In the two previous papers (Stengele et al., 2001; Stengele et al., 2002) it was shown, that the Clausius-Mossotti-Debye equation for the quasi-static dielectric constant (ϵ) can be extended to liquids if the parameter E_i/E is introduced. E_i corresponds to the local mean field due to close molecule-molecule interactions after the application of an external electric field E . In the present paper it is demonstrated that the value of E_i/E at room temperature can be 1) related to the density of hydroxy groups and the density of the squared dipole moment per molar volume for polar liquids and 2) also to the total (δ_t) and partial solubility parameter, for polar (δ_p) and hydrogen bond forming molecules (δ_h).

Keywords:

Modification of the Clausius-Mossotti-Debye-Equation; Hildebrand and Hansen solubility parameters; Dimroth-Reichardt E_T parameter; Polar solvent.

* Corresponding author: Tel.: +41-61-267-1501; fax: +41-61-267-1516.

E-mail address: hans.leuenberger@unibas.ch (H. Leuenberger).

4.4.2 Introduction

As it was shown in previous papers (Stengele et al., 2001; Stengele et al., 2002) pure polar liquids can be characterized by the parameter E_i/E of the Clausius-Mossotti-Debye equation modified according to Leuenberger for the quasi-static dielectric constant (Stengele et al., 2001).

In the present paper the emphasis was put on the study of the nature of the parameter E_i/E and its origin in case of pure polar liquids at room temperature.

4.4.3 Theoretical

4.4.3.1 The Clausius-Mossotti-Debye equation modified according to Leuenberger for the quasi-static dielectric constant (Stengele et al., 2001)

The original Clausius-Mossotti-Debye equation is only valid for molecules in the ideal gas phase, i.e. in the case, where the molecules are located far from each other and do not show any interaction:

$$\frac{\varepsilon - 1}{\varepsilon + 2} \frac{M_r}{\rho} = \frac{N_A}{3\varepsilon_0} \left(\alpha + \frac{\mu_g^2}{3KT} \right) \quad (1)$$

with ε = quasi-static relative dielectric constant; M_r = molecular weight; ρ = density; N_A = Avogadro number, 6.023×10^{23} (mol⁻¹); ε_0 = electric field constant in the vacuum, 8.854×10^{-12} (C² J⁻¹ m⁻¹); α = polarizability of the molecule (Cm²V⁻¹); μ_g = dipole moment in the state of an ideal gas (C m); K = Boltzmann's constant, 1.38×10^{-23} (J K⁻¹); T = temperature (K).

The essential point of the original derivation of the Clausius-Mossotti-Debye equation consisted in the fact that the local mean field E_i being the result of short range Van der Waals interactions and of hydrogen bonding of neighboring molecules was neglected. The introduction of the term E_i/E with $E =$ applied external electric field leads to the following modification:

$$\frac{\varepsilon - 1}{3 \frac{E_i}{E} + (\varepsilon + 2)} \frac{Mr}{\rho} = \frac{N_A}{3\varepsilon_0} \left(\alpha + \frac{\mu_g^2}{3KT} \right) \quad (2)$$

The classical Clausius-Mossotti-Debye equation (Eq. (1)) it is not valid for polar liquids but can be used to estimate quite accurately the dipole moment μ_g of water in a highly diluted solution of water in 1,4-dioxane simulating an ideal gas state condition (Hedestrand, 1929).

The Clausius-Mossotti-Debye equation modified according to Leuenberger for the quasi-static dielectric constant (Stengele et al., 2001) (Eq. (2)) can be used to characterize polar liquids. In case of a highly polar liquid such as water the value of E_i/E is -21.0 at room temperature. The parameter E_i/E is temperature dependent and can be modeled as follows:

$$\frac{E_i}{E} = -|m| \left(\frac{1}{T} \right) + b \quad (3)$$

where $|m|$ = absolute value for the slope m of $(E_i/E) = f(1/T)$ and b = intercept from the linear regression $(E_i/E) f(1/T)$.

Interestingly an empirical relationship between $|m|$ and the Hildebrand parameter (δ) could be established (Stengele et al., 2001). This relationship has to be judged with caution as it is often neglected that δ is temperature dependent. The values of δ which are listed in tables such as in the book of Barton (Barton, 1991) are estimated values valid at room temperature. The slope $|m|$ on the other hand is a temperature independent parameter. If the temperature T is kept constant, the parameter $(|m|/T)$ is a constant, too, and the

correlation between the Hildebrand solubility parameter (δ) and ($|m|/T$) is still valid. One can expect that as a consequence the value E_i/E at room temperature may directly yield a good correlation with the total Hildebrand solubility parameter (δ_t). Thus, it should be possible to find an empirical relationship between the values of E_i/E and the total Hildebrand solubility parameter (δ_t) at room temperature. This evaluation will be part of this paper as well as the study of the correlation of E_i/E value with the partial Hansen solubility parameters for polar and hydrogen bond forming molecules (δ_p, δ_h).

4.4.3.2 *Dimroth-Reichardt E_T parameter: an empirical solvent polarity parameter*

The notion of solvent polarity is often used to choose a solvent or to explain solvent effects. With the exception of some mixtures of two solvents, solvent polarity is not conveniently measured either by the dipole moment or by the dielectric constant. However very useful correlations were obtained with empirical solvent polarity parameters (Griffiths and Pugh, 1979; Reichardt, 1979) such as the $E_T(30)$ scale of Dimroth-Reichardt (Reichardt, 1994), Z scale of Kosower (Kosower, 1958) or the π^* scale of Kamlet (Kamlet and Taft, 1976).

$E_T(30)$ values (Reichardt, 1994) are defined as the molar electronic transition energies (E_T) of the *negatively solvatochromic pyridinium N-phenolate betaine dye* (Fig. 1) in a given solvent measured in kilocalories per mol (kcal/mol) at room temperature (25°C) and normal pressure (1 bar), according to Eq. (4). The number (30) was added by its originators in order to avoid confusion with ET, often used in photochemistry as abbreviation for triplet energy.

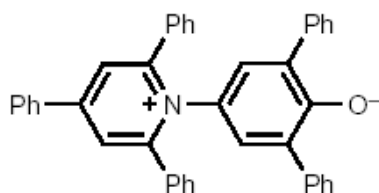


Figure 1: Negatively solvatochromic pyridinium N-phenolate betaine dye

$$E_T(30)(Kcalmol^{-1}) = hc\bar{\nu}_{\max} N_A = (2.8591 * 10^{-3}) \bar{\nu}_{\max} (cm^{-1}) = 28591 / \lambda_{\max} (nm) \quad (4)$$

where $\bar{\nu}_{\max}$ = frequency and λ_{\max} = wavelength of the maximum of the longest wavelength, intramolecular charge-transfer π - π^* absorption band of the negatively solvatochromic pyridinium N-phenolate betaine dye.

In addition, so-called normalized E_T^N values have been introduced (Reichardt, 1994). They are defined according to Eq. (5) as dimensionless figures, using water and tetramethylsilane (TMS) as extreme polar and nonpolar reference solvents, respectively. Hence, the E_T^N scale ranges from 0.000 for TMS, the least polar solvent, to 1.000 for water, the most polar solvent (Reichardt, 1994).

$$E_T^N = \frac{E_T(solvent) - E_T(TMS)}{E_T(water) - E_T(TMS)} = \frac{E_T(solvent) - 30.7}{32.4} \quad (5)$$

A comparison between E_i/E parameter and $E_T(30)$ parameter and also between the E_i/E parameter and the so-called normalized E_T^N values for polar substances will be performed.

4.4.4 Materials and methods

4.4.4.1 Data analysis

The molar volume of a pure liquid is defined as:

$$V_m = \frac{M_r}{\rho} \quad [cm^3/mol] \quad (6)$$

where M_r = molecular weight [$gmol^{-1}$] and ρ = density [gcm^{-3}].

In order to get a parameter, which defines the density of OH-groups per volume (D_{OH}), and the density of the squared dipole moment per molar volume ($D_{\mu\mu}$), the following variables were defined:

$$D_{OH} = \frac{(n^0 OH - groups \text{ per molecule})}{V_m} [\text{cm}^{-3}] \quad (7)$$

$$D_{\mu\mu} = \frac{\mu^2}{V_m} [\text{D}^2 \text{mol/cm}^3] \quad (8)$$

The dipole moment (μ) is given in debye units (D). The conversion factor to SI units is 1 D = 3.33564×10^{-30} C m.

The E_i/E parameter result of the modified Debye equation according to Leuenberger was calculated according to Eq. (2). As the external electric field E varies in a cylinder condenser as a function of the radius r (Frauenfelder and Huber, 1967), it does not make sense to calculate E and to estimate E_i . The values for the polarizability α were calculated using the Lorentz–Lorenz equation (Lorentz, 1880), which gave excellent results compared with literature data (Riddick and Bunger, 1970) both for polar and nonpolar compounds (see Eq. (9)).

$$\frac{n^2 - 1}{n^2 + 2} \frac{Mr}{\rho} = \frac{N_A}{3\epsilon_0} \alpha \quad (9)$$

For the study of the correlation between the parameter E_i/E and the total and partial solubility parameters and also for the correlation between the parameter E_i/E and D_{OH} the data compiled in Table 1 were analyzed.

The squared value of the Hansen parameters was taken according to the Hansen equation (see Eq. (10)).

$$\delta_t^2 = \delta_d^2 + \delta_p^2 + \delta_h^2 \quad (10)$$

For the study of the correlation between the E_i/E parameter and $D_{\mu\mu}$, as well as for the correlation between E_i/E parameter and the $E_T(30)$ parameter and the normalized E_T^N values the data also compiled in Table 1 were analyzed.

Substance	OH -groups	E_i/E - value ¹⁾	D_{OH} (cm^{-3})	²⁾ δ_t^2 (MPa)	²⁾ δ_p^2 (MPa)	²⁾ δ_h^2 (MPa)	²⁾ δ_d^2 (MPa)	$(\delta_p^2 + \delta_h^2)^{1/2}$
Methanol	1	-5.190	0.025	876.160	151.290	497.290	228.010	25.470
Ethanol	1	-2.390	0.017	702.250	77.440	376.360	249.640	21.300
Benzylalcohol	1	-0.570	0.010	566.440	39.690	187.690	338.560	15.080
2-Methyl-1-butanol	1	-0.550	0.009	470.890	20.250	193.210	256.000	14.610
1-Propanol	1	-0.140	0.013	600.250	46.240	302.760	256.000	18.680
2-Propanol	1	-0.100	0.013	552.250	37.210	268.960	249.640	17.500
2-Methyl-1-propanol	1	-0.170	0.011	515.290	32.490	256.000	228.010	16.980
Water	1.33	-20.620	0.074	2284.840	256.000	1789.290	243.360	45.220
1,2-Ethanediol	2	-8.210	0.036	1082.410	121.000	676.000	289.000	28.230
1,2-Propanediol	2	-4.560	0.027	912.040	88.360	542.890	282.240	25.120
1,2-Butanediol	2	-3.110	0.022	n.a	n.a	n.a	n.a	n.a
Glycerol	3	-8.540	0.041	1303.210	146.410	858.490	302.760	31.700
	$D_{\mu\mu}$ (D^2mol cm^{-3})	³⁾ $E_T(30)$ (Kcal mol^{-1})	³⁾ E_T^N					
Methanol	0.071	55.400	0.762					
Ethanol	0.049	51.900	0.654					
Benzylalcohol	0.028	50.400	0.608					
2-Methyl-1-butanol	0.033	48.000	0.534					
1-Propanol	0.032	50.700	0.617					
2-Propanol	0.032	48.400	0.546					
2-Methyl-1-propanol	0.034	48.600	0.552					
Water	0.190	63.100	1.000					
1,2-Ethanediol	0.093	56.300	0.790					
1,2-Propanediol	0.066	54.100	0.722					
1,2-Butanediol	n.a	52.600	0.676					
Glycerol	0.092	57.000	0.812					

Table 1: Physical properties of pure solvents (¹⁾ source: Stengele, 2002; ²⁾ source: Barton, 1991; ³⁾ source: Reichardt, 1994)

4.4.5 Results

4.4.5.1 *The correlation of E_i/E with the total Hildebrand solubility parameter δ_t and the partial Hansen solubility parameters (δ_p , δ_h) at room temperature.*

According to Eq. (3) a linear dependence between E_i/E and $1/T$ exists. The slope m of the Eq. (3) could be correlated to the Hildebrand solubility parameter (δ), more precisely to the total solubility parameter (δ_t). A close inspection of the data obtained (see Table 1) so far leads now to the following result. If T is kept constant it is possible to correlate the parameter E_i/E directly to the Hildebrand solubility parameter (δ_t) with a mean correlation coefficient $r^2 = 0.99$ (Fig. 2, Eq. (11)):

$$E_i/E = -0.01 \delta_t^2 + 5.83 \quad r^2 = 0.99 \quad (11)$$

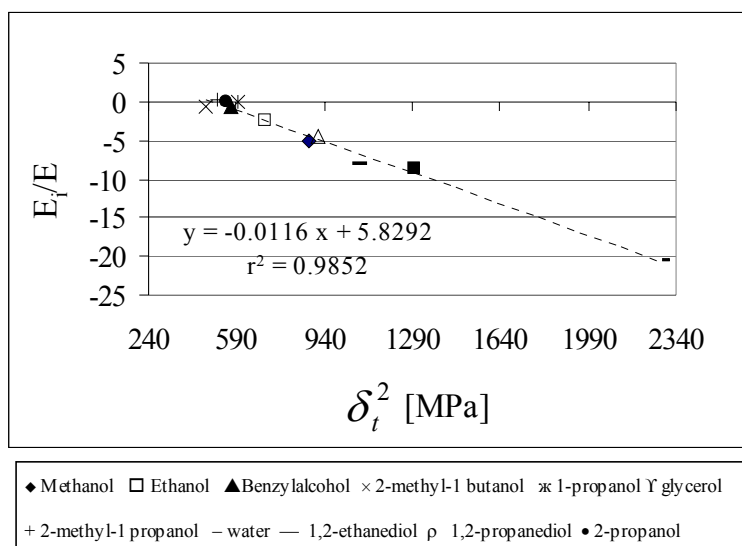


Figure 2: E_i/E values as a function of the squared total Hildebrand solubility parameter δ_t at 298.2K

Interestingly it is also possible to correlate E_i/E directly with the partial Hansen solubility parameter δ_h for molecules being capable to form hydrogen bonds with a $r^2 = 0.98$ (Fig. 3, Eq. (12)).

$$E_i/E = -0.01 \delta_h^2 + 2.53 \quad r^2 = 0.98 \quad (12)$$

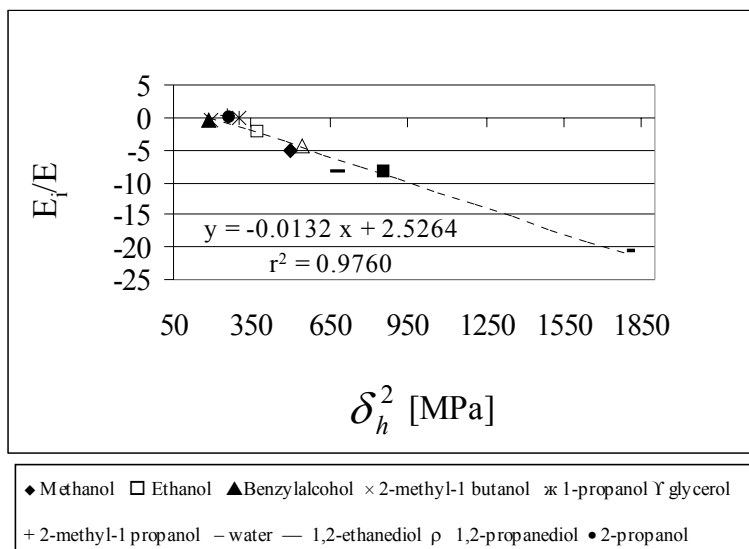


Figure 3: E_i/E values as a function of the squared partial Hansen solubility parameter δ_h at 298.2K

A good correlation is also found between the parameter E_i/E and the partial Hansen solubility parameter δ_p for polar molecules having a dipole moment ($r^2 = 0.92$, Fig. 4, Eq. (13)).

$$E_i/E = -0.08 \delta_p^2 + 3.10 \quad r^2 = 0.92 \quad (13)$$

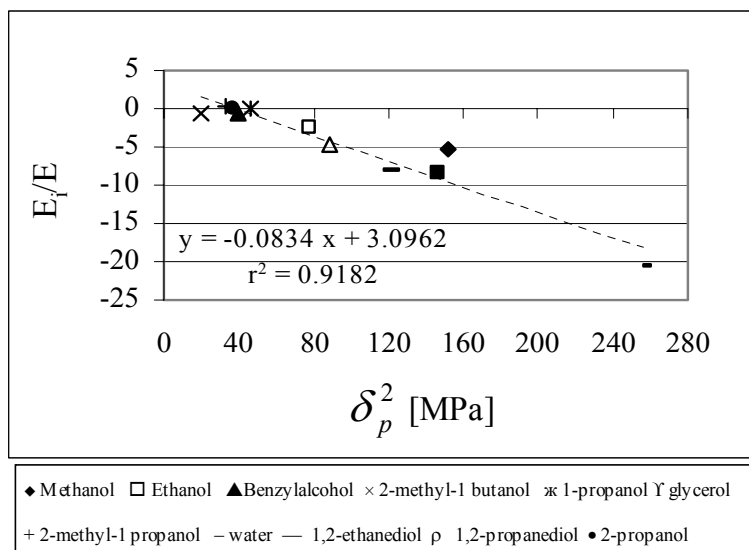


Figure 4: E_i/E values as a function of the squared partial Hansen solubility parameter δ_p at 298.2K

E_i/E can also be correlated with the combined partial solubility parameter $\delta_{hp} = (\delta_h^2 + \delta_p^2)^{1/2}$, which leads to a correlation coefficient of $r^2 = 0.96$.

As E_i/E can be determined rather accurately, a good estimate for the total (δ_t) and partial solubility parameters (δ_p, δ_h) can be obtained. As expected no correlation can be observed with the dispersive partial solubility parameter δ_d ($r^2 < 0.01$).

4.4.5.2 The correlation of E_i/E with D_{OH}

Interestingly the following empirical relationship could be obtained, which correlates the D_{OH} with the value of E_i/E in a polar solvent (see Fig. 5) For this relationship the following correlation coefficient was obtained $r^2 = 0.99$ (Eq. (14))

$$E_i/E = -318.91 D_{OH} + 3.43 \quad r^2 = 0.99 \quad (14)$$

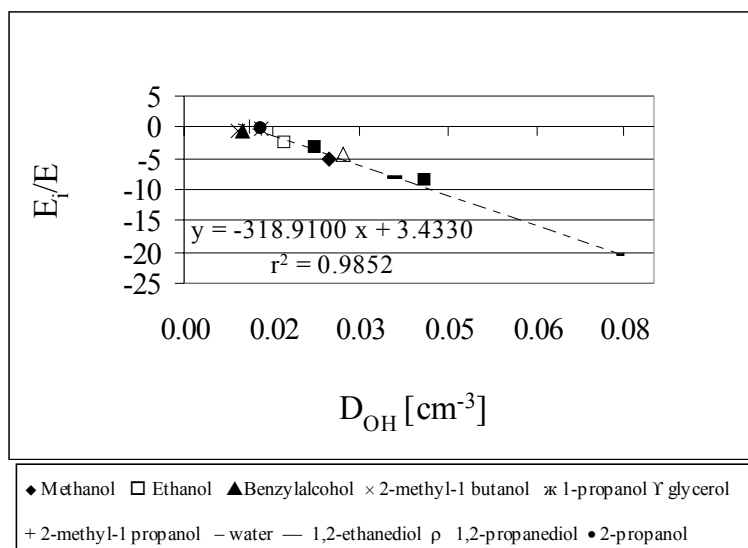


Figure 5: E_i/E values as a function of D_{OH} at 298.2 K

It has to be kept in mind that a correlation of E_i/E with the Hildebrand and Hansen solubility parameters exist and that it is possible to estimate theoretically the solubility parameter δ_t and δ_h with the help of a group number concept, i.e. with group cohesion

parameters (Barton, 1991). The application of this concept is based on the knowledge of the functional groups of the molecule contributing per unit molar volume a specific value to the solubility parameter. Thus, it is not so surprising that the above empirical correlation between D_{OH} of the solvent was found. As a conclusion it can be postulated that the value of E_i/E can be estimated on the basis of a new group number concept, which can be established on the basis of Eq. (14).

4.4.5.3 The correlation of E_i/E with $D_{\mu\mu}$ at room temperature

According to Eq. (15) a linear dependence between E_i/E and $D_{\mu\mu}$ exists (see Fig. 6). However no correlation exists between E_i/E and the dipole moment ($r^2 = 0.16$).

$$E_i/E = -129.20 D_{\mu\mu} + 3.85 \quad r^2 = 0.99 \quad (15)$$

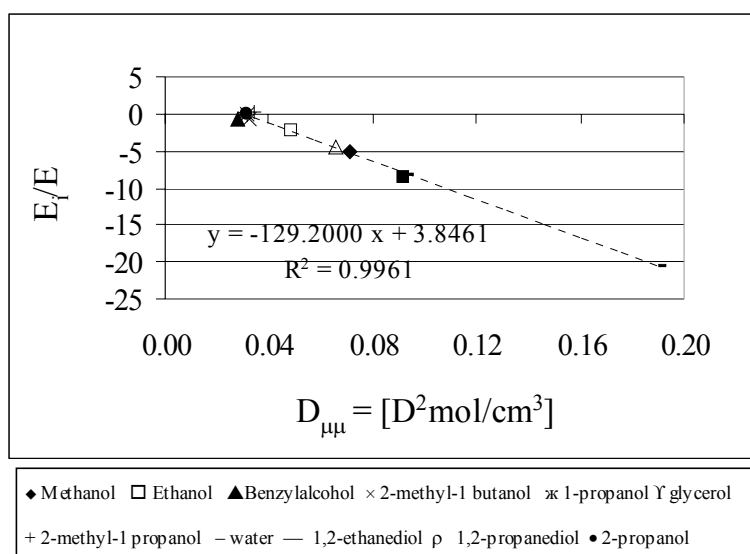


Figure 6: E_i/E values as a function of $D_{\mu\mu}$ at 298.2 K

The squared solubility parameter corresponds to the endoergic process of separating the solvent molecules to provide a suitably sized enclosure for the solute and measures the work required to produce a cavity of unit volume in the solvent. This term is related to the tightness or structuredness of solvents as caused by intermolecular solvent/solvent interactions (Barton, 1991). Therefore, the squared solubility parameter gives us the amount

of Van der Waals forces that held the molecules of the liquid together per molar volume. Therefore, it is not surprising that if a good correlation between E_i/E and the solubility parameter is found (see section 4.4.5.1), it is also possible to find an excellent correlation between E_i/E and $D_{\mu\mu}$ ($r^2 = 0.99$ according to Eq. (15)) as can be expected according to modified Clausius-Mossotti-Debye equation by Leuenberger (see Eq. (2)).

4.4.5.4 The correlation between the D_{OH} and $D_{\mu\mu}$ at room temperature

It could be shown a good correlation ($r^2=0.99$) between D_{OH} and $D_{\mu\mu}$ (see Fig.7 and Eq. (16)).

$$D_{OH} = 0.400 D_{\mu\mu} - 0.001 \quad r^2 = 0.985 \quad (16)$$

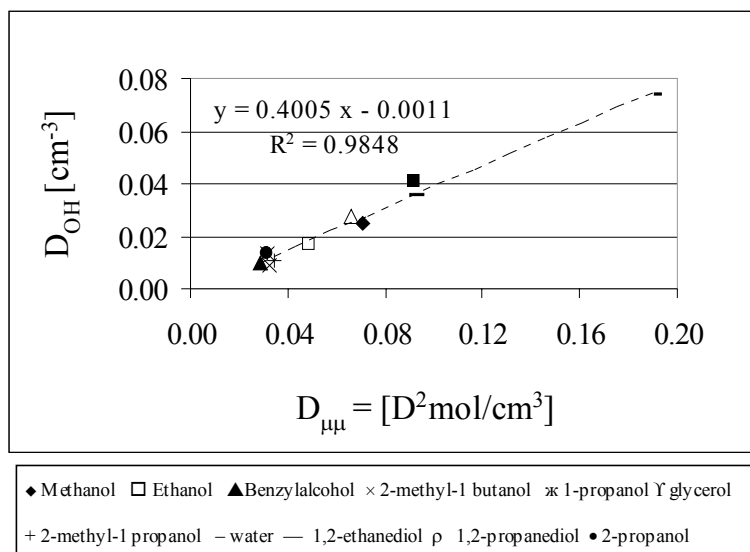


Figure 7: D_{OH} as a function of $D_{\mu\mu}$ at 298.2 K

It indicates that both parameters are to some extent exchangeable.

4.4.5.5. The correlation of E_i/E with the Dimroth-Reichardt $E_T(30)$ at room temperature.

A good correlation (see Eqs. (17), and (18)) is found between the E_i/E parameter and the empirical solvent polarity parameter $E_T(30)$ at room temperature and also between the E_i/E parameter and the normalized E_T^N parameter (see Fig. 8 and 9). That confirms the important role of the E_i/E parameter in the characterization of polar liquids.

$$E_i/E = -1.28 E_T(30) + 63.82 \quad r^2 = 0.92 \quad (17)$$

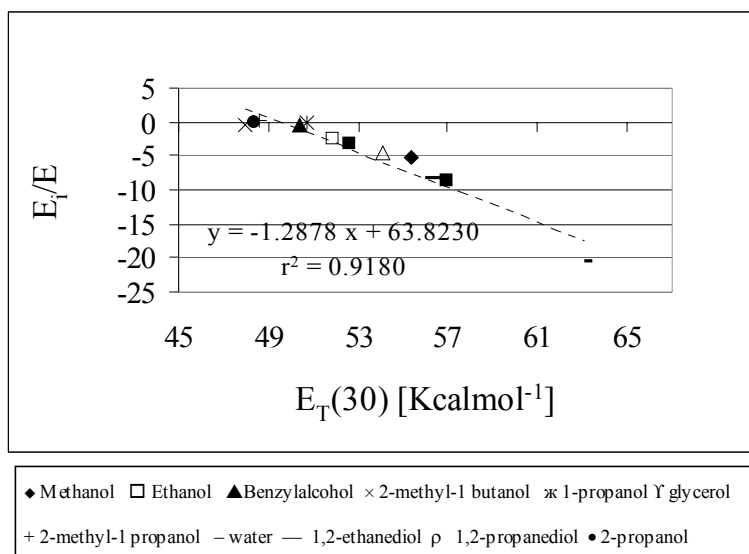


Figure 8: E_i/E values as a function of $E_T(30)$ at 298.2 K

$$E_i/E = -41.70 E_T^N + 24.27 \quad r^2 = 0.92 \quad (18)$$

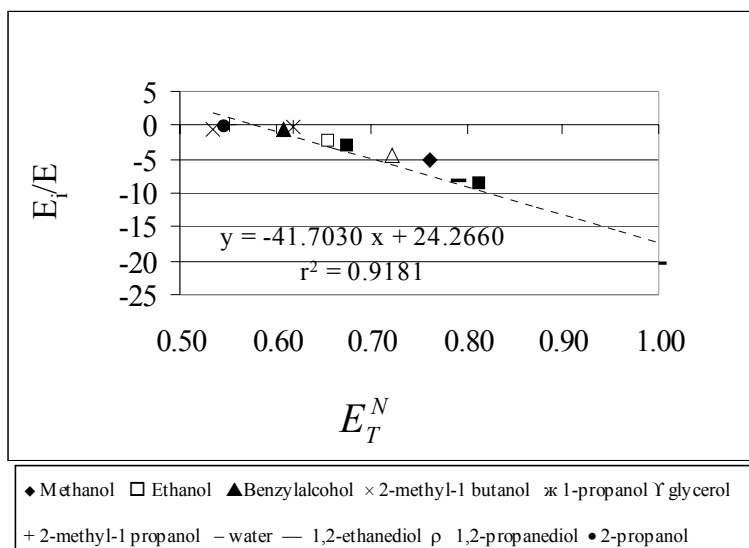


Figure 9: E_i/E values as a function of E_T^N at 298.2 K

4.4.6 Conclusions

An excellent correlation between E_i/E and D_{OH} and D_{μ} could be found. This confirms that E_i/E describes the close range dipolar and hydrogen bonding interactions.

It could also be shown that due to the possibility of determining rather accurately the E_i/E values of polar liquids in both pure liquid and in binary mixtures of different polarities, it is possible without an enormous experimental effort to get a good estimates for the Hildebrand total (δ_t) and for the Hansen partial solubility parameter for polar molecules capable of forming hydrogen bonds (δ_h).

A good correlation between the E_i/E parameter and the empirical solvent polarity parameter $E_T(30)$ could be established showing that the E_i/E parameter are an easily measurable alternative parameter to describe the polarity of liquids.

4.4.7 References

Barton, A.F.M., 1991. CRC Handbook of Solubility Parameters and Other Cohesion Parameters, Second ed. CRC Press, Boca Raton.

CRC Handbook of Chemistry and Physics 77th edition, 1997. CRC Press Inc., Boca Raton.

Frauenfelder, P., Huber, P., 1967. Einführung in die Physik, Band 2, 2. Auflage, Ernst Reinhardt, Basel, pp. 75–77.

Griffiths, T.R., Pugh, D.C., 1979. Correlations among solvent polarity scales, dielectric constant and dipole moment, and a means to reliable predictions of polarity scale values from cu. *Coordn. Chem. Rev.* 29, 129-211.

Hedestrand, G., 1929. Die Berechnung der Molekularpolarisation gelöster Stoffe bei unendlicher Verdünnung. *J. Physik. Chemie Abt. B* 2, 428-444.

Kamlet, M.J., Taft, R.W., 1976. The solvatochromic comparison method. I. The .beta.-scale of solvent hydrogen-bond acceptor (HBA) basicities. *J. Am. Chem. Soc.* 98, 377-383.

Kosower, E.M., 1958. The Effect of Solvent on Spectra. I. A New Empirical Measure of Solvent Polarity: Z-Values. *J. Am. Chem. Soc.* 80, 3253-3260.

Lorenz, L.V., 1880. Ueber die Refraktionsconstante. *Ann. Phys.* 11, 70–103.

Reichardt, C., 1994. Solvatochromic dyes as solvent polarity indicators. *Chem. Rev.* 94, 2319-2358.

Reichardt, C., 1988. Solvents and Solvent Effects in Organic Chemistry, 2nd revision and enlarged edition. VCH, Weinheim.

Riddick, J.A., Bunger, W.B., 1970. Techniques of Chemistry, vol. 2, Third ed. Wiley, New York.

Stengele, A., Rey, St., Leuenberger, H., 2001. A novel approach to the characterization of polar liquids. Part 1: pure liquids. *Int. J. Pharm.* 225, 123-134.

Stengele, A., 2002. A contribution to the description of the behavior of polar and hydrogen-bonding liquids. Ph.D Thesis, University of Basel, Switzerland.

Stengele, A., Rey, St., Leuenberger, H., 2002. A novel approach to the characterization of polar liquids. Part 2: binary mixtures. *Int. J. Pharm.* 241, 231-240.

The Merck Index. 1983. An encyclopedia of chemicals, drugs, and biologicals, 10th ed. Merck & Co., U.S.A

4.5 Detection of percolation phenomena in binary polar liquids by broadband dielectric spectroscopy

Graci Hernandez-Perni, Andrea Stengele, Hans Leuenberger*

Institute of Pharmaceutical Technology, Pharmacenter University of Basel,

Klingelbergstrasse 50, CH-4056 Basel, Switzerland

4.5.1 Abstract

In the previous papers (Stengele et al., 2001; Stengele et al., 2002) it was shown, that the Clausius-Mossotti-Debye equation for the quasi-static dielectric constant (ϵ) can be extended to liquids if the parameter E_i/E is introduced. E_i corresponds to the local mean field due to close molecule-molecule interactions after the application of an external electric field E . In the present paper it is demonstrated that the E_i/E parameter and the relaxation behavior of the dipole moment of the polar molecule in binary mixtures of water, respectively methanol or benzylalcohol with 1,4-dioxane can be used for the detection of percolation phenomena. As 1,4-dioxane has no intrinsic dipole moment but can form hydrogen bonds and is completely miscible with water, respectively methanol or benzylalcohol, percolation phenomena can be related to the relaxation behavior of the dipole moment of the polar co-solvent. The relaxation behavior of the binary mixtures can be modeled by applying the Debye equation, and the Cole-Davidson distribution function. Superpositions such as the Debye equation and the Cole-Davidson distribution function or a sum (Σ_i) of Debye equations are also considered.

Keywords: Broadband dielectric spectroscopy; Percolation phenomena; Modification of the Clausius-Mossotti-Debye equation; Binary polar solvent mixtures.

* Corresponding author: Tel.: +41-61-267-1501; fax: +41-61-267-1516.

4.5.2 Introduction

As it was shown in previous papers (Stengele et al., 2001; Stengele et al., 2002) pure polar liquids can be characterized by the parameter E_i/E of the Clausius-Mossotti-Debye equation modified according to Leuenberger for the quasi-static dielectric constant (Stengele et al., 2001). In the present paper the emphasis was put on the analysis of binary mixtures of a polar liquid with 1,4-dioxane by applying broadband (0.2-20 GHz) dielectric spectroscopy (Kremer and Schönhals, 2003). 1,4-dioxane was chosen as it has no dipole moment and is fully miscible with water, methanol and benzylalcohol due to the formation of hydrogen bonds (The Merck index, 1983). Interestingly, the relaxation behavior of the water dipole can be described in its state as a pure liquid with a single relaxation time τ , i.e. with the Debye equation for the complex permittivity (Smith et al., 1995). Thus, it is of interest to study first the relaxation behavior of the pure liquid and subsequently the change of its behavior as a result of the addition of 1,4-dioxane (V_{dx}/V). One can imagine that the volumetric addition of 1,4-dioxane to water may destroy totally or partially the water structure as a function of the volume percentage of 1,4-dioxane added. It can be speculated that the structure of water is fundamentally changed if 1,4-dioxane starts to percolate the water structure forming itself an infinite cluster. In case of water the question arises immediately whether a discrete number of additional relaxation times $\tau_1, \tau_2, \tau_3 \dots$ show up after a partial destruction of the water structure or whether a continuity of relaxation times appear, which can only be described on the basis of a suitable distribution function such as the Cole-Davidson or the Havriliak-Negami equation (Kremer and Schönhals, 2003). In this paper superpositions such as the Debye and the Cole-Davidson distribution function or a sum (Σ_i) of Debye equations with different but discrete relaxation times τ_i were studied. The aim of this work is to detect percolation phenomena by analyzing the relaxation process and the E_i/E parameter for the binary mixtures of 1,4-dioxane with water, methanol and benzylalcohol.

4.5.2.1 *Broadband dielectric spectroscopy*

4.5.2.1.1 General remarks

The properties of polar solvents in the dipole relaxation region are usually described in terms of complex permittivity $\varepsilon^*(\omega)$:

$$\varepsilon^*(\omega) = \varepsilon'(\omega) - i\varepsilon''(\omega) \quad (1)$$

where $\varepsilon'(\omega)$ = the real part of the permittivity that is proportional to the energy stored reversibly in the system per period and $\varepsilon''(\omega)$ = imaginary part that its proportional to the energy which is dissipated per period.

In a simplest case, when the polarization drop is characterized by only one relaxation time τ , the frequency dependence of the real $\varepsilon'(\omega)$ and imaginary $\varepsilon''(\omega)$ components of complex permittivity $\varepsilon^*(\omega)$ are expressed by the Debye equation (Eq. (4)) which is the most simplest equation but not all the systems show a Debye response. Usually the measured dielectric functions are much broader than predicted by the Debye function. It is therefore useful to consider the developments to the original Debye theory that have been proposed over subsequent years like the Cole-Davidson or the Havriliak-Negami relaxation behavior (Kremer and Schönhals, 2003). As already mentioned, we will also analyze the superposition of two Debye equations and the superposition of Debye equation with the Cole-Davidson distribution function. In this context it has to be kept in mind that the models may yield satisfying mean corrected coefficient R^2 which do not differ from each other very much. Thus, it becomes difficult to make a choice of the best model.

4.5.2.1.2 *The Clausius-Mossotti-Debye equation modified according to Leuenberger for the quasi-static dielectric constant (Stengele et al., 2001)*

The original Clausius-Mossotti-Debye equation is only valid for molecules in the ideal gas phase, i.e. in the case, where the molecules are located far from each other and do not show any interaction:

$$\frac{\varepsilon - 1}{\varepsilon + 2} \frac{M_r}{\rho} = \frac{N_A}{3\varepsilon_0} \left(\alpha + \frac{\mu_g^2}{3KT} \right) \quad (2)$$

With ε = quasi-static relative dielectric constant; M_r = molecular weight; ρ = density; N_A = Avogadro number, 6.023×10^{23} (mol⁻¹); ε_0 = electric field constant in the vacuum, 8.854×10^{-12} (C² J⁻¹ m⁻¹); α = polarizability of the molecule (cm² V⁻¹); μ_g = dipole moment in the state of an ideal gas (C m); K = Boltzmann's constant, 1.38×10^{-23} (J K⁻¹); T = temperature (K).

The essential point of the original derivation of the Clausius-Mossotti-Debye equation consisted in the fact that the local mean field E_i being the result of short range Van der Waals interactions and of hydrogen bonding of neighboring molecules was neglected. The introduction of the term E_i/E with E_i = internal electric field, caused by interactions with other induced neighbouring dipoles; E = external electric field, produced by the applied voltage leads to the following modification:

$$\frac{\varepsilon - 1}{3 \frac{E_i}{E} + (\varepsilon + 2)} \frac{Mr}{\rho} = \frac{N_A}{3\varepsilon_0} \left(\alpha + \frac{\mu_g^2}{3KT} \right) \quad (3)$$

The classical Clausius-Mossotti-Debye equation (Eq. (2)) it is not valid for polar liquids but can be used to estimate quite accurately the dipole moment μ_g of water in a highly diluted solution of water in 1,4-dioxane simulating an ideal gas state condition (Hedestrand, 1929).

The Clausius-Mossotti-Debye equation modified according to Leuenberger for the quasi-static dielectric constant (Stengele et al., 2001) (Eq. (3)) can be used to characterize polar liquids. In case of a highly polar liquid such as water the value of E_i/E is -21.0 at room temperature.

The aim of the present work is to detect percolation phenomena in liquid binary mixtures by analyzing the E_i/E parameter from the Clausius-Mossotti-Debye equation modified according to Leuenberger.

4.5.2.1.3 The Debye equation for the complex dielectric permittivity ε^* .

The Debye equation describes the behavior of the frequency ω dependence of the complex dielectric permittivity $\varepsilon^* = \varepsilon', \varepsilon''$:

$$\varepsilon^*(\omega) = \varepsilon_\infty + \frac{\varepsilon - \varepsilon_\infty}{1 + i\omega\tau} \quad (4)$$

With ε^* = complex permittivity; ε = quasi-static dielectric permittivity (dielectric constant at ca. zero frequency); ε_∞ = dielectric permittivity for induced polarization, measured at a frequency low enough that both atomic and electronic polarization are the same as in the static field and high enough so that the permanent dipoles can no longer follow the field ($\omega \rightarrow \infty$); τ = characteristic relaxation time [s^{-1}]; ω = angular frequency [s^{-1}] and i = imaginary unit = $(-1)^{1/2}$.

Eq. (4) can be split for the real (ε') and imaginary part (ε'') of the complex permittivity:

$$\varepsilon'(\omega) = \varepsilon_\infty + (\varepsilon - \varepsilon_\infty) \frac{1}{1 + \omega^2\tau^2}, \quad (5)$$

and

$$\varepsilon''(\omega) = (\varepsilon - \varepsilon_\infty) \frac{\omega\tau}{1 + \omega^2\tau^2}. \quad (6)$$

Eqs. (5) and (6) can be interpreted as follows: If we consider the behavior of a sample containing mobile dipole which is being subjected to an oscillating electric field of

increasing frequency, in the absence of the field, the dipoles will experience random motion due to thermal energy in the system and no ordering will be present. At low frequencies the dipole moment of the polar molecules, i.e. the entire molecule, orients in the applied electric field. Thus, the real part (ϵ') is approximately constant and the imaginary part (ϵ'') is close to zero. At higher frequencies the dipole can no longer follow the directions of the external applied field. The dipoles are unable to reorientate with that field and the total polarization of the system falls. Thus, ϵ' and ϵ'' assume rather low values (see Fig. 1). However, at a specific frequency called resonance frequency (ω_{res}) located between these two extremes, the efficiency of the reorientation process is at maximum, as the rate of change in direction of the applied field matches the relaxation time of dipoles. Those dipoles will therefore undergo maximum reorientation, but the random oscillations superimposed on that system would be at minimum. At the resonance frequency (ω_{res}) the imaginary part (ϵ'') assumes a maximum value, which corresponds to the frequency of maximum energy absorption.

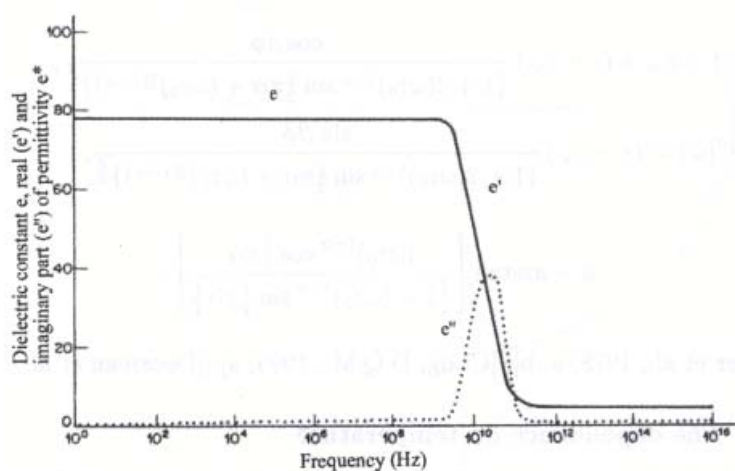


Figure 1: Dielectric permittivity of a polar substance as a function of frequency (Decareau and Mudgett, 1985).

In practice, the Debye relaxation is seldom seen, as systems usually contain more than one relaxation time. In an organized system all dipoles relax “in phase”, i.e. in a cooperative way, highly synchronized. Materials assumed to be composed of clusters would belong to that group of systems where a long range forces must exist to achieve a high order of its dynamical behavior. The relaxation behavior of these clusters will affect the overall shape

of the response, as well as the absolute values at any particular frequency. In a less organized system more than one relaxation time exists. The dipoles of water in its pure state can be described with a single relaxation time. Therefore, it may be assumed that the addition of a certain volume percentage of 1,4-dioxane to water may only slightly modify the water structure leading to more than one single relaxation time.

Thus, the case for two relaxation times τ_1 , τ_2 the real and imaginary part of the Eq. (5), respectively Eq. (6) can be modeled as follows:

The real part being

$$\varepsilon'(\omega) = \varepsilon_\infty + (\varepsilon - \varepsilon_\infty) \left\{ \frac{l_1}{1 + \omega^2 \tau_1^2} + \frac{l_2}{1 + \omega^2 \tau_2^2} \right\} \quad (7)$$

and the imaginary part

$$\varepsilon''(\omega) = (\varepsilon - \varepsilon_\infty) \left\{ \frac{l_1 \omega \tau_1}{1 + \omega^2 \tau_1^2} + \frac{l_2 \omega \tau_2}{1 + \omega^2 \tau_2^2} \right\} \quad (8)$$

with l_1 = weight factor of the relaxation time τ_1 and l_2 = weight factor of the relaxation time τ_2 being $l_1 + l_2 = 1$.

4.5.2.1.4 The Cole-Davidson relaxation behavior and its superposition with the Debye equation

$$\varepsilon^*(\omega) = \varepsilon_\infty + \frac{\varepsilon - \varepsilon_\infty}{(1 + i\omega\tau_0)^\beta} \quad (9)$$

The Cole-Davidson relaxation behavior (Eq. (9)) can be described as follows, taking into account the real and imaginary part:

$$\varepsilon'(\omega) = \varepsilon_\infty + (\varepsilon - \varepsilon_\infty)(\cos \phi)^\beta \cos \beta\phi, \quad (10)$$

$$\varepsilon''(\omega) = (\varepsilon - \varepsilon_\infty)(\cos \phi)^\beta \sin \beta\phi, \quad (11)$$

$$\text{with } \phi = \arctan(\omega\tau_0). \quad (12)$$

where τ_0 = Cole-Davidson relaxation time [s^{-1}], β ($0 < \beta \leq 1$) describes an asymmetric broadening of relaxation function. In case of $\beta=1$ the Cole-Davidson equation is identical with the Debye equation (Eq. (4)).

It is evident to check first whether the application of the Debye equation may be sufficient in order to avoid a distribution with the additional parameter β . Thus, before using a more complex distribution, which is just “descriptive” we analyze first the relaxation behavior with the superposition of two Debye equations (Eqs. (7) and (8)) second the relaxation behavior with the Cole-Davidson distribution function and third whether a superposition of the Debye equation with the Cole-Davidson distribution function (Eqs. (13) and (14)) describes satisfactory the relaxation behavior of the binary mixtures:

$$\varepsilon'(\omega) = \varepsilon_\infty + (\varepsilon - \varepsilon_\infty) \left[l_1 \left(\frac{1}{1 + \omega^2 \tau_1^2} \right) + l_2 ((\cos \phi)^\beta \cos \beta\phi) \right] \quad (13)$$

$$\varepsilon''(\omega) = (\varepsilon - \varepsilon_\infty) \left[l_1 \left(\frac{\omega\tau_1}{1 + \omega^2 \tau_1^2} \right) + l_2 ((\cos \phi)^\beta \sin \beta\phi) \right] \quad (14)$$

with $\phi = \arctan(\omega\tau_0)$, and $l_1 + l_2 = 1$

4.5.2.1.5 Application of percolation theory

Percolation theory (Stauffer and Aharony, 1998) is a mathematical concept that can be applied in many different fields. The starting point is the definition of a *lattice* (see Fig. 2

(A)). In the present case the lattice is formed by substance A (e.g. water, methanol or benzylalcohol). We will increase the amount of substance B (e.g. 1,4-dioxane) in the system formed by substance A and at the same time, different dielectric spectroscopy parameters for each concentration will be measured.

If we start adding substance B we pass from Fig. 2 (A) to Fig. 2 (B). At that point clusters of substance B will appear. A *cluster* is a group of occupied nearest neighbour lattice sites. On Fig. 2 (B) we find two clusters formed by two B-molecules and a cluster of three B-molecules. Those clusters are inserted into the structure of substance A.

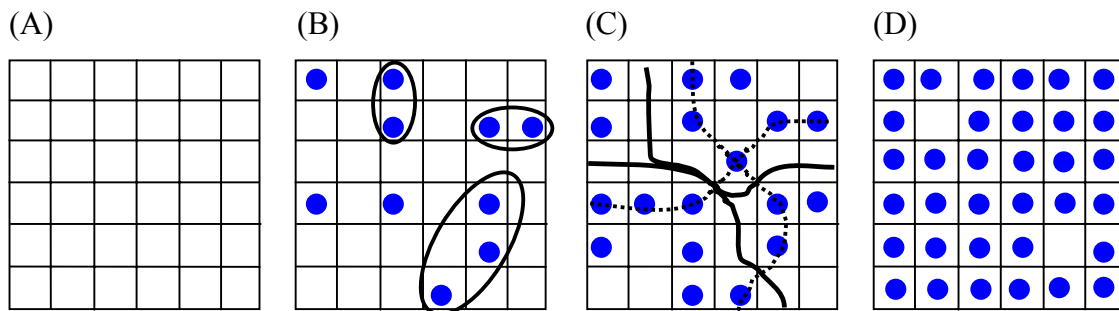


Figure 2: (A)-(D) Percolation on a square lattice.

If we increase the B concentration it arrives a point represented by Fig. 2 (C) where we observe the existence of a cluster that connects the top with the bottom, and the left with the right side of the lattice. On Fig. 2 (C) it is possible to see the infinite cluster for B-molecules in dotted line and the infinite cluster for A-molecules in solid line. We passed from a disconnected state to a connected one. At that concentration we have a *percolation cluster*. B starts to dominate the system. That transition suggests an important transformation of the system and should be therefore detected when we measure different dielectric spectroscopy parameters. That critical concentration is called the *lower percolation threshold* (p_c). Finally and if we add volumetrically more and more B it arrives a critical concentration where the binary system is completely dominated by B and we find the *upper percolation threshold* (p_c) as the component A is no longer percolating and starts to form isolated clusters. That transition also suggests an important transformation of the system and should also be detected when we measure different dielectric spectroscopy parameters. According to the explanation above we have to bear in mind that in three dimensions the lower p_c should be detected in the range of 5%-45% (V_{dx}/V) and the upper p_c at ca. 55%-95% (V_{dx}/V) depending on the “microscopic” lattice structure. In the section of materials and

methods it will be explained how to detect the lower and upper percolation thresholds by subdivision of curves into segments by means of nonlinear regression analysis.

4.5.3 Materials and methods

4.5.3.1 Solvents

The binary mixtures of water/1,4-dioxane, methanol/1,4-dioxane, and benzylalcohol/1,4-dioxane were examined at 298.2 K. Bidistilled water was freshly prepared by means of a Fontavapor 285 (Büchi AG CH-Flawil). The organic solvents of high purity were acquired commercially from Fluka Chemie GmbH CH- Buchs [benzylalcohol (art. No. 13160), 1,4-dioxane (art. No. 42512) and methanol (art. No. 65550)] (see Table 1)

	¹⁾ Dipole Moment [D]	¹⁾ MW [g _{mol} ⁻¹]
Methanol	1.70	32.04
Benzylalcohol	1.71	108.14
Water	1.85	18.02
1,4-Dioxane	0.00	88.11

Table 1: Physical properties of the solvents studied at room temperature (¹⁾ source: CRC Handbook of Chemistry and Physics, 1997). The dipole moment is given in debye units (D). The conversion factor to SI units is 1 D = 3.33564 x 10⁻³⁰ C m.

The samples were prepared by weighing the necessary amounts of solvents/solutes into glass flasks. The samples were then shaken vigorously for 15 seconds and then stirred for 1 minute using a Vortex mixer.

4.5.3.2 Experimental setup and data analysis

4.5.3.2.1 Measurement of the static permittivity and conductivity

The static permittivity and conductivity in this work were measured via the impedance and conductance, respectively, by means of a LCR (inductance L, capacitance C, and resistance R) Meter at a low ac frequency, so the measured permittivity corresponds to the dielectric constant measured in direct current (dc).

For the measurement of the static permittivity and conductivity the following apparatus were used: *Precision LCR Meter* (Agilent Technologies Inc. HP 4284A; 2940J01533), and *Test Fixture* (Agilent Technologies Inc. USA-Palo Alto CA 94304-1185 HP 16047C).

To the test fixture it was connected a *Cylinder Condensator* (by courtesy of Ramsden and the Mechanische Werkstatt Biozentrum, Universität Basel). The inner electrode has a diameter 12.92mm, and height 9.85 mm, and the outer electrode has a diameter 18.74 mm.

To the cylinder condensator it was connected a *Thermostat* (B. Braun Biotech International GmbH D-34209 Melsungen: Thermomix UB; 852 042/ 9; 9012 498/ Frigomix U-1; 852 042/ 0; 8836 004), allowing temperature control of ± 0.1 K. The temperature was checked by means of a *Digital Thermometer* (Haake GmbH D-76227 Karlsruhe DT 10, Pt. 100 platinum resistance thermometer (± 0.1 K)).

For the measurement set-up used in this work the capacitance C and the conductance G were measured in a parallel circuit mode (Lehnert, 1992). As test frequency 100 kHz was chosen, giving stable results and being $10^3 - 10^5$ lower than the relaxation frequencies of the dipoles of the liquids measured in this work.

The measurements were made by means of a personal computer connected to the LCR Meter, using the software HP VEE 5.01 (Agilent Technologies Inc. USA-Palo Alto CA 94304-1185).

The cylinder condensator was brought to the measuring temperature (298.2 K) and filled with the sample. 5 minutes after the required temperature was reached, the sample was measured 5 times, waiting for 1 minute after each measurement.

4.5.3.2.1.1 *Data analysis: Calculation of the E_i/E parameter for binary polar liquid mixtures*

For a Capacitor C_{MUT} filled with the material under test (MUT) The static permittivity ε - for $\omega \ll \omega_{res}$ - equals the real part of the permittivity.

$$\varepsilon' = \frac{C_{MUT}}{C_{vacuum}} \quad (15)$$

with ε' = real part of permittivity ε^* ; C_{MUT} = capacitance of material under test (F); C_{vacuum} = capacitance of vacuum (F).

In the present work, the measured C_{air} is substituted for C_{vacuum} , the calculated values for ε are corrected via a calibration curve (Eq. (16)).

$$\varepsilon_{lit} = 2.7394 \cdot \varepsilon_{exp} - 1.8031 \quad r^2=1.000. \quad (16)$$

E_i/E for binary mixtures was calculated according to the following equation (Stengele et al., 2002):

$$\frac{E_i}{E} = \frac{M_{r,m}}{3 \cdot \rho_m} \cdot \frac{\varepsilon_m - 1}{\frac{N_A}{3 \cdot \varepsilon_0} \left[V_1 \left(\alpha_1 + \frac{\mu_{g,1}^2}{3 \cdot K \cdot T} \right) + V_2 \left(\alpha_2 + \frac{\mu_{g,2}^2}{3 \cdot K \cdot T} \right) \right]} - \frac{\varepsilon_m + 2}{3} \quad (17)$$

where ρ_m = density of mixture; $M_{r,m}$ = molecular weight of the mixture; ε_m = quasi-static relative dielectric constant for the mixture; V_1 = volume fraction of liquid 1; V_2 = volume fraction of liquid 2.

For calculating the respective contributions of the liquids, their volume contributions are considered. For the description of binary mixtures by means of percolation theory, the

volume fractions are used, as they are more meaningful for the characterization of three-dimensional networks than molar fractions (Stengele et al., 2002).

4.5.3.2.2 *Measurement of the complex permittivity*

The measuring system consists of a dielectric probe connected to a network analyzer by means of a semi-rigid coaxial cable. An electromagnetic signal is generated by the network analyzer and transmitted into the material under test (MUT) via cable and probe. The signal is reflected by the MUT its phase and amplitude are compared by the network analyzer to those of the incident electromagnetic wave.

For the measurement of the complex permittivity the following apparatus was used: *Network Analyzer* Agilent Technologies Inc. USA-Palo Alto CA 94304-1185 HP 8720D; US38111202.

To the Network Analyzer it was connected a *High-Temperature Dielectric Probe Kit* Agilent Technologies Inc. USA-Palo Alto CA 94304-1185 HP 85070B OPT 002.

The sample was kept at the required temperature through immersion in a *Thermostat* (B. Braun Biotech International GmbH D-34209 Melsungen: Thermomix UB; 852 042/ 9; 9012 498 / Frigomix U-1; 852 042/ 0; 8836 004), allowing temperature control of ± 0.1 K.

The temperature was checked by means of a *Digital Thermometer* (Haake GmbH D-76227 Karlsruhe DT 10; Pt. 100 platinum resistance thermometer (± 0.1 K)).

The measurements were made by means of a personal computer connected to the Network Analyzer, using *software HP 85070B Probe Software Program* (Agilent Technologies Inc. USA-Palo Alto CA 94304-1185).

The Measurements were made between 0.2 and 20 GHz at 401 frequencies. The Auto Sweep Time Mode was selected. This mode maintains the fastest sweep speed possible for

the current measurement settings. A sweep time = 13.052 s was obtained for measurements between 0.2 and 20 GHz at 401 frequencies.

The dielectric probe was calibrated at the measurement temperature ($T_{\text{meas}} = 298.2$ K) by air, a metal block, and bidistilled water. The computer software requires a fast performance of these calibration steps, which does not allow for an exact temperature adjustment. Therefore, this operation was followed by a calibration refresh procedure, using bidistilled water at $T_{\text{meas}} \pm 0.1$ K. Calibration and refresh calibration were made before starting measurements at T_{meas} and after every fifth sample.

For measurement, the probe was immersed in the sample, which was brought to T_{meas} by means of a water bath/refrigerator. Special attention has to be paid to avoid air bubbles in the probe and the stability of the coaxial cable. Using the thermostat as a water bath, the sample was stabilized at $T_{\text{meas}} \pm 0.1$ K before starting the measurement.

4.5.3.2.2.1 *Data analysis: Calculation of the relaxation time τ*

The following softwares were used for data analysis: *Excel* Microsoft corp. USA-Redmond WA 98052-6399 Version 97 SR-2 and *SYSTAT for Windows* SPSS Inc. USA-Chicago IL 60606-6307 Version 7.0.

In order to find the values for the dielectric spectroscopy parameters such as the relaxation time τ or distribution parameter β , the raw data $\varepsilon'(\omega)$, $\varepsilon''(\omega)$ obtained directly from the dielectric relaxation measurements must be fitted to an equation describing the process.

Close attention must be paid to choose an adequate equation and fitting procedure, and the number of fitting parameters. Usually a compromise has to be found between a large number of free parameters, offering a most adequate fit of the data, and a small number, providing robust and meaningful results, especially when data of e.g. various water concentrations are to be compared.

It has to be kept in mind that the resulting relaxation time τ depends on the mathematical model applied. The choice of best equation describing the process was based on literature and on the comparison of the mean corrected coefficient R^2 obtained after fitting the raw data $\varepsilon'(\omega)$, $\varepsilon''(\omega)$ for every concentration into different equations. If the mean corrected coefficient R^2 coefficient does not differ significantly between the different mathematical models, it is not possible to make an unambiguous choice of a model. The choice of the best equation describing the process was also based on the overall look of the obtained curves.

As the Havriliak-Negami equation did not lead to a significantly better mean corrected coefficient R^2 -values but includes an additional free parameter α (symmetric distribution parameter) and in order facilitate the understanding these results are not included in this paper.

The fitting software used for evaluation was *Systat for Windows* SPSS Inc. USA-Chicago IL 60606-6307 Version 7.0 where the inclusion of both real and imaginary parts for fitting can be made as the term $(\varepsilon - \varepsilon_\infty)$ occurs in both parts. This allows reformulation of equations as following: Considering the real and imaginary part of the Debye equation (Eqs. (5) and (6))

$$\varepsilon'(\omega) = \varepsilon_\infty + (\varepsilon - \varepsilon_\infty) \frac{1}{1 + \omega^2 \tau^2} = \varepsilon_\infty + (\varepsilon - \varepsilon_\infty)A \quad (18)$$

$$\varepsilon''(\omega) = (\varepsilon - \varepsilon_\infty) \frac{\omega \tau}{1 + \omega^2 \tau^2} = (\varepsilon - \varepsilon_\infty)B \quad (19)$$

$$(\varepsilon - \varepsilon_\infty) = \frac{\varepsilon'(\omega) - \varepsilon_\infty}{A} = \frac{\varepsilon''(\omega)}{B} \quad (20)$$

Therefore,

$$\varepsilon''(\omega) = (\varepsilon - \varepsilon_\infty) \frac{\omega\tau}{1 + \omega^2\tau^2} = (\varepsilon'(\omega) - \varepsilon_\infty) \frac{B}{A} \quad (21)$$

$$\varepsilon'(\omega) = \varepsilon_\infty + (\varepsilon - \varepsilon_\infty) \frac{1}{1 + \omega^2\tau^2} = \varepsilon_\infty + (\varepsilon - \varepsilon_\infty)A = \varepsilon_\infty + \varepsilon''(\omega) \frac{A}{B} \quad (22)$$

The data, i.e. the mean based on three separate measurements, are fitted to the chosen equation (e.g. Eq. (21) or (22)) by using nonlinear regression (Gauss-Newton with Least Squares estimation).

4.5.3.2.2.2 *Subdivision of curves into segments by means of nonlinear regression: detection of percolation thresholds*

From theory, we assume that the properties of a binary mixture should behave like the volume-wise addition of the properties if the pure liquids. If deviations from this theoretical assumption occur, the splitting up of the curve onto small number of segments leads to the distinction of percolation thresholds, critical volume fractions, and to a better description of properties of the system. The subdivision of data into a number of segments may be appropriate if the number of segments is small, the mathematical model describing the segments simple, viz straight lines, and if there are sharp transitions between the segments. (Bellman and Roth, 1969; Seber and Wild, 1989).

The software used was: *Systat for Windows* SPSS Inc. USA-Chicago IL 60606-6307 Version 7.0.

The data were inspected in order to decide about a suitable number of sub-segments and potential critical concentrations. For the following example (see Table 2), three sub-segments seem appropriate with critical values for volume fraction $(V_x/V)_{\text{crit}} \approx 4-6$ and 8-10.

The data were arbitrary split into three straight subsegments around these possible $(V_x/V)_{\text{crit}}$, e.g. the first four points to subsegment A, the next four to subsegment B, the last

four to subsegment C. Using nonlinear regression, the data were fitted to the following equation:

$$y = A (m_1x + b_1) + B (m_2x + b_2) + C (m_3x + b_3) \quad (23)$$

x	y	Data belong to segment		
		A	B	C
1.0	12.7	1	0	0
2.0	12.6	1	0	0
3.0	12.1	1	0	0
4.0	12.0	1	0	0
5.0	10.0	0	1	0
6.0	8.5	0	1	0
7.0	7.0	0	1	0
8.0	5.0	0	1	0
9.0	3.0	0	0	1
10.0	3.5	0	0	1
11.0	4.0	0	0	1
12.0	4.6	0	0	1

Table 2: Subdivision of curves into segments: example

The final decision to which segment the data are to be assigned is made considering the mean corrected coefficient R^2 for the overall fit. For this example, the best fit ($R^2 = 0.999$) was received for a distribution 4 / 4 / 4 (A: $y = -0.26x + 13.00$; B: $-1.65x + 18.35$; C: $0.53x - 1.79$).

The critical values correspond with the intersection points of the segments. In the example they are located at the following volume fractions: $(V_x/V)_{\text{crit1}} = 3.85$ and $(V_x/V)_{\text{crit2}} = 9.24$. Those intersections points correspond to the lower and upper percolation thresholds.

For the description of binary mixtures by means of percolation theory, the volume fractions are used, as they are more meaningful for the characterization of three-dimensional networks than molar fractions.

4.5.3.2.3 *Other measurements*

The measurements of the density ρ were made using a *vibrating-tube densimeter*, refractive indices n_D were measured by means of an *Abbé refractometer*.

Physical properties which were necessary for calculations, such as the dipole moment in the gas phase μ_g (CRC Handbook of Chemistry and Physics, 1997) and the polarizability α of the investigated compounds were obtained as follows: The values of the dipole moment in the gas phase μ_g were taken from the literature. The polarizability was determined via the Lorentz-Lorenz-equation, which gave excellent results compared with literature data (Riddick and Bunger, 1970) both for polar and nonpolar compounds (see Eq. (24)).

$$\frac{n^2 - 1}{n^2 + 2} \frac{Mr}{\rho} = \frac{N_A}{3\epsilon_0} \alpha \quad (24)$$

4.5.4 Results and discussion

4.5.4.1 *Percolation phenomena observed in binary mixtures based in the results of the modified Clausius-Mossotti-Debye equation (Eq. 17)*

The E_i/E -values for the investigated binary mixtures at 298.2K are represented in Fig. 3, 4 and 5. For the water/1,4-dioxane and methanol/1,4-dioxane binary mixtures data can be clearly divided in two segments (Fig. 3 and 4): A convex curve of slightly positive values, and a linear relationship between E_i/E and the % of the volume fraction of 1,4-dioxane (V_{dx}/V). The E_i/E -values of water/1,4-dioxane, methanol/1,4-dioxane and benzylalcohol/1,4-dioxane can be subdivided in three linear segments that will be explained according to percolation theory.

4.5.4.1.1 *Water/1,4-dioxane binary mixtures*

The data for the E_i/E values of the water/1,4-dioxane binary mixtures as a function of the % of the volume fraction of 1,4-dioxane (V_{dx}/V) were inspected in order to decide about a suitable number of sub-segments and potential critical concentrations which could correspond with the lower and upper percolation thresholds (see Fig. 3). By means of nonlinear regression the curve for water/1,4-dioxane mixtures could be split into three sections whose intersections are located at 62% (V_{dx}/V) and 86% (V_{dx}/V) (see Fig. 3).

It can be assumed that water forms isolated clusters and is definitely no longer percolating the system for (V_{dx}/V) percentages above 86%. That intersection point corresponds with the upper p_c of 1,4-dioxane. Thus, water may start to percolate at a volume fraction of $100\% - 86\% = 14\%$ (V_{wa}/V). However, the detailed analysis indicates that only above 38% (V_{wa}/V), i.e. below 62% (V_{dx}/V), water may assume its normal structure leading to the value of $E_i/E = -20.4$ for the pure liquid (see linear part of the curve). It is evident that 38% (V_{wa}/V) represents a critical concentration corresponding to a structural change with a lower coordination number but it cannot be excluded that it could also be a percolation threshold.

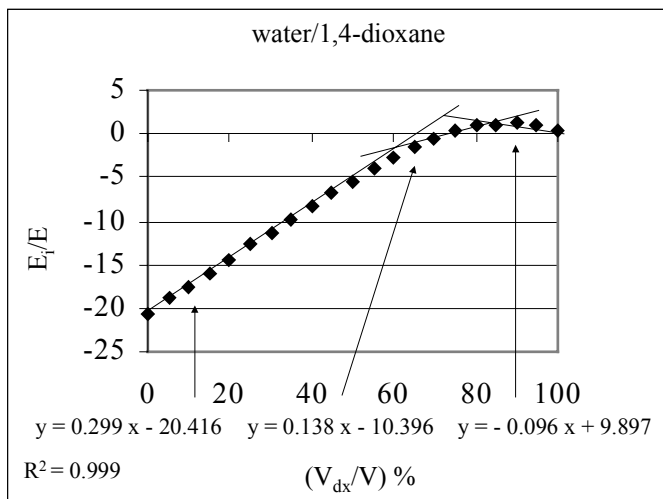


Figure 3: E_i/E values as a function of the % volume fraction of 1,4-dioxane (V_{dx}/V) for water/1,4 dioxane binary mixtures at 298.2 K. The critical points are located at ca. 62% and 86% (V_{dx}/V).

It is important to realize that between 0% (V_{dx}/V) and 62% (V_{dx}/V) (linear part of the curve), the lower p_c could not be detected by analyzing the E_i/E parameter. One has to assume that 1,4-dioxane fits well into the water structure and the lower p_c of 1,4-dioxane cannot be detected for this reason.

4.5.4.1.2 Methanol/1,4-dioxane binary mixtures

For 1,4-dioxane/methanol mixtures, the dependence of the E_i/E -values as a function of % of the volume fraction of 1,4-dioxane (V_{dx}/V) can be divided into three segments whose intersections are located at 45% (V_{dx}/V) and 74% (V_{dx}/V) (see Fig. 4). It can be assumed that methanol forms isolated clusters above 74% (V_{dx}/V), i.e. that methanol percolates the system, above 26% (V_{metOH}/V). The final structure of methanol seems to be achieved at a higher concentration of methanol, i.e. above 55% (V_{metOH}/V), i.e. below 45% (V_{dx}/V). It seems that 1,4-dioxane starts to percolate the system above 45% (V_{dx}/V). Thus, above 45% (V_{dx}/V) and below 74% (V_{dx}/V) both 1,4-dioxane and methanol percolate the system. The critical concentration at ca. 45% (V_{dx}/V) could correspond with a structural change in the lattice. It is a rather high value for a lower p_c . Nevertheless, we cannot exclude that possibility. It is convenient to see section 4.5.4.2.2. in order to compare the critical

concentrations obtained with the E_i/E -values with those obtained after analyzing the relaxation time.

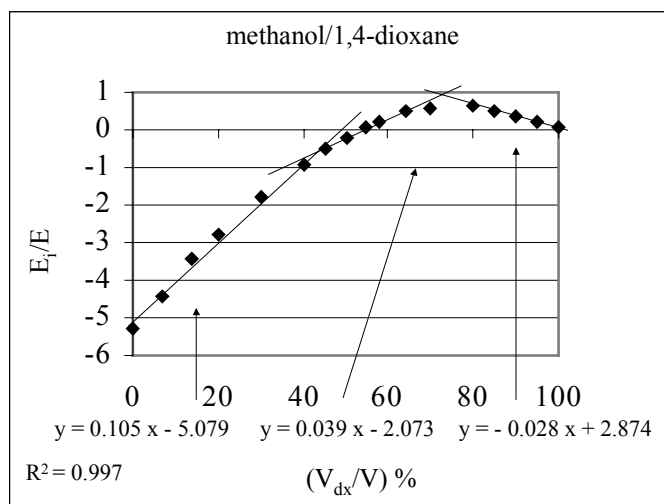


Figure 4: E_i/E values as a function of the % volume fraction of 1,4-dioxane (V_{dx}/V) for methanol/1,4 dioxane binary mixtures at 298.2 K. The critical points are located at ca. 45% and 74% (V_{dx}/V).

4.5.4.1.3 Benzylalcohol/1,4-dioxane binary mixtures

In Fig. 5 the dependence of E_i/E as a function of % of the volume fraction of 1,4-dioxane (V_{dx}/V) added to benzylalcohol can be subdivided into three segments with the intersections located at 27% (V_{dx}/V) and 55% (V_{dx}/V). The first intersection at ca. 27% (V_{dx}/V) can be interpreted as the lower p_c of 1,4 -dioxane. The second one at 55% (V_{dx}/V) can be assumed as the upper p_c , where benzylalcohol starts to form isolated clusters. One has to keep in mind, that the determination of the upper p_c is not very precise as the slopes of the line of the middle and upper segments are not very different.

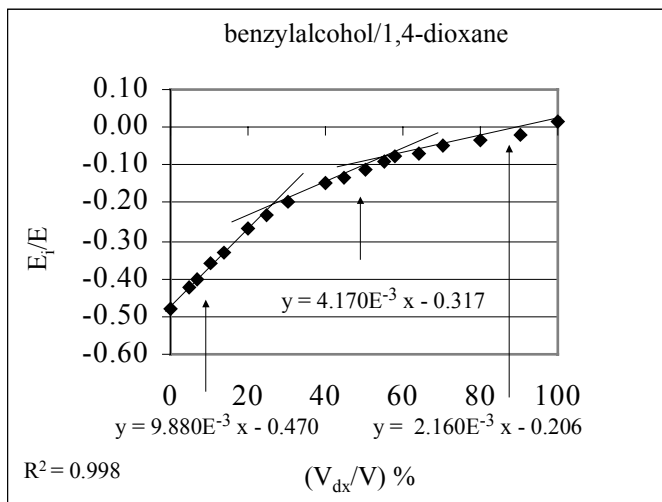


Figure 5: E_r/E values as a function of the % volume fraction of 1,4-dioxane (V_{dx}/V) for benzylalcohol/1,4-dioxane binary mixtures at 298.2 K. The critical points are located at ca. 27% and 55% (V_{dx}/V).

4.5.4.2 *Percolation phenomena observed in binary mixtures based in the results of broadband dielectric spectroscopy of binary mixtures at 298.2 K*

4.5.4.2.1 *Water/1,4-dioxane binary mixtures*

The binary system water 1, 4-dioxane was analyzed as follows: first with the approximation of the relaxation behavior with a single Debye function and second with the superposition of a Debye function and Cole-Davidson distribution function, as a function of the % of the volume fraction of 1,4-dioxane (V_{dx}/V) added.

In Fig. 6 the relaxation behavior of the dipole moment of water at 298.2 K in 1,4-dioxane and water mixtures is modeled by one Debye function (see section 4.5.3.2.2.1) and with the superposition of one Debye function with the Cole-Davidson distribution. With one Debye equation we only obtain a mean correlated coefficient R^2 between 0.99 and 0.98 for the range of 0%-25% (V_{dx}/V). In the range above 25% (V_{dx}/V) R^2 starts decreasing adopting a minimum of $R^2 = 0.66$ for 90% (V_{dx}/V).

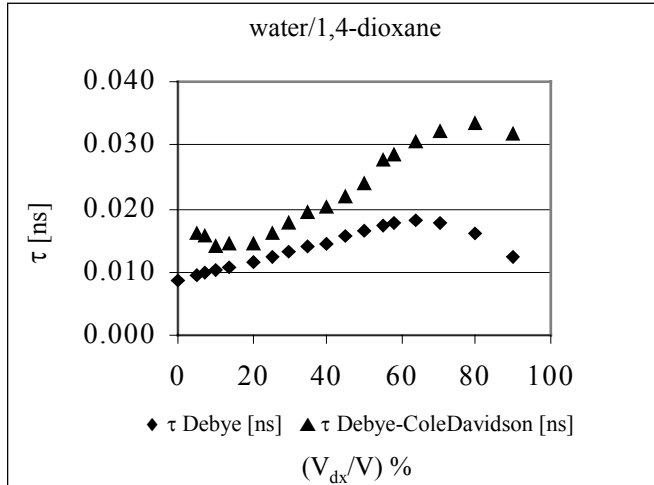


Figure 6: Two different models for the description of the relaxation behavior of the water dipole in water/1,4-dioxane mixtures at 298.2 K as a function of the % volume fraction of dioxane (V_{dx}/V).

According to Fig. 6 the superposition of the Debye and Cole-Davidson equations yields a good fit with $R^2 = 0.99-0.98$ for the whole range. In the latter case (see Fig. 7) l_1 belonging to the Debye part of the superposition becomes zero at the presumed lower p_c of ca. 20% (V_{dx}/V). Thus, below the lower p_c , it is possible to describe the relaxation behavior just with one Debye function based on the excellent fitting of the data with R^2 -values > 0.99 . Above the lower p_c the relaxation behavior is well described by the Cole-Davidson distribution function only ($l_2=1, l_1=0$, see Fig. 7). Compared to the dependence of E_i/E -parameter (see Fig. 3) the lower p_c is clearly visible.

In Fig. 8 the β -parameter (skewness) of the Cole-Davidson equation is plotted as a function of the % of the volume fraction of 1,4-dioxane (V_{dx}/V) added. In this plot the lower p_c at ca. 24% (V_{dx}/V) and the upper one at ca. 62% (V_{dx}/V) are visible. These findings are compatible with the findings of Fig. 6 (τ -values) for the lower p_c but not with Fig. 3 (E_i/E -values) for the upper p_c .

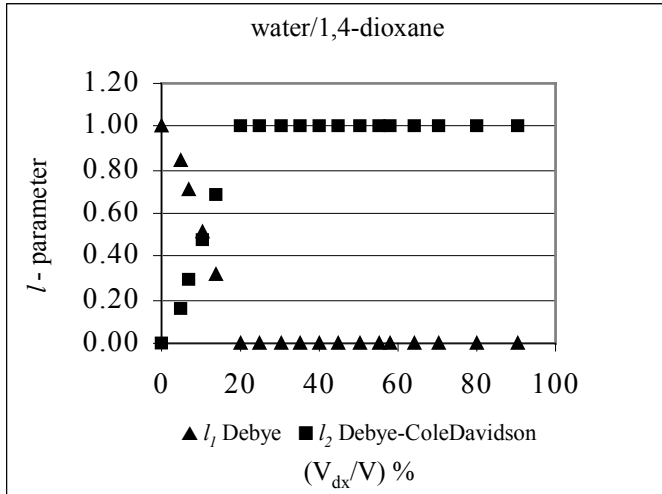


Figure 7: Weight factor of relaxation time (l - parameter: l_1 , l_2) for water/1,4-dioxane binary mixtures at 298.2 K as a function of the % volume fraction of dioxane (V_{dx}/V) calculated with the superposition of one Debye equation (l_1) with the Cole-Davidson distribution function (l_2).

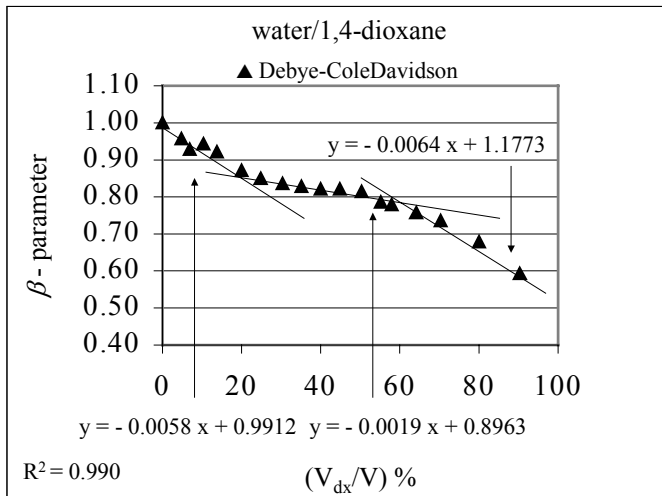


Figure 8: Skewness of the distribution of relaxation times (β -parameter) for water/1,4-dioxane binary mixtures at 298.2 K as a function of the % volume fraction of dioxane (V_{dx}/V) calculated with the superposition of Debye and Cole-Davidson equations. The critical points are located at ca. 24% and 62% (V_{dx}/V).

Summarizing, the lower p_c would be located at ca. 20% (V_{dx}/V) and the upper p_c at ca. 86% (V_{dx}/V). The critical point obtained at ca. 62% (V_{dx}/V) would be interpreted as a structural

change in the lattice. Nevertheless, it cannot be excluded that the critical point obtained at ca. 62% (V_{dx}/V) could also be a p_c .

4.5.4.2.2 *Methanol/1,4-dioxane binary mixtures*

In case of the binary mixtures methanol/1, 4-dioxane the best fits were obtained with the Debye and Cole-Davidson distribution function (Fig. 9). The values can be subdivided into three segments with the intersections located at 20% (V_{dx}/V) and 48% (V_{dx}/V). Below 20% (V_{dx}/V) it is possible to describe the relaxation behavior of methanol with one Debye function. However, the R^2 -values being in the range of 0.96 to 0.99 are not as high as in the case of water with R^2 -values > 0.99

The data of Fig. 9 allow only a rough estimate of the two percolation thresholds and the three ranges: range I (0% ~20% (V_{dx}/V)) with a decrease of the main relaxation time τ , range II (20%~48% (V_{dx}/V)), i.e. where both components percolate and range III (48%~1% (V_{dx}/V) 1,4-dioxane) with a significant decrease of the main relaxation time.

The relaxation behavior of the dipole of methanol can be best described by one Debye function in the range of 0% (V_{dx}/V) to ca. 20% (V_{dx}/V). For higher percentages of 1,4-dioxane the behavior can be best approximated by a superposition of one Debye with a Cole-Davidson distribution function (see Fig. 9). However the plot of the β -parameter does not reveal clearly percolation thresholds.

The comparison of these results with the findings of the critical concentrations of the E_i/E -values indicates that it is difficult to decide whether the critical concentration describes a percolation threshold or a structural change of the lattice.

The critical concentrations obtained with the E_i/E -values are located at ca. 45% (V_{dx}/V) and 74% (V_{dx}/V). With the relaxation time we find the critical concentrations at ca. 20% (V_{dx}/V) and 48% (V_{dx}/V). We can conclude with a high probability that the lower p_c would be located at 20% (V_{dx}/V), the upper p_c at ca. 74% (V_{dx}/V) and the critical concentration

founded with E_i/E and τ at ca. 45% (V_{dx}/V) respectively 48% (V_{dx}/V) could be interpreted as a structural change without changing the subsequent upper p_c . However it cannot be excluded that this point could also reflect a p_c .

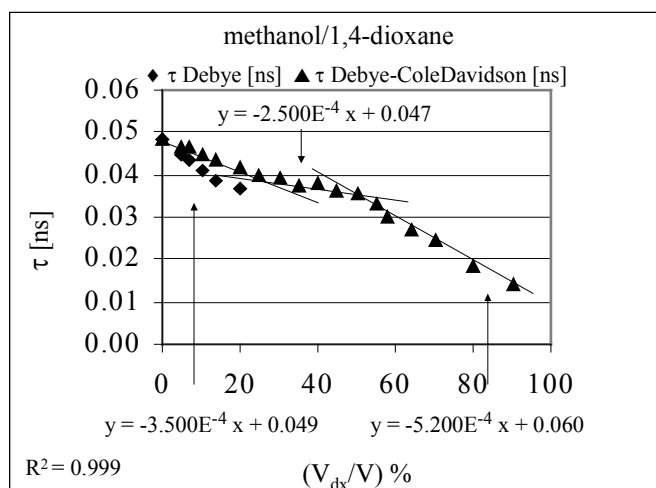


Figure 9: Relaxation behavior of the dipole of methanol in 1,4-dioxane mixtures calculated on the basis of one Debye function (range 0%-20% (V_{dx}/V)) and on the basis of the superposition of one Debye equation with the Cole-Davidson distribution function at 298.2 K as a function of the % volume fraction of dioxane (V_{dx}/V). The critical points are located at ca. 20% and 48% (V_{dx}/V).

4.5.4.2.3 Benzylalcohol/1,4-dioxane binary mixtures

With benzylalcohol/1,4-dioxane binary mixtures the situation is as follows.

Fig. 10 shows two different models to fit the relaxation time behavior for benzylalcohol/1,4-dioxane binary mixtures at 298.2 K as a function of the % volume fraction of 1,4-dioxane (V_{dx}/V). With one Debye equation we only obtain a mean corrected coefficient R^2 between 0.99 and 0.97 for the range 0% - ca. 20% (V_{dx}/V). Thus, in the 1,4-dioxane poor region, i.e. till 1,4-dioxane starts to percolate the system (as ca. 20% (V_{dx}/V)), the behavior of the relaxation of the benzylalcohol dipole can be described by the simple Debye equation.

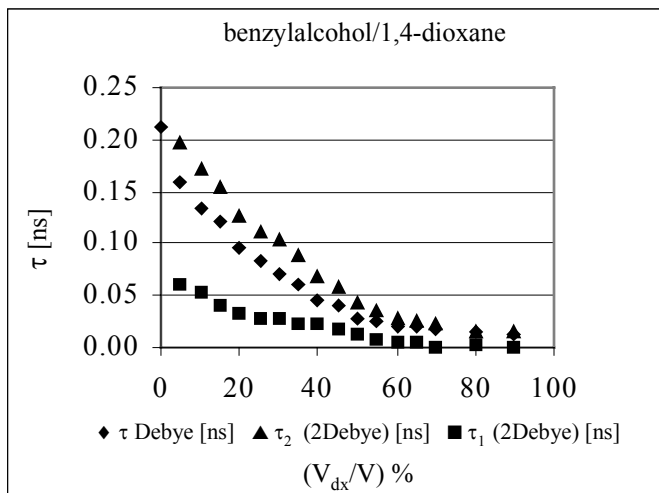


Figure 10: Two different models to fit the relaxation time behavior for benzylalcohol/1,4-dioxane binary mixtures at 298.2 K as a function of the % volume fraction of 1,4-dioxane (V_{dx}/V).

Interestingly the superposition of two Debye equations is able to characterize nearly the whole range of benzylalcohol/1, 4-dioxane mixtures with $R^2 > 0.97$ for less than 70% (V_{dx}/V), i.e. below the upper p_c of ca. 58-63% (V_{dx}/V) (see Fig. 10). In fact it is possible to conclude that the addition of 1,4-dioxane leads to two distinct modes of relaxation, which can be described by two relaxation times τ_1 , τ_2 . The values of the relaxation times depend on the mixture ratio. A closer inspection of both relaxation times τ_1 , τ_2 as a function of the amount of 1,4-dioxane added reveal percolation phenomena, as shown in Figs. 11 (A) and 11 (B), showing a lower p_c at ca. [19-22]% (V_{dx}/V) and an upper p_c at ca. [58-63]% (V_{dx}/V).

A closer inspection of the weights l_1 and l_2 of the superposition of the two Debye equations leads to a symmetric behavior of the relaxation times τ_1 , τ_2 (see Fig. 12).

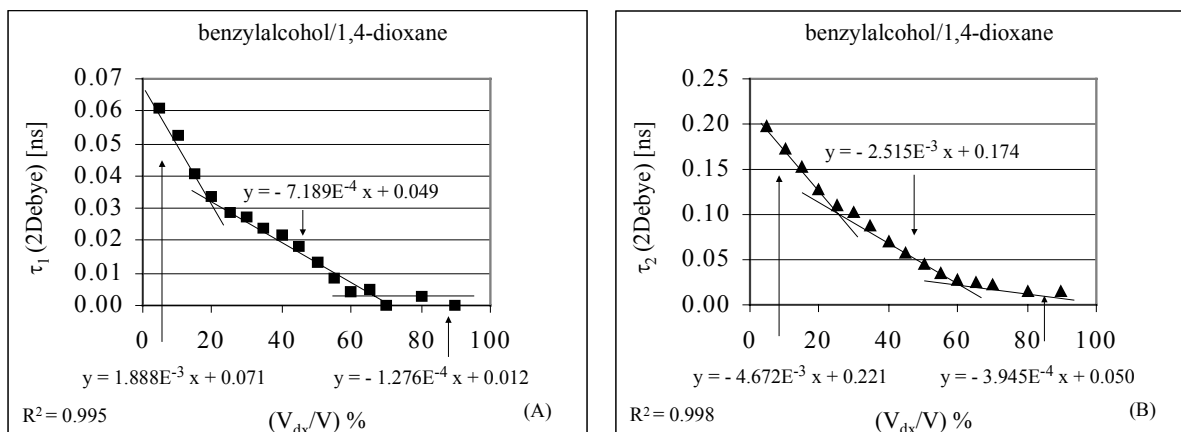


Figure 11: Relaxation times obtained from the superposition of two Debye equations for Benzylalcohol at 298.2 K as a function of the % volume fraction of 1,4-dioxane (V_{dx}/V). (A) Relaxation time τ_1 with critical points located at ca. 19% and 63% (V_{dx}/V). (B) Relaxation time τ_2 with critical points located at ca. 22% and 58% (V_{dx}/V).

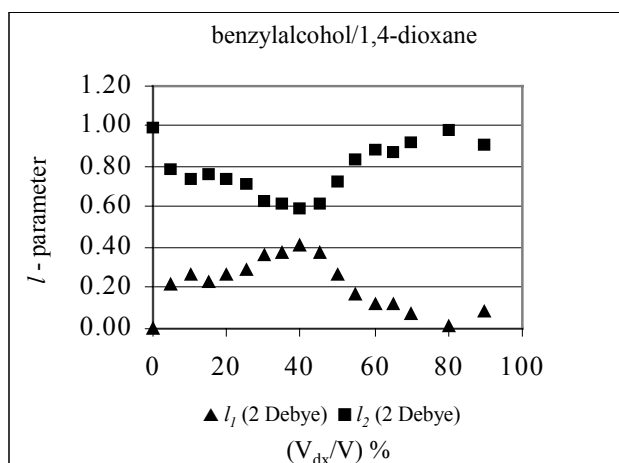


Figure 12: Weight factor of relaxation time (l - parameter: l_1, l_2) for benzylalcohol/1,4-dioxane binary mixtures at 298.2 K as a function of the % volume fraction of 1,4-dioxane (V_{dx}/V) calculated with the superposition of two Debye equations.

These findings are also compatible with the findings of Fig. 5 (E_i/E -values) for the lower and upper p_c .

If we compare with water/1,4-dioxane and methanol/1,4-dioxane we observe that for benzylalcohol/1,4-dioxane mixtures the upper p_c is detected at lower concentration and no

critical concentration are related to a structural change. We can conclude that the behavior between water/1,4-dioxane and methanol/1,4-dioxane is similar due to more similarities in the lattice structure.

4.5.5 Conclusions

It could be shown that the application of the broad range dielectric spectroscopy together with the analysis of the quasi-static permittivity using the modified Clausius-Mosotti-Debye equation can be used to detect percolation phenomena in binary polar liquid mixtures. It leads to a valuable insight into the structure of polar liquids and to a better understanding of binary systems. However, it has to be kept in mind, that besides of percolation thresholds as critical concentrations it is also possible to detect a change of the coordination number as a function of the volume ratio of the components, which involves a change of the lattice type. It is sometimes difficult to discriminate between p_c or lattice change and more studies are needed in order to distinguish between those processes.

4.5.6 References

Bellmann, R., Roth, R., 1969. Curve fitting by segmented straight lines. *J. Am. Stat. Assoc.*, 64, 1079-1084.

CRC Handbook of Chemistry and Physics 77th edition, 1997. CRC Press Inc., Boca Raton.

Decareau, R.V., Mudgett, R.E., 1985. *Microwaves in the Food Processing Industry*, Academic Press, Orlando, pp. 1-54.

Hedestrand, G., 1929. Die Berechnung der Molekularpolarisation gelöster Stoffe bei unendlicher Verdünnung. *J. Physik. Chemie Abt. B* 2, 428-444.

Kremer, F., Schönhals, A, 2003. Broadband Dielectric Spectroscopy, Springer Germany.

Riddick, J.A., Bunger, W.B., 1970. Techniques of Chemistry, vol. 2, Third ed. Wiley, New York.

Seber, G.A.F., Wild, C.J., 1989. Nonlinear regression, Wiley, New York, pp. 433-489.

Smith, G., Duffy, P.D., Shen, J., Olliff, C.J., 1995. Dielectric relaxation spectroscopy and some applications in the pharmaceutical sciences. *J. Pharm. Sci.* 84, 1029-1044

Stauffer, D., Aharony, A., 1998. Introduction to Percolation Theory, second ed. Taylor & Francis, London.

Stengele, A., Rey, St., Leuenberger, H., 2001. A novel approach to the characterization of polar liquids. Part 1: pure liquids. *Int. J. Pharm.* 225, 123-134.

Stengele, A., Rey, St., Leuenberger, H., 2002. A novel approach to the characterization of polar liquids. Part 2: binary mixtures. *Int. J. Pharm.* 241, 231-240.

The Merck Index. 1983. An encyclopedia of chemicals, drugs, and biologicals, tenth ed. Merck & co., U.S.A

4.6 The characterization of aprotic polar liquids and percolation phenomena in DMSO-water mixtures

Graci Hernandez-Perni, Hans Leuenberger*

*Institute of Pharmaceutical Technology, Pharmacenter University of Basel,
Klingelbergstrasse 50, CH-4056 Basel, Switzerland*

4.6.1 Abstract

In the previous papers of our research group it was shown, that the Clausius-Mossotti-Debye equation for the quasi-static dielectric constant (ϵ) can be extended to liquids if the parameter E_i/E is introduced. Thus, it is possible to characterize polar liquids with the easily accessible parameter E_i/E . This property is also reflected by the fact that the parameter E_i/E can be directly related to the empirical $E_T(30)$ and the normalized E_T^N parameter to describe the polarity of polar liquids proposed by Reichardt (Chem. Rev. 94, 2319-2358):

$$E_T^N = \frac{E_T(\text{solvent}) - E_T(\text{TMS})}{E_T(\text{water}) - E_T(\text{TMS})} = \frac{E_T(\text{solvent}) - 30.7}{32.4} \quad (1)$$

E_i corresponds to the local mean field due to close molecule-molecule interactions after the application of an external electric field E . In a recent work of our research group it was also demonstrated that the modified Clausius-Mossotti-Debye equation and the study of the relaxation time can be related to percolation phenomena in the binary solvent mixtures leading to a valuable insight of the structure of polar liquids and to a better understanding of binary systems. In the present paper it is demonstrated that percolation phenomena for DMSO-water binary mixtures, become visible due to changes of parameters describing the dielectric spectrums. Thus, these parameters can

* Corresponding author: Institute of Pharmaceutical Technology, Pharmacenter University of Basel, Klingelbergstrasse 50, CH-4056 Basel, Switzerland. Tel.: +41-61-267-1501; fax: +41-61-267-1516.

E-mail address: hans.leuenberger@unibas.ch (H. Leuenberger).

be used in place of other parameters such as viscosity or other properties of the liquid mixture as demonstrated by other authors.

Keywords: Modification of the Clausius-Mossotti-Debye-Equation; Percolation phenomena; empirical solvent solubility parameter $E_T(30)$ and the normalized E_T^N parameter; Binary polar solvent mixtures; Dielectric spectroscopy.

4.6.2 Introduction

Dimethyl sulphoxide (DMSO) [(CH₃)₂SO)] is a widely used solvent with pharmacological action including anti-inflammatory and bacteriostatic activity, analgesia, nerve blockade, diuresis, cholinesterase inhibitor, vasodilation, and muscle relaxation (Wood and Wood, 1975). DMSO also has the unique capability of penetrating living tissues without causing significant damage (Chen et al., 2003). It has been used as a carrier to enhance the bladder absorption of chemotherapeutics such as Paclitaxel (Chen et al., 2003), cisplatin, pirarubicin, and doxorubicin (Rangel et al., 1994; Roth, 1995). One of the most interesting and significant properties of DMSO is its ability to act as a carrier for transferring other drugs through the cell membrane (Soper and Luzar, 1992). By this we mean that the liquid DMSO can be applied on the sole of the foot and within a very few seconds you will be able to taste the DMSO in your mouth. It has a very distinctive taste, something like kerosene or garlic. As a second step, if you mix any of many other different substances with the DMSO, and again apply this mixture (liquid) to the sole of your foot you will get a different taste in your mouth, in the same few seconds. The difference in the taste will depend on the other substance, which was added to the DMSO and then carried very quickly through the body to the tongue to be tasted. Due to that fact, DMSO with a relatively low intrinsic toxicity of 14.5 g/Kg Oral-Rat measured by LD50 is an interesting absorption enhancer but on the other hand DMSO as a component in a formulation is problematic as it can facilitate other substances to cross the cell barrier including the blood-brain barrier, which may lead to undesired interactions with other drugs. Therefore, many drugs have an enhanced physiological effect when they are mixed with DMSO, which means that the dose can be reduced, which can lead to a reduction of possible side effects due to drug toxicity. DMSO plays also an important role as a cryoprotector to prevent

denaturalization of proteins. This cryoprotective action appears to stem from its ability to prevent water crystal formation within the cells. DMSO is at the same time a common used solvent in the industry. It is often used to test new drugs in an early preclinical study because DMSO can typically dissolve lipophilic drugs and hydrophilic drugs (Jorjani and Rastegar, 2003). In this context it has to be kept in mind that DMSO is completely miscible with water and that water is the key solvent for the existence of life.

As we can see many properties are closely related to its properties in water solutions. Therefore, it is important to study its ability to affect the structure of water. DMSO-water binary mixtures are also of great interest due to the fact that both solvents have a dipole moment and that hydrogen bonds can be formed between water and DMSO molecules. However, DMSO is an aprotic solvent, i.e. no hydrogen bonding between pure DMSO molecules exists. Hence, the hydrogen bonding involving DMSO leads to a decrease in the number of hydrogen bonds among water molecules. Therefore, DMSO-water mixtures represents one of the more complicated binary systems, namely an associating component (water) plus a second component (DMSO) acting only as a hydrogen bond acceptor (Luzar, 1990).

There have been many attempts to reveal the structure of the DMSO-water mixture in order to understand the non-linear behavior of this system as a function of the composition. Extreme deviations from additivity are observed for a wide range of properties, such as density and viscosity. The maximum deviations occur at 30–40 mol % DMSO (63–72% (V_{DMSO}/V)) corresponding to 60–70 mol % water (28–37 % (V_{wa}/V)) and suggest the probable existence of a stable DMSO hydrate or at least a strong hydrogen-bonded association between the two kind of molecules (Soper and Luzar, 1992). The aim of this paper is to interpret that behavior in the framework of the percolation theory by using parameters derived from low frequency dielectric spectroscopy such as the E_i/E parameter, g -values obtained from the Kirkwood-Fröhlich, and dielectric constant, and the relaxation time derived from high frequency dielectric spectroscopy.

4.6.3 Theoretical background

4.6.3.1 *The Clausius-Mossotti-Debye equation modified according to Leuenberger for the quasi-static dielectric constant (Stengele et al., 2001)*

The original Clausius-Mossotti-Debye equation is only valid for molecules in the ideal gas phase, i.e. in the case, where the molecules are located far from each other and do not show any interaction:

$$\frac{\varepsilon - 1}{\varepsilon + 2} \frac{M_r}{\rho} = \frac{N_A}{3\varepsilon_0} \left(\alpha + \frac{\mu_g^2}{3kT} \right) \quad (2)$$

With ε = quasi-static relative dielectric constant; M_r = molecular weight; ρ = density; N_A = Avogadro number, 6.023×10^{23} (mol⁻¹); ε_0 = electric field constant in the vacuum, 8.854×10^{-12} (C² J⁻¹ m⁻¹); α = polarizability of the molecule (cm² V⁻¹); μ_g = dipole moment in the state of an ideal gas (C m); k = Boltzmann's constant, 1.38×10^{-23} (J K⁻¹); T = temperature (K).

The essential point of the original derivation of the Clausius-Mossotti-Debye equation consisted in the fact that the local mean field E_i being the result of short range Van der Waals interactions and of hydrogen bonding of neighboring molecules was neglected. The introduction of the term E_i/E with E_i = internal electric field, caused by interactions with other induced neighbouring dipoles; E = external electric field, produced by the applied voltage leads to the following modification:

$$\frac{\varepsilon - 1}{3 \frac{E_i}{E} + (\varepsilon + 2)} \frac{M_r}{\rho} = \frac{N_A}{3\varepsilon_0} \left(\alpha + \frac{\mu_g^2}{3KT} \right) \quad (3)$$

The Clausius-Mossotti-Debye equation modified according to Leuenberger for the quasi-static dielectric constant (Stengele et al., 2001) (Eq. (3)) can be used to

characterize polar liquids. In case of a highly polar liquid such as water the value of E_i/E is -21.0 at room temperature.

4.6.3.2 *g-values obtained form the Kirkwood-Fröhlich Equation (Stengele et al., 2001)*

Short-range interactions between dipoles are considered by the Kirkwood–Fröhlich Equation (Eq. (4)), which was introduced by Kirkwood (Kirkwood, 1939) and further developed by Fröhlich (Fröhlich, 1958).

$$\frac{(\varepsilon - \varepsilon_\infty)(2\varepsilon + \varepsilon_\infty)}{\varepsilon(\varepsilon_\infty + 2)^2} = \frac{N_A}{9\varepsilon_0 kT} \frac{\rho}{M_r} \mu_g^2 g \quad (4)$$

Where ε , respectively ε_∞ corresponds to the dielectric constant characteristic for induced polarization, measured at a frequency low enough that both atomic and electronic polarization are the same as in the static field, respectively high enough so that the permanent dipoles can no longer follow the field; g = correlation factor; M_r = molecular weight; ρ = density; N_A = Avogadro number, 6.023×10^{23} (mol⁻¹); ε_0 = electric field constant in the vacuum, 8.854×10^{-12} (C² J⁻¹ m⁻¹); μ_g = dipole moment in the state of an ideal gas (C m); k = Boltzmann's constant, 1.38×10^{-23} (J K⁻¹); T = temperature (K).

The correlation factor g is a measure of intermolecular correlations, considering one dipole surrounded by its z next neighbors:

$$g = 1 + z \langle \cos \phi_{ij} \rangle \quad (5)$$

$\langle \cos \phi_{ij} \rangle$ is the average of the cosine of the angle between the two neighboring molecules i and j .

So we find for a parallel alignment of molecules, i.e. $\langle \cos \phi_{ij} \rangle = 1$, $g > 1$, and for an antiparallel alignment, i.e. $\langle \cos \phi_{ij} \rangle = -1$, $g < 1$.

The Kirkwood–Fröhlich Equation (Eq. (4)) is only valid for polar molecules. The value of g is ambiguous, as $g = 1$ stands either for disorder or equal amounts of parallel and antiparallel aligned molecules outweighing each other.

4.6.3.3 The Debye equation for the complex dielectric permittivity ε^*

The Debye equation describes the behavior of the frequency (ω) dependence of the complex dielectric permittivity $\varepsilon^* = \varepsilon', \varepsilon''$:

$$\varepsilon^*(\omega) = \varepsilon_\infty + \frac{\varepsilon - \varepsilon_\infty}{1 + i\omega\tau} \quad (6)$$

With $\varepsilon^* =$ complex permittivity; $\varepsilon =$ quasi-static dielectric permittivity (dielectric constant at ca. zero frequency) and $\varepsilon_\infty =$ dielectric permittivity for large frequencies ($\omega \rightarrow \infty$); $\tau =$ characteristic relaxation time (s^{-1}); $\omega =$ angular frequency (s^{-1}) and $i =$ imaginary unit $= (-1)^{1/2}$. Equation (6) can be split for the real (ε') and imaginary part (ε'') of the complex permittivity:

$$\varepsilon'(\omega) = \varepsilon_\infty + (\varepsilon - \varepsilon_\infty) \frac{1}{1 + \omega^2\tau^2}, \quad (7)$$

and

$$\varepsilon''(\omega) = (\varepsilon - \varepsilon_\infty) \frac{\omega\tau}{1 + \omega^2\tau^2}. \quad (8)$$

Eqs. (7) and (8) can be interpreted as follows: If we consider the behavior of a sample containing mobile dipole which is being subjected to an oscillating electric field of increasing frequency, in the absence of the field, the dipoles will experience random motion due to thermal energy in the system and no ordering will be present. At low frequencies the dipole moment of the polar molecules, i.e. the entire molecule, orients in the applied electric field. Thus, the real part (ε') is approximately constant and the

imaginary part (ϵ'') is close to zero. At higher frequencies the dipole can no longer follow the directions of the external applied field. The dipoles are unable to reorientate with that field and the total polarization of the system falls. Thus, ϵ' and ϵ'' assume rather low values (Fig. 1). However, at a specific frequency called resonance frequency (ω_{res}) located between these two extremes, the efficiency of the reorientation process is at maximum, as the rate of change in direction of the applied field matches the relaxation time of dipoles. Those dipoles will therefore undergo maximum reorientation, but the random oscillations superimposed on that system would be at minimum. At the resonance frequency (ω_{res}) the imaginary part (ϵ'') assumes a maximum value, which corresponds to the frequency of maximum energy absorption.

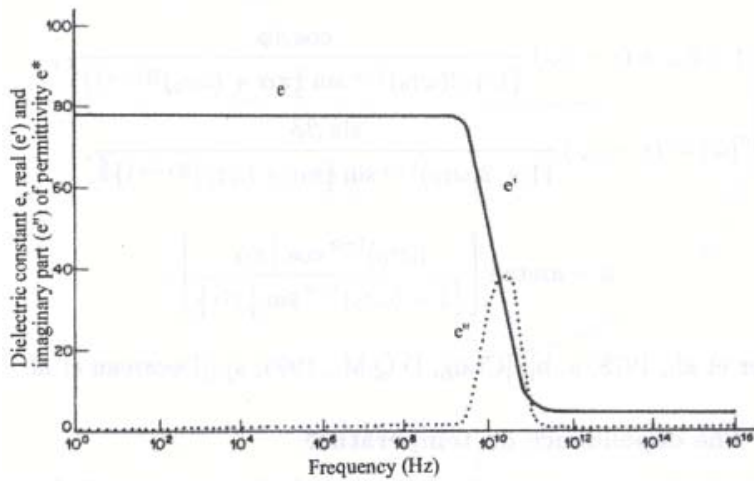


Figure 1: Dielectric permittivity of a polar substance as a function of frequency (after Decareau and Mudget, 1985)

4.6.3.4 Application of percolation theory

Peyrelasse et al., 1988 studied the conductivity and permittivity of various water/AOT/oil systems (AOT = surfactant active agent = sodium bis(2-ethylhexyl) sulfosuccinate) being able to interpret the results according to the phenomenon of percolation. In a second step they studied the viscosity of those systems and they concluded that the shape of viscosity curves could also be interpreted, at least qualitatively, in the framework of percolation theory. They also suggested that the phenomenon of percolation must be involved in other physical properties.

The aim of this work is to study the phenomenon of percolation in binary solvent mixtures parameters by analysing parameters derived from dielectric spectroscopy trying to find a connection between different physical properties.

We chose the DMSO-water system for our study because the mixtures exhibit higher viscosities than either of the two pure components, with a large viscosity maximum near 35% mole fraction in DMSO (32% (V_{wa}/V)) (Marshall et al., 1987). Moreover, there have been many attempts to reveal the structure of the DMSO-water mixture in order to understand the maximum deviations detected at 30–40 mol % DMSO (63–72% (V_{DMSO}/V)) corresponding to 60–70 mol % water (28–37 % (V_{wa}/V)) observed for a wide range of properties, such as freezing point (Havemeyer, 1966), density and viscosity (Soper and Luzar, 1992). Kaatze et al., 1990 found a typically minimum at mole fraction around 30% of DMSO (37% (V_{wa}/V)) for the adiabatic compressibility suggesting the existence of homogeneous hydrogen-bonded networks rather than the presence of stoichiometrically well-defined DMSO: 2H₂O complexes.

Soper and Luzar, 1992, could moreover demonstrate through a neutron diffraction study of DMSO-water mixtures that although there is clearly some disordering of the water structure, the broadly tetrahedral coordination of water molecules remains intact: part of the hydrogen bonding has simply been transferred from the water-water complex to water-DMSO complex, and the proportion of this transfer increases with increasing concentration of DMSO (Fig. 2).

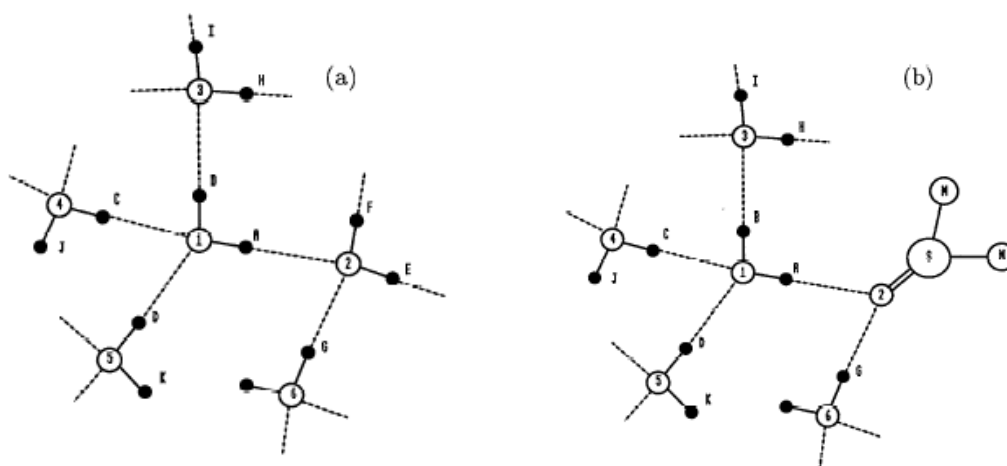


Figure 2: Schematic view of hydrogen bonding in pure water (a) and DMSO/water (b). Solid lines represent intramolecular bonds, dashed lines represent hydrogen bonds. In (a) water molecule 1 is

coordinated by 5 other molecules, 2, 3, 4, 5, and 6, with the first four at roughly tetra-hedral positions the hydrogen A at the origin it sees 1 hydrogen (B) at 1.55 Å, 4 hydrogens (C, D, E, F) at ≈ 2.3 Å, 1 hydrogen (G) at ≈ 3.0 Å, and 4 hydrogens (H, I, J, K) at ≈ 3.8 Å, with a broad range of additional positions available due to the disorder. In (b) molecule 2 has been replaced by a DMSO molecule, which is roughly 50% larger than the water molecule it replaces and adds two or three lone pair electrons, but no hydrogens, to form hydrogen bonds. Now hydrogens E and F have disappeared, so substantially reducing the height of the peaks at 2.3 Å and 3.8 Å, and, if DMSO contributes three lone pairs, emphasizing the peak at ≈ 3 Å. If DMSO were to form much stronger hydrogen bonds with water than water does to itself, this reduction in peak height should become marked at high concentration (Soper and Luzar, 1992).

Percolation thresholds of an ideal system occupied by isometric particles depends on the lattice type, the type of percolation (bond or site) and on the euclidean dimension of the lattice (see Table 1). In the following work only the case of site percolation is discussed. In an ideal system the lattice size is extremely large, i.e. infinite compared to the size of a unit lattice cell. Unfortunately, for most of the lattices the percolation thresholds (p_c) cannot be calculated in a straightforward way, but have to be estimated experimentally by computer simulation of such a lattice and its random occupation.

Lattice	Site	Bond	Coordination number z
Honeycomb	0.696	0.653	3
Square	0.593	0.500	4
Triangular	0.500	0.347	6
Diamond	0.430	0.388	4
Simple cubic	0.312	0.249	6
BCC	0.246	0.180	8
FCC	0.198	0.119	12
Bethe	$1/(z-1)$	$1/(z-1)$	z

Table 1: Values of the bond and site percolation thresholds for various two and three dimensional lattices. Also given is the coordination number defined as the number of bonds meeting at an interior lattice site (Sahimi, 1994).

4.6.3.5 Structural differences between a solid, liquid and a gas

The case of an ideal gas is very clear: the atoms, molecules do not interact due to the large distances in between. The difference between a liquid and a gas becomes difficult in case that the distances between the atoms and molecules are reduced. In case of CO₂ (see phase diagram in Fig. 3) above the critical point it is difficult to decide, whether it behaves like a gas or a liquid. Officially this phase is called a supercritical gas.

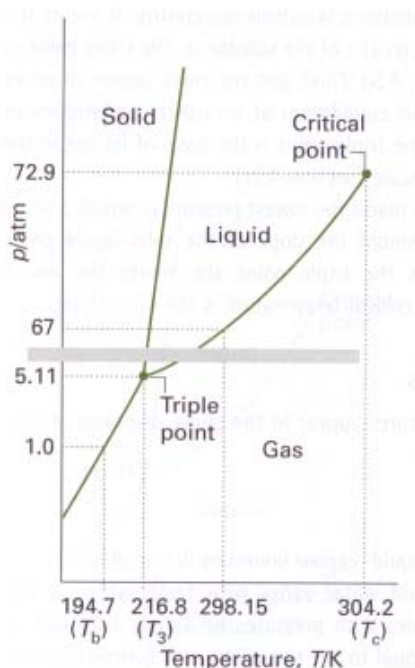


Figure 3: The phase diagram of CO₂ according to Atkins, 1998

On the other hand a crystalline solid has a perfect structure (see Fig. 4). A liquid can be considered as a modified solid. The information obtained by diffraction experiments is often presented graphically by means of the “radial distribution function”. The radial distribution function is a measure of the average density as a function of distance from some arbitrary origin. In Fig. 4 we see that liquid Hg resembles more the solid than the gaseous state, suggesting the existence of short-range order in liquids and the legitimate description of liquid as a modified solid. It is therefore evident that a liquid is somehow structured but the structure is not perfect. It should be possible however to give an estimate concerning e.g. the coordination number of the structure of the liquid. In case of water it can be assumed that the coordination number is in the vicinity of 4. This reasoning is supported by the fact that water is present in the form of H₂O clusters, which disintegrate and/or formed again. The half-life of these structures is considered to be around 10⁻¹⁰ to 10⁻¹¹s (“flickering clusters”, “formation and dissolution of Nano-Icebergs”). Solidified water (ice) has a coordination number $z=4$ having a diamond structure (Frank et al., 1957).

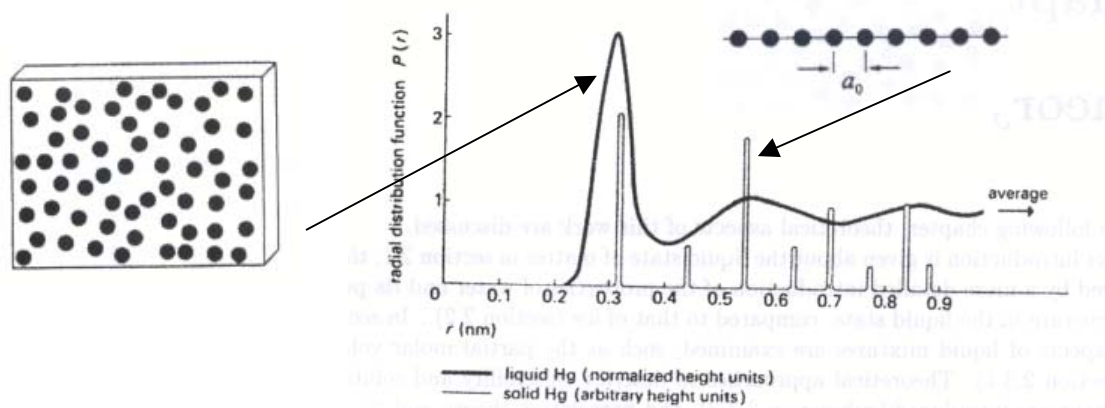


Figure 4: Radial distribution function in liquid and solid mercury. The radius is measured from an arbitrary atom chosen as origin (Tabor, 1991)

4.6.4 Materials and methods

4.6.4.1 Solvents

The binary mixtures of DMSO-water, diglycerol-water and 1,4-dioxane-water were examined at 298.2 K. Bidistilled water was freshly prepared by means of a Fontavapor 285 (Büchi AG CH-Flawil). Dimethylsulfoxid of high purity ($\geq 99.5\%$) was acquired commercially from Fluka Chemie GmbH CH (art. No. 41644) DMSO-water solutions were stored tightly covered since DMSO is strongly hygroscopic. 1,4-Dioxane of high purity was acquired commercially from Fluka Chemie GmbH CH- Buchs (art. No. 42512) Diglycerol was supplied by Solvay GmbH D-Rheinberd (art.No. 71021328).

4.6.4.2 Experimental setup and data analysis

4.6.4.2.1 Measurement of the static permittivity and conductivity: The use of the E_i/E parameter in the characterization of aprotic liquids at room temperature: Data analysis

The measurement of the static permittivity and conductivity as well as the calculation of the E_i/E parameter for binary liquid mixtures is described in detail elsewhere (Hernandez-Perni et al., 2004b)

For the determination of the dielectric constant, the precision LCR meter at 100 KHZ, Agilent Technologies Inc. USA-Palo Alto, CA was used. The sample was kept at 298.2 K (± 0.1 K) with a thermostat (Thermomix UB and Frigomix U-1, B. Braun Biotech International GmbH D-Melsungen).

E_i/E for binary mixtures was calculated according to the following equation (Stengele et al., 2002):

$$\frac{E_i}{E} = \frac{M_{r,m}}{3 \cdot \rho_m} \cdot \frac{\varepsilon_m - 1}{\frac{N_A}{3 \cdot \varepsilon_0} \left[V_1 \left(\alpha_1 + \frac{\mu_{g,1}^2}{3 \cdot K \cdot T} \right) + V_2 \left(\alpha_2 + \frac{\mu_{g,2}^2}{3 \cdot K \cdot T} \right) \right]} - \frac{\varepsilon_m + 2}{3} \quad (9)$$

where ρ_m = density of mixture; $M_{r,m}$ = molecular weight of the mixture; ε_m = quasi-static relative dielectric constant for the mixture; V_1 = volume fraction of liquid 1; V_2 = volume fraction of liquid 2.

The dipole moments μ_g used for calculations are literature values for the gas phase (CRC Handbook of Chemistry and Physics, 1997)

The polarizability was determined via the Lorentz-Lorenz-equation, which gave excellent results compared with literature data (Riddick and Bunger, 1970) both for polar and nonpolar compounds (see Eq. (10)).

$$\frac{n^2 - 1}{n^2 + 2} \frac{M_r}{\rho} = \frac{N_A}{3\varepsilon_0} \alpha \quad (10)$$

The measurements of the density ρ were made using a vibrating-tube densimeter (Density Meter Anton Paar AG A-8054 Graz DMA 58;8), refractive index n_D were

measured by means of the Abbé refractometer (A. Krüss Optronic GmbH D-22297 Hamburg AR8; 30098).

For calculating the respective contributions of the liquids, their volume contributions are considered. For the description of binary mixtures by means of percolation theory, the volume fractions are used, as they are more meaningful for the characterization of geometric three-dimensional networks than molar fractions (Stengele et al., 2002).

The correlation factor g was calculated following the Kirkwood-Fröhlich equation for binary mixtures, using the volume fractions for calculations instead of molar fractions, so that the results are comparable to the values for E_i/E [21].

$$\frac{(\varepsilon_m - \varepsilon_{\infty,m}) \cdot (2 \cdot \varepsilon_m + \varepsilon_{\infty,m})}{\varepsilon_m (\varepsilon_{\infty,m} + 2)^2} = \frac{N_A}{9 \cdot \varepsilon_0 \cdot K \cdot T} \cdot \frac{\rho_m}{M_{r,m}} \cdot (V_1 \mu_{g,1}^2 + V_2 \mu_{g,2}^2) \cdot g \quad (11)$$

For $\varepsilon_{\infty,m}$, the square of the refractive index of the mixture at $\lambda=589.3$ nm was used.

The molar volume of a pure liquid is defined as:

$$V_m = \frac{M_r}{\rho} \quad [\text{cm}^3 \text{mol}^{-1}] \quad (12)$$

where M_r = molecular weight (gmol^{-1}) and ρ = density (gcm^{-3}).

In order to get a parameter, which defines the density of the squared dipole moment per molar volume ($D_{\mu\mu}$), the following variables were defined (Hernandez-Perni et al., 2004a):

$$D_{\mu\mu} = \frac{\mu^2}{V_m} \quad [\text{D}^2 \text{molcm}^{-3}] \quad (13)$$

The dipole moment μ is given in debye units (D). The conversion factor to SI units is $1 \text{ D} = 3.33564 \times 10^{-30} \text{ C m}$.

The squared value of the Hansen parameters ($\delta_d^2, \delta_p^2, \delta_h^2$) was taken according to the Hansen equation (see Eq. (14)).

$$\delta_t^2 = \delta_d^2 + \delta_p^2 + \delta_h^2 \quad (14)$$

Substance	E_i/E -value	$^1) \delta_t^2$ (MPa)	$^1) \delta_p^2$ (MPa)	$^1) \delta_h^2$ (MPa)	$^1) \delta_d^2$ (MPa)
DMSO	-13.26	712.89	268.96	104.04	338.56
Acetonitrile	-10.97	595.36	324.00	37.21	234.09
Dimethylformamide	-10.08	615.04	187.69	127.69	302.76
Dimethylacetamide	-9.78	515.29	132.25	104.04	282.24
Methylpyrrolidone	-8.79	524.41	151.29	51.84	324.00
Acetone	-5.37	400.00	108.16	49.00	240.25
Methyl ethyl ketona	-3.92	361.00	81.00	26.01	256.00
Tetrahydrofuran	-1.04	376.36	32.49	64.00	282.24
Ethyl acetate	-0.79	327.61	28.09	51.84	249.64
1,4-Dioxane	0.02	420.25	3.24	54.76	361.00
Substance	$(\delta_p^2 + \delta_h^2)^{1/2}$	$D_{\mu\mu}$ ($\text{D}^2 \text{ mol cm}^{-3}$)	$^2) E_T(30)$ (Kcal mol $^{-1}$)	$^2) E_T^N$	
DMSO	19.31	0.220	45.10	0.44	
Acetonitrile	19.01	0.294	45.60	0.46	
Dimethylformamide	17.76	0.199	43.20	0.39	
Dimethylacetamide	15.37	0.148	42.90	0.38	
Methylpyrrolidone	14.25	0.175	-	-	
Acetone	12.54	0.113	42.20	0.36	
Methyl ethyl ketona	10.34	0.086	41.30	0.33	
Tetrahydrofuran	9.82	0.038	37.40	0.21	
Ethyl acetate	8.94	0.032	38.10	0.23	
1,4-Dioxane	7.62	0.000	36.00	0.16	

Table 2: Physical properties of pure solvents ($^1)$ source: Barton, 1991; $^2)$ source: Reichardt, 1994)

For the study of the correlation between the parameter E_i/E and $D_{\mu\mu}$ and the squared value of the total and the partial solubility parameters as well as for the correlation

between E_i/E parameter and the $E_T(30)$ parameter (Reichardt, 1994) and the normalized E_T^N values (Reichardt, 1994) the data compiled in Table 2 were analyzed.

4.6.4.2.2 Measurement of the complex permittivity: Calculation of the relaxation time (τ)

The measurement of the complex permittivity as well as the calculation of the relaxation time (τ) for binary liquid mixtures is described in detail elsewhere (Hernandez-Perni et al., 2004b)

For the determination of the real (ϵ') and imaginary (ϵ'') permittivity the HP 8720D Vector Network Analyzer, Agilent Technologies Inc. USA-Palo Alto, CA was used. The sample was kept at 298.2 K (± 0.1 K) with a thermostat (Thermomix UB and Frigomix U-1, B. Braun Biotech International GmbH D-Melsungen). Measurements were made between 0.2 and 20 GHz at 401 frequencies. The Auto Sweep Time Mode was selected. This mode maintains the fastest sweep speed possible for the current measurement settings. A sweep time = 13.052 s was obtained for measurements between 0.2 and 20 GHz at 401 frequencies.

The following software were used for data analysis: *Excel* Microsoft corp. USA-Redmond WA 98052-6399 Version 97 SR-2 and *SYSTAT for Windows* SPSS Inc. USA-Chicago IL 60606-6307 Version 7.0, where the inclusion of both real and imaginary parts for fitting can be made as the term $(\epsilon - \epsilon_\infty)$ occurs in both parts (see Eqs. (7) and (8)). Data were fitted in these equations by using nonlinear regression (Gauss-Newton with Least Squares estimation).

4.6.4.2.3 Subdivision of curves into segments by means of nonlinear regression: detection of percolation thresholds

The Subdivision of curves into segments by means of nonlinear regression in order to detect percolation thresholds is described in detail elsewhere (Hernandez-Perni et al., 2004b)

The data were inspected in order to decide about a suitable number of sub-segments and potential critical concentrations. In a second step they were arbitrary split into three straight subsegments around these possible critical volume fractions $(V_x/V)_{crit}$. Using nonlinear regression, the data were fitted to the following equation:

$$y = A (m_1x + b_1) + B (m_2x + b_2) + C (m_3x + b_3) \quad (15)$$

The final decision to which segment the data are to be assigned is made considering the mean corrected coefficient R^2 for the overall fit.

The software used was: *Systat for Windows* SPSS Inc. USA-Chicago IL 60606-6307 Version 7.0.

For the description of binary mixtures by means of percolation theory, the volume fractions are used, as they are more meaningful for the detection of the percolation thresholds, described by Stauffer and Aharony, 1998 (Introduction to Percolation Theory) as “geometrical phase transitions”.

4.6.5 Results and discussion

4.6.5.1 *The use of the E_i/E parameter in the characterization of aprotic liquids at room temperature*

It was possible to show in a previous paper (Hernandez-Perni et al., 2004a) that there is a correlation between E_i/E and the total and the partial solubility parameters. It became evident that the squared correlation coefficient could be still improved if E_i/E is correlated to the squared value of the total and partial solubility parameters. Thus, for the following analysis the E_i/E –values were correlated as a first choice with the squared value of the total and partial solubility parameters. A close inspection of the data in Table 2 leads to the following results. A satisfactory correlation between the E_i/E parameter and the squared value of the total Hildebrand solubility parameter was obtained (see Fig. 5, Eq. (16)).

This result is not as good as in the case of polar substances able to form hydrogen bonds ($E_i/E = f(\delta_t^2)$: $r^2 = 0.99$), where we also found an excellent respectively good correlation between the E_i/E parameter and the squared of the partial Hildebrand solubility parameters δ_h and δ_p ($E_i/E = f(\delta_h^2)$: $r^2 = 0.98$ respectively $E_i/E = f(\delta_p^2)$: $r^2 = 0.92$). For aprotic substances a satisfying correlation can be established with the polar component of the Hansen equation (see Fig. 6, Eq. (17)). However no correlation exists between the E_i/E parameter and the hydrogen-bonding component of the Hansen equation (see Fig. 7, Eq. (18)), which is not surprise due to the fact that no hydrogen bonding between pure aprotic molecules exists.

However, it is of interest that E_i/E can also be correlated with the combined partial solubility parameter $\delta_{hp} = (\delta_h^2 + \delta_p^2)^{1/2}$, which leads to an improved correlation coefficient of $r^2 = 0.95$.

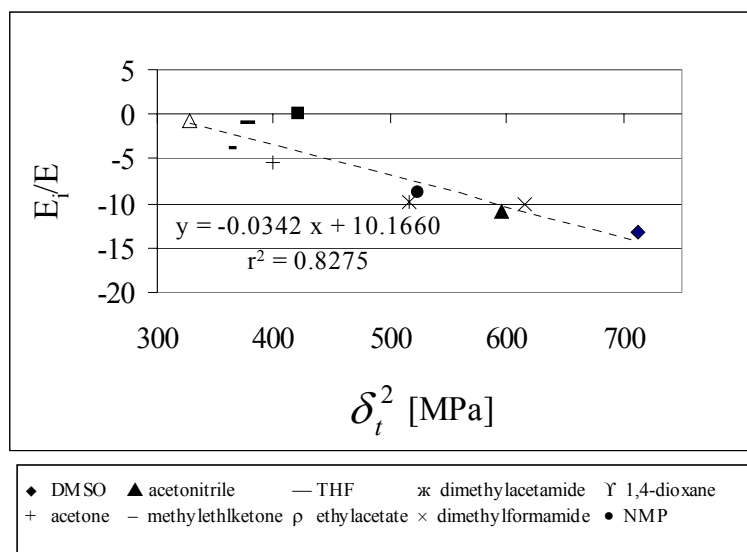


Figure 5: E_i/E values as a function of the squared total Hildebrand solubility parameter for aprotic substances at 298.2K

$$E_i/E = -0.03 \delta_t^2 + 10.17 \quad r^2 = 0.83 \quad (16)$$

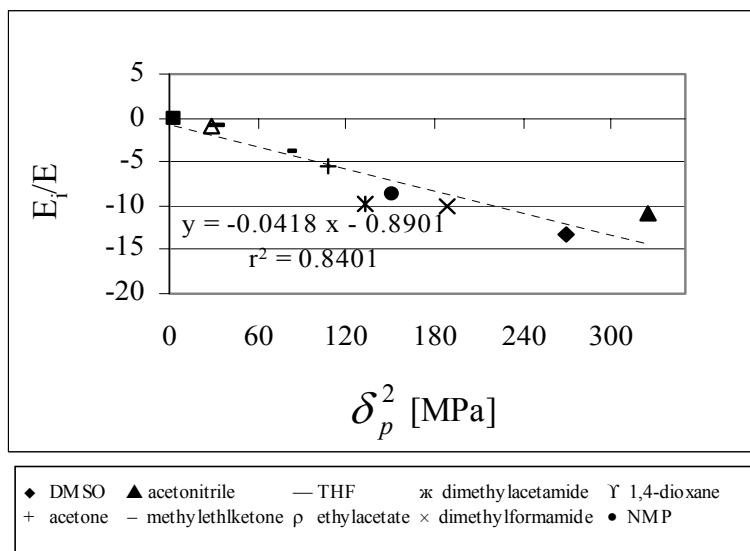


Figure 6: E_i/E values as a function of the squared partial Hansen solubility parameter δ_p for aprotic substances at 298.2K

$$E_i/E = -0.04 \delta_p^2 - 0.89 \quad r^2 = 0.84 \quad (17)$$

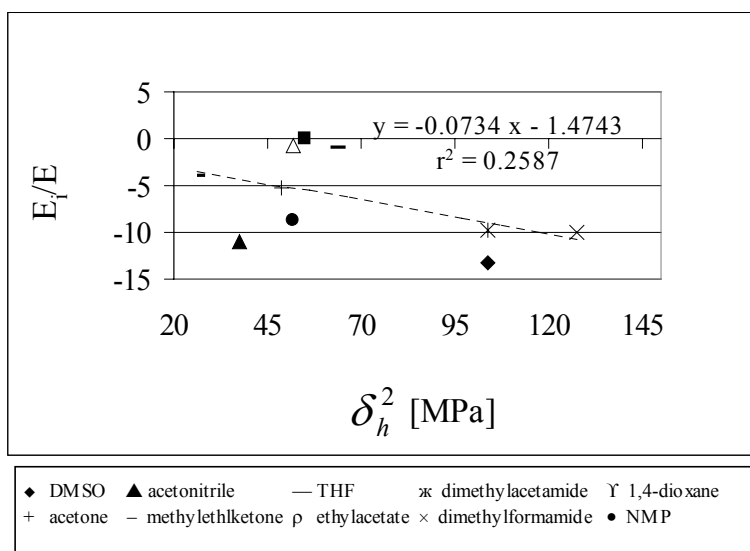


Figure 7: E_i/E values as a function of the squared partial Hansen solubility parameter δ_h for aprotic substances at 298.2K

$$E_i/E = -0.07 \delta_h^2 - 1.47 \quad r^2 = 0.26 \quad (18)$$

As expected no correlation can be observed with the dispersive partial solubility parameter, i.e. δ_d ($r^2 < 0.01$).

It is important to keep in mind that the squared values of the solubility parameters were taken for two reasons:

a) For polar substances the relation $E_i/E = f(D_{OH})$ was analyzed (D_{OH} defines the density of OH-groups per volume). We were therefore looking at the system per volume. The close molecular-molecular interactions per volume are correlated with the density of hydroxy groups per molar volume (D_{OH}). When the relation $E_i/E = f$ (solubility parameter) is investigated, the squared value of the solubility parameters is taken due to the fact that the squared solubility parameter corresponds to the endoergic process of separating the solvent molecules to provide a suitably sized enclosure for the solute and measures the work required to produce a cavity of unit volume in the solvent. This term is related to the tightness or structuredness of solvents as caused by intermolecular solvent/solvent interactions (Barton, 1991). Therefore, the squared solubility parameter gives us the amount of Van der Waals forces that held the molecules of the liquid together per molar volume.

$$\delta = \sqrt{c} = \left[\frac{\Delta H - R \cdot T}{V_m} \right]^{\frac{1}{2}} \quad \text{or} \quad \delta^2 = c = \frac{\Delta H - R \cdot T}{V_m} \quad (19)$$

For aprotic substances the squared value of the solubility parameters was taken for the same reason. We need a relation per molar volume.

b) The squared values of the total and partial solubility parameters have the advantage that the dimension is equal to energy per volume having a clear meaning. Nevertheless, It is important to point out that the squared values were slightly better for δ_h i.e. $E_i/E = f(\delta_h^2)$; in the same order for δ_t i.e. $E_i/E = f(\delta_t^2)$ and slightly worse for δ_p i.e. $E_i/E = f(\delta_p^2)$. It is of interest, that a very good correlation is found for combined solubility parameters δ_{ph} and δ_{ph}^2 ($E_i/E = f((\delta_h^2 + \delta_p^2))$) and $E_i/E = f((\delta_h^2 + \delta_p^2)^{1/2})$ (see Table 3)

Similar polar substances being able to form hydrogen bonds only a good estimation for the total (δ_t) and the squared value of the partial solubility parameter (δ_p) can be obtained by determining the corresponding E_i/E values.

Aprotic Substances			
	r^2		r^2
$E_i/E = f(\delta_t^2)$	0.828	$E_i/E = f(\delta_t)$	0.832
$E_i/E = f(\delta_p^2)$	0.840	$E_i/E = f(\delta_p)$	0.901
$E_i/E = f(\delta_h^2)$	0.259	$E_i/E = f(\delta_h)$	0.226
$E_i/E = f(\delta_d^2)$	0.005	$E_i/E = f(\delta_d)$	0.005
$E_i/E = f(\delta_h^2 + \delta_p^2)$	0.915	$E_i/E = f((\delta_h^2 + \delta_p^2)^{1/2})$	0.949

Table 3: correlation coefficient obtained for different correlations between the E_i/E parameter and the total and partial solubility parameters for aprotic liquids.

According to Eq. (20) a linear dependence between E_i/E and $D_{\mu\mu}$ also exists for aprotic liquids (see Fig. 8).

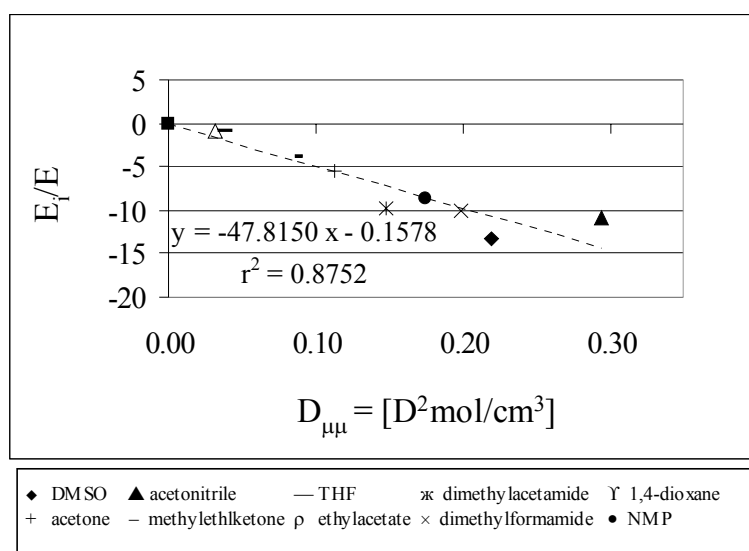


Figure 8: E_i/E values as a function of $D_{\mu\mu}$ for aprotic substances at 298.2 K

$$E_i/E = -47.82 D_{\mu\mu} - 0.16 \quad r^2 = 0.87 \quad (20)$$

Finally, it was also possible to find a good correlation between the E_i/E parameter and the empirical solvent polarity parameter $E_T(30)$ at room temperature and also between the E_i/E parameter and the normalized E_T^N parameter (see Figs. 9 and 10 corresponding Eqs. (21) and (22)). That confirms the important role of the E_i/E parameter in the characterization of not only polar liquids able to form hydrogen bonds but also aprotic liquids.

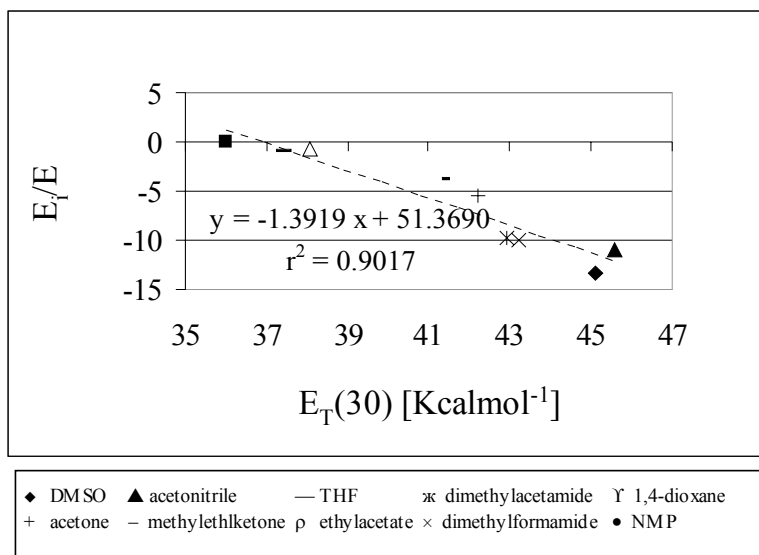


Figure 9: E_i/E values as a function of $E_T(30)$ for aprotic substances at 298.2 K

$$E_i/E = -1.39 E_T(30) + 51.37 \quad r^2 = 0.90 \quad (21)$$

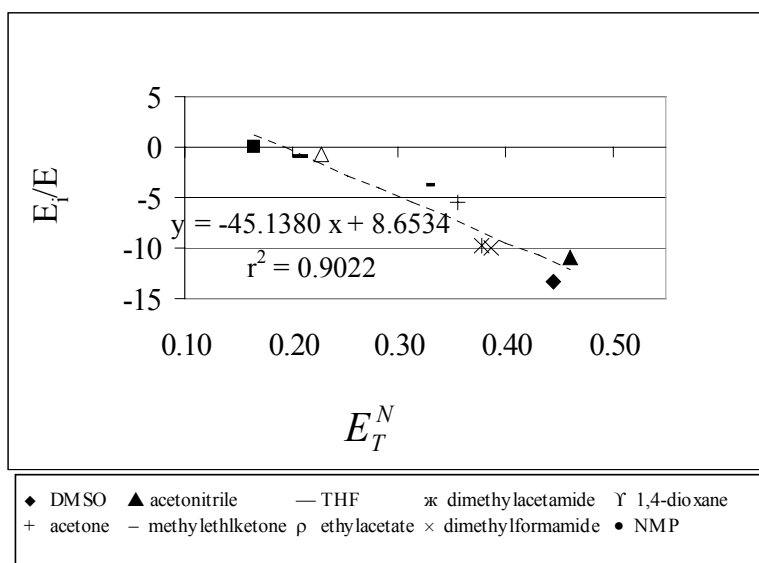


Figure 10: E_i/E values as a function of E_T^N for aprotic substances at 298.2 K

$$E_i/E = -45.14 E_T^N + 8.65 \quad r^2 = 0.90 \quad (22)$$

4.6.5.2 *Percolation phenomena observed in DMSO-water mixtures based in the results of the modified Clausius-Mossotti-Debye equation*

The E_i/E -values for the investigated DMSO-water binary mixtures at 298.2K are represented in Fig. 11. The E_i/E -values can be subdivided in three linear segments. The intersections are located at ca. 32% and 74% (V_{wa}/V). The lower intersection at ca. 32% (V_{wa}/V) can be interpreted as the percolation threshold of water. The second one at 74% (V_{wa}/V) can be assumed as the upper percolation threshold, where DMSO starts to form isolated clusters and is no longer percolating the system.

DMSO-water mixtures represents one of the more complicated binary systems, namely an associating component (water) plus a second component (DMSO) acting only as a hydrogen bond acceptor (Luzar, 1990).

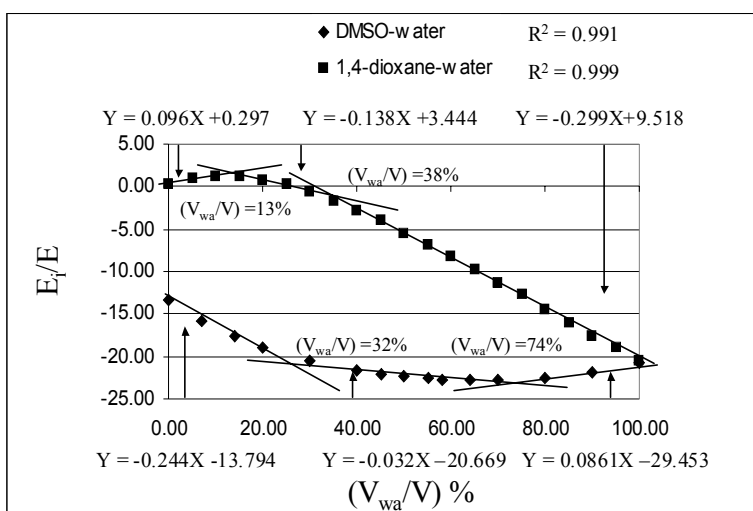


Figure 11: E_i/E values of the DMSO-water binary mixtures at 298.2 K. The intersections are located at ca. 32% and 74% (V_{wa}/V) and E_i/E values of the 1,4-dioxane-water binary mixtures at 298.2 K with intersections at ca. 13% and 38% (V_{wa}/V)

It is interesting to compare the behavior of 1,4-dioxane-water and DMSO-water mixtures (see Fig. 11). In 1,4-dioxane-water binary mixtures it is not possible to detect percolation threshold between 38% (V_{wa}/V) and 100% (V_{wa}/V). It is possible that water starts to percolate at ca 13% (V_{wa}/V), or that a change of the “lattice structure” of the 1,4-dioxane-water systems occurs. It can be shown that the water molecules form isolated islands in a continuous phase of 1,4-dioxane as it is possible to get a better estimate of the dipole moment of water using the classical Debye equation for decreasing water concentration below 13% (V_{wa}/V). A second critical concentration is

observed at 38% (V_{wa}/V), which would correspond in fact to a percolation threshold of lattices with a coordination number close to 4 (diamond lattice) (see Table 1)

In this context it has to be kept in mind that the structure of ice at normal pressure and close to 0°C corresponds to a tetrahedral configuration with the coordination number 4. According to the model of water described by a dynamic equilibrium of “nano-icebergs” which are formed and dissolve a coordination number close to 4 can be adopted. The upper percolation threshold is not visible, which indicates that 1,4-dioxane fits well into the water. It can be assumed that the volume of a single water cluster with 5 water units has a similar molar weight [$mw = 90.10 \text{ gmol}^{-1}$], and a similar volume as one 1,4-dioxane molecule [$mw = 88.11 \text{ gmol}^{-1}$]. With DMSO-water binary mixtures both percolation threshold can be detected: The lower one at ca. 32% (V_{wa}/V) water and the upper one at 74% (V_{wa}/V). If the E_i/E values of the pure solvents are not taken into account the following percolation thresholds are obtained for DMSO-water binary mixtures: the lower value at ca. 34% (V_{wa}/V), and the upper value at ca. 66% (V_{wa}/V). If we consider our binary mixture being somehow structured it complies with the idea of having a critical concentration at 34% (V_{wa}/V) for the lower p_c respectively 66% ($34\%(V_{dmsO}/V)$) for the upper p_c , which corresponds to the percolation thresholds of a three dimensional lattice with a coordination number of $z \approx 4$. Thus, it can be concluded that DMSO does not seem to induce a major disruption of the water structure. Between the two percolation thresholds both components percolate. Thus, more hydrophobic substances can be dissolved in the continuous phase of DMSO. Thus, the special physiological properties of the DMSO-water mixtures may be related to the fact, that the water structure is not heavily modified. It seems to be the case, that the tetrahedral coordination remains intact (Soper and Luzar, 1992) with the whole range of DMSO-water mixtures. On the other hand, the value of E_i/E decreases to a minimum at the upper percolation threshold indicating a higher local electric field E_i . This effect can be related to the high dipole moment of DMSO. This dipole moment is also responsible for the different behavior of DMSO-water mixtures compared to 1,4-dioxane-water mixtures of the E_i/E values (see Fig. 11).

4.6.5.3 Percolation phenomena observed in DMSO-water binary mixtures based in the results of g -values according to the Kirkwood-Fröhlich equation

The g -values for the binary mixtures of DMSO-water binary mixtures at 298.2K are presented in Fig. 12. The curve can be subdivided into three linear segments. The intersections of the linear segments are located at ca. 35% (V_{wa}/V) and ca. 77% (V_{wa}/V). These findings are compatible with the findings of Fig. 11 (E_i/E -values) for the lower and upper p_c as it is well known that the location of the critical concentrations may be influenced by the sensitivity of the of the parameter to be chosen to detect the p_c .

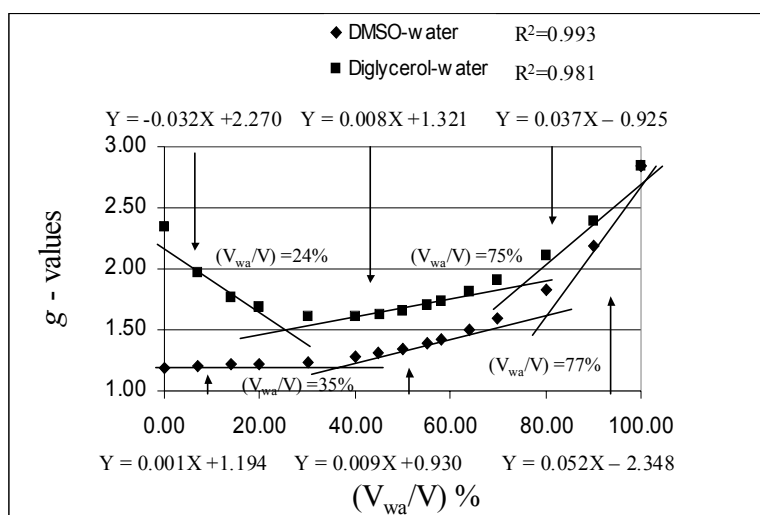


Figure 12: The values of the correlation factor g of the Kirkwood-Fröhlich Eq. (Eq. (3)) for the binary mixtures of DMSO-water with intersections at ca. 35% and 77% (V_{wa}/V) at 298.2K, and Diglycerol-water binary mixtures with intersections at ca. 24% and 75% (V_{wa}/V) at 298.2K.

Unlike polar liquids capable of forming hydrogen bonds (Stengele et al., 2002) such as diglycerol in a mixture with water, the aprotic DMSO behaves differently with respect to the g -values (see Fig. 12). In the case of DMSO we find a region nearly constant with g -values close to $g \approx 1$ till ca. 35% (V_{wa}/V). Thus, this finding confirms that there is no structure breaking effect of the DMSO structure by adding water. Below 35% (V_{wa}/V), i.e. below the lower percolation threshold the water molecules fit well into the DMSO-structure of the liquid. Due to the value of $g \approx 1$ the water molecules are either randomly distributed in the solvent mixture or in an antiparallel alignment with the dipole moment of DMSO.

Above the critical concentration of 35% (V_{wa}/V) the g-values are increasing i.e. the dipole moments of water and DMSO assume more and more a parallel alignment. A parallel alignment of the dipole moments is being formed due to the increase in the hydrogen bonding formation. From the point of view of percolation theory 35% (V_{wa}/V) corresponds with the lower percolation threshold (see section 4.6.5.2) where water starts to form infinite clusters, both water and the DMSO percolate the system up to ca. 77% (V_{wa}/V) where the second percolation threshold is found. From that point DMSO starts to form isolated clusters and is no longer percolating the system.

4.6.5.4 *Relaxation time according to the Debye equation for the complex dielectric permittivity ϵ^**

The Debye equation is able to characterize the whole range of DMSO-water mixtures with $R^2 = 0.997$ showing with respect to the relaxation time (τ) a lower percolation threshold ca. 32% (V_{wa}/V) and an upper percolation threshold ca. 73% (V_{wa}/V) (Fig. 13). It is of interest to point out that in the case of the methanol-water mixtures the behavior of the relaxation time can be only be described by a single Debye equation with a $R^2 \geq 0.997$ between 58%-100% (V_{wa}/V). The fact that the Debye equation is able to describe the whole range of DMSO-water mixtures is another strong evidence that the lattice type seems to remain intact. It is worth to realize that the percolation thresholds remain more or less at the same positions (see Table 4) independent of the choice of the parameters for their detection. In case of the 1,4-dioxane-water mixture [20] the behavior of the relaxation time can only be described by a single Debye function with an adequate correlation coefficient R^2 between 80%-100% (V_{wa}/V). Only the superposition of a Debye equation with the Cole-Davidson equation leads to a satisfactory R^2 values (see Fig. 13).

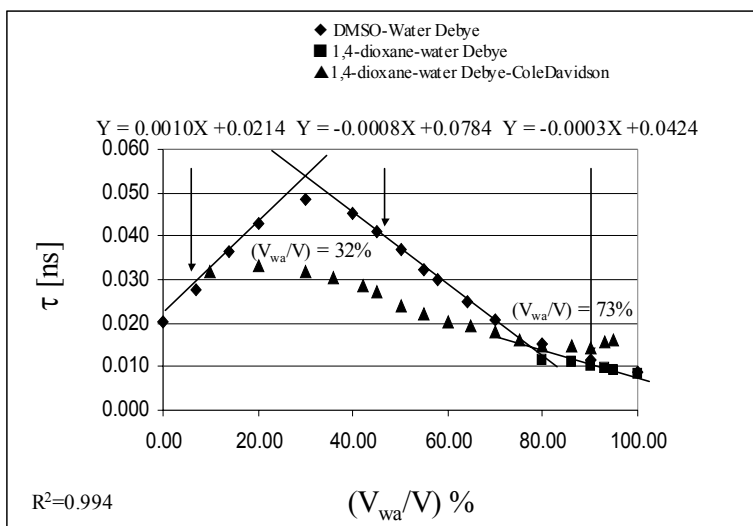


Figure 13: Relaxation behavior of the dipole of DMSO in water mixtures as a function of the % volume fraction of water (V_{wa}/V) with intersections at ca. 32% and 73% (V_{wa}/V) at 298.2 K which can be described by the Debye equation. In the case of 1,4-dioxane (no dipole moment)-water mixtures the relaxation behaviour of the water dipole moment can be only described by a single Debye function with an adequate correlation coefficient R^2 ($R^2 \geq 0.99$) in the range of 80% (V_{wa}/V) to 100% (V_{wa}/V). In the range of 0% (V_{wa}/V) to 100% (V_{wa}/V) the relaxation behavior needs to be described by a superposition of the Debye function with the Cole-Davidson distribution function to obtain an $R^2 \gg 0.98$.

4.6.5.5 *Other physical properties explaining the phenomenon of percolation in DMSO-water binary mixtures.*

It is evident that percolation thresholds can also be detected with other physical parameters. The results are compiled in Table 4 together with literature data concerning the viscosity, adiabatic compressibility and freezing point of binary mixtures and in Figs. 14, 15 and 16. With the dielectric constant we can detect not only the lower but also the upper percolation threshold. With refractive and density it is only possible to detect the lower percolation threshold. Tommila et al., 1969 also measured the dielectric constant of several DMSO-water binary mixtures observing a maximum at 72 mol % water (40% (V_{wa}/V)) but they did not give a clear interpretation. Cowie et al., 1961 also measured the viscosity, density and refractive index of several DMSO-water binary mixtures. They also observed a positive deviation from linearity in those properties but could not give a clear interpretation. They only suggested a greater *degree of association* in DMSO-water mixtures than in water alone, i.e. they did not seem to realize the percolation phenomenon.

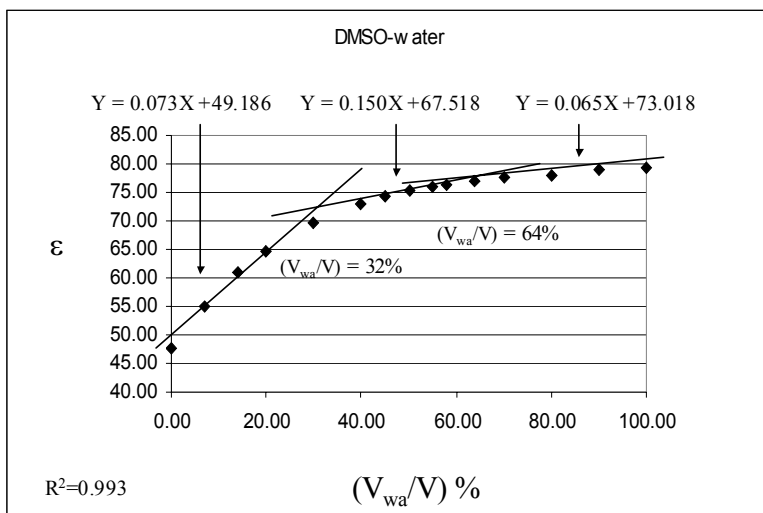


Figure 14: Dielectric constant values for the DMSO-water binary mixtures with intersections at ca. 32% and 64% (V_{wa}/V) at 298.2K.

	<i>Low percolation threshold</i> (% (V_{wa}/V).	<i>Upper percolation threshold</i> (% (V_{wa}/V).
E_i/E -parameter	32	74
g-values	35	77
Relaxation time (τ)	32	73
Dielectric constant (ϵ)	32	64
Viscosity ¹	32	Not detectable
Density	34	Not detectable
Refractive index	28	Not detectable
Adiabatic compressibility ²	37	Not detectable
Freezing point ³	32	Not detectable

Table 4: Percolation thresholds found for E_i/E -parameter from the modified Clausius-Mossotti-Debye equation, g-values obtained from the Kirkwood-Fröhlich Eq., τ , dielectric constant, viscosity, density, refractive index, adiabatic compressibility and freezing point as a function of the volume fraction of water in the investigated DMSO-water binary mixtures (¹ source: Marshall et al., 1987; ² source: Kaatze et al., 1990; ³ source: Havemeyer, 1966)

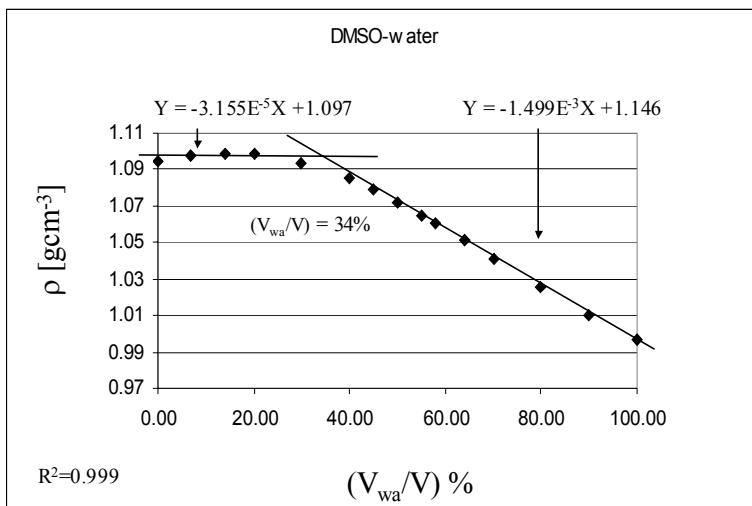


Figure 15: Density values for the DMSO-water binary mixtures with an intersection at ca. 34% (V_{wa}/V) at 298.2K.

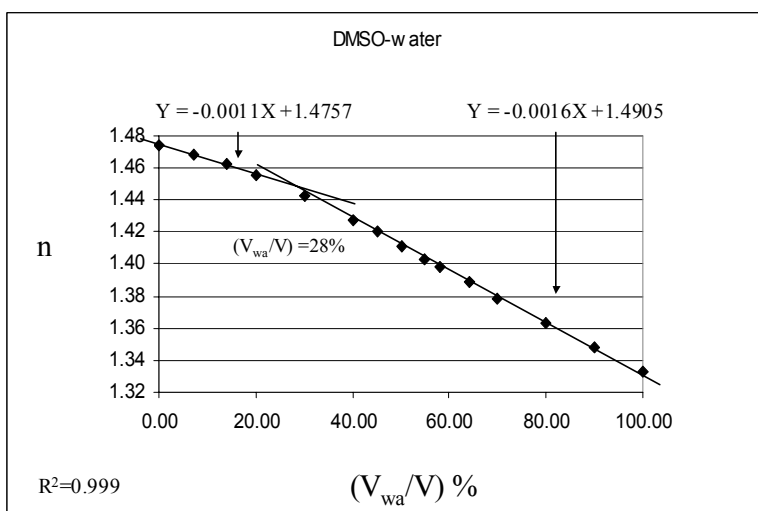


Figure 16: Refractive index values for the DMSO-water binary mixtures with an intersection at ca. 28% (V_{wa}/V) at 298.2K

4.6.6 Conclusions

It is demonstrated the important role of the E_i/E parameter in the characterization of not only polar liquids able to form hydrogen bonds but also aprotic liquids being an easier measurable alternative parameter to describe the polarity of liquids.

The phenomenon of percolation could be well demonstrated in the case of DMSO-water binary liquid mixtures.

The value of E_i/E at room temperature in the binary mixtures can also be related to the viscosity changes, which was earlier shown by Peyrelasse et al. [12] to be a percolation phenomenon.

It was possible to clarify the maximum value of the viscosity detected at 33% mole fraction in DMSO (34% (V_{wa}/V)) in the frame of percolation theory. This was possible by measuring the following parameters: E_i/E parameter obtained through the modified Clausius-Mossotti-Debye equation, g -values obtained from the Kirkwood-Fröhlich equation, relaxation time and dielectric constant data by using dielectric spectroscopy and density and refractive index. The results are listed together with literature data concerning the viscosity, adiabatic compressibility and freezing point of binary solvent mixtures. The values of the lower and upper percolation thresholds are comparable and it is of interest, that as a function of the parameter studied, only one or two percolation thresholds can be detected.

In Hernandez-Perni et al., [20] we saw that for 1,4-dioxane-water binary mixtures, the upper percolation threshold is not visible, which indicates that 1,4-dioxane fits well into the water. With DMSO-water binary mixtures both percolation thresholds can be detected. Nevertheless, it seems to be the case, that the tetrahedral coordination remains intact. For DMSO-water binary mixtures we also observe that the value of E_i/E decreases to a minimum at the upper percolation threshold indicating a higher local electric field E_i . This effect can be related to the high dipole moment of DMSO.

Unlike polar liquids capable of forming hydrogen bonds (Stengele et al., 2002) such as diglycerol in a mixture with water, the aprotic DMSO behaves differently with respect to the g -values. Here we find a region nearly constant with g -values close to $g \approx 1$ till ca. 35% (V_{wa}/V). Thus, there seems to be no structure breaking effect of the DMSO structure by adding water. Below the lower percolation threshold the water molecules fit well into the DMSO-structure of the liquid. Due to the value of $g \approx 1$ the water molecules are either randomly distributed in the solvent mixture or in an antiparallel alignment with the dipole moment of DMSO. It can be concluded that DMSO and water

have as a liquid a similar lattice structure with a coordination number 4, which facilitates the complete miscibility and seem to be one of the reasons for the special physiological behavior of DMSO-water mixtures.

As a final conclusion it is demonstrated that the use of percolation theory revealing percolation thresholds give insight into the “lattice structure” of DMSO-water mixtures and contribute to lift a bit the mystery of the behavior of DMSO-water mixtures.

4.6.7 References

Atkins, P.W., 1998. *Physical Chemistry*. Oxford University Press, Oxford, Melbourne, Tokyo.

Barton, A.F.M., 1991. *CRC Handbook of Solubility Parameters and Other Cohesion Parameters*, Second ed. CRC Press, Boca Raton.

Chen Danny, Song Di, Guillaume Wientjes M., Jessie L-S., 2003. Effect of dimethyl sulfoxide on bladder tissue penetration of intravesical Paclitaxel. *Clin. Cancer Res.*, 9, 363-369.

Cowie, J.M.G., Toporowski, P.M., 1961. Association in the binary liquid system dimethyl sulphoxide-water. *Can. J. Chem.* 39, 2240-2243.

CRC Handbook of Chemistry and Physics 77th edition, 1997. CRC Press Inc., Boca Raton.

Decareau, R.V., Mudgett, R.E., 1985. *Microwaves in the Food Processing Industry*, Academic Press, Orlando, pp. 1-54.

Frank, H.S., Wen, W.-Y., 1957. III. Ion-Solvent Interaction. Structural Aspects of Ion-Solvent Interaction in Aqueous Solutions: A Suggested Picture of Water Structure. *Disc. Farad. Soc.*, 24, 133-140.

Fröhlich, H., 1958. Theory in the liquid. Theory of Dielectrics. Oxford University Press, Oxford.

Havemeyer, R.N., 1966. Freezing point curve of dimethyl sulfoxide-water solutions. J. Pharm. Sci. 55(8), 851-3.

Hernandez-Perni, G., Stengele, A., Leuenberger, H., 2004a. Towards a better understanding of the parameter E_i/E in the characterization of polar liquids. Proceedings of the 5th Central European Symposium on Pharmaceutical Technology and Biotechnology, Ljubljana 2003. Int. J. Pharm. (submitted)

Hernandez-Perni, G., Stengele, A., Leuenberger, H., 2004b. Detection of percolation phenomena in binary polar liquids by broadband dielectric spectroscopy. Proceedings of the 5th Central European Symposium on Pharmaceutical Technology and Biotechnology, Ljubljana 2003. Int. J. Pharm. (submitted)

Jorjani, M., Rastegar, H., et al. 2003. Synthesis and Biological Evaluation of New 1, 4-Dihydropyridines as Antihypertensives Agents in Rats. Iranian J. Pharm. Res. 43-46

Kaatze, U., Brai, M., Scholle, F.D., Pottel, R., 1990. Ultrasonic absorption and sound velocity of dimethyl sulfoxide/water mixtures in the complete composition range. J. Mol. Liq. 44, 197-209.

Kirkwood, J.G., 1939. The dielectric polarization of polar liquids. J. Chem. Phys. 7, 911-919.

Luzar, A. 1990. Dielectric behavior of DMSO-water mixtures: a hydrogen-bonding model. J. Mol. Liq. 46, 221-38.

Marshall, D.B., McHale, J. L., Carswell, S., Erne, D., 1987. Properties of nonideal binary solutions. An integrated physical chemistry experiment. J. Chem. Educ. 64(4), 369-70.

Peyrelasse, J., Moha-Ouchane, M., Boned, C. 1988. Viscosity and the phenomenon of percolation in microemulsions. *Phys. Rev. A* 38(8), 4155-61.

Rangel, C., Niell, H., Miller, A., Cox, C. 1994. Taxol and taxotere in bladder cancer: *in vitro* activity and urine stability. *Cancer Chemoth. Pharm.*, 33, 460–464.

Reichardt, C., 1994. Solvatochromic dyes as solvent polarity indicators. *Chem. Rev.* 94, 2319-2358.

Riddick, J.A., Bunger, W.B., 1970. *Techniques of Chemistry*, vol. 2, Third ed. Wiley, New York.

Roth, B. J., 1995. Preliminary experience with paclitaxel in advanced bladder cancer. *Semin. Oncol.*, 22, 1–5.

Sahimi, M., 1994. *Applications of percolation theory*, Taylor & Francis, London.

Soper, A. K., Luzar, Alenka. 1992. A neutron-diffraction study of dimethyl sulfoxide-water mixtures. *J. Chem. Phys.* 97(2), 1320-31.

Stauffer, D., Aharony, A., 1998. *Introduction to Percolation Theory*, second ed. Taylor & Francis, London.

Stengele, A., Rey, St., Leuenberger, H., 2001 A novel approach to the characterization of polar liquids Part 1: pure liquids. *Int. J. Pharm.* 225, 123-134.

Stengele, A., Rey, St., Leuenberger, H., 2002. A novel approach to the characterization of polar liquids. Part 2: binary mixtures. *Int. J. Pharm.* 241, 231-240.

Tabor, D., 1991. *Gases, liquids and solids*, 3rd Ed., Cambridge University Press, Cambridge, pp. 253-295.

Tommila, E., Pajunen, A., 1969. The dielectric constants and surface tensions of dimethyl sulphoxide-water mixtures. *Suom. Kemistil. B* 41, 172-176.

Wood, D.C., Wood, J., 1975. Pharmacologic and biochemical considerations of dimethyl sulfoxide, *Ann. N.Y. Acad. Sci.*, 243, 7-18

Outlook

In the present work it was shown the important role of the E_i/E parameter in the characterization of polar liquids. It could be demonstrated that the application of the broad range dielectric spectroscopy together with the analysis of the quasi-static permittivity using the modified Clausius-Mosotti-Debye equation can be used to detect percolation phenomena in binary polar liquid mixtures. It leads to a valuable insight into the structure of polar liquids and to a better understanding of binary systems. However, it has to be kept in mind, that besides of percolation thresholds as critical concentrations it is also possible to detect a change of the coordination number as a function of the volume ratio of the components, which involves a change of the lattice type. It is sometimes difficult to discriminate between p_c or lattice change and more studies are needed in order to distinguish between these two processes. It might also be useful to add additional analytical methods.

It was possible to clarify the non-linear behavior of the DMSO-water mixtures founded in different measured physical properties. This was possible by measuring dielectric spectroscopy parameters such as the E_i/E parameter obtained through the modified Clausius-Mosotti-Debye equation, g -values obtained from the Kirkwood-Fröhlich equation, relaxation time and dielectric constant and comparing them with literature data concerning the viscosity, adiabatic compressibility and freezing point of binary solvent mixtures. The results were interpreted in the frame of percolation theory. The values of the lower and upper percolation thresholds are comparable and it is of interest, that as a function of the parameter studied, only one or two percolation thresholds can be detected. It is necessary to remark that despite the large number of techniques that have been applied to the study of the DMSO-water system, the behavior of this system is still a mystery.

For future pharmaceutical research it could be interesting to extend the dielectric spectroscopy studies to the Nanotechnology. This is in my view an exciting perspective. Stromme (Proc. SPIE Int. Soc. Opt. Eng. 5118 pp 310-322, 2003) demonstrated how dielectric spectroscopy can be used as a tool to obtain insight about properties on the nano-scale of interfaces of pharmaceutical interest. An outline for studying the adhesion in terms of a compatibility factor between pharmaceutical gels and biological tissue was put forward.

Appendix A

E_i/E values of diglycerol/water, PEG200/water, acetone/water, DMSO/water, NMP/water and methanol/water at 298.2 K and compared with literature values for the binary mixtures of glycerol/water, and ethanol/water (¹ Stengele, 2002).

% (V_{wa}/V)	E_i/E-values diglycerol/water	% (V_{wa}/V)	¹E_i/E-values glycerol/water	% (V_{wa}/V)	E_i/E-values methanol/water
0	-6.16	0	-8.54	0	-5.26
7	-8.66	6	-9.90	7	-6.62
14	-10.53	12	-11.18	14	-7.83
20	-11.92	17	-12.23	20	-8.88
30	-13.71	26	-13.71	30	-10.56
40	-15.35	35	-15.00	40	-12.27
45	-16.08	40	-15.67	45	-13.21
50	-16.74	44	-16.23	50	-13.90
55	-17.41	49	-16.82	55	-14.67
58	-17.69	53	-17.25	58	-15.00
64	-18.36	59	-17.89	64	-15.86
70	-19.02	65	-18.49	70	-16.70
80	-19.74	76	-19.38	80	-18.04
90	-20.31	88	-20.23	90	-19.46
100	-20.73	100	-20.62	100	-20.73
% (V_{wa}/V)	¹E_i/E-values ethanol/water	% (V_{wa}/V)	E_i/E-values PEG200/water	% (V_{wa}/V)	E_i/E-values acetone/water
0	-2.45	0	-3.11	0	-5.37
7	-3.76	7	-5.85	7	-6.85
14	-5.04	14	-7.87	14	-8.35
20	-6.15	20	-9.31	20	-9.41
30	-7.92	25	-10.46	30	-11.43
40	-9.85	30	-12.18	40	-13.30
45	-10.91	35	-12.56	45	-14.24
50	-11.88	40	-12.83	50	-15.06
55	-12.84	45	-14.22	55	-15.91
58	-13.50	50	-15.30	58	-16.43
64	-14.67	55	-16.20	64	-17.31
70	-15.72	58	-16.61	70	-18.10
80	-17.43	64	-17.47	80	-19.28
90	-19.05	70	-18.32	90	-20.12
100	-20.62	80	-19.52	100	-20.73
		90	-20.39		
		100	-20.66		

% (V_{wa}/V)	E_i/E-values DMSO/water	% (V_{wa}/V)	E_i/E-values NMP/water	% (V_{wa}/V)	¹E_i/E-values 1,4dioxane/water
0	-13.26	0	-8.91	0	0.22
7	-15.74	7	-10.00	5	0.93
14	-17.69	14	-12.62	10	1.18
20	-18.96	20	-14.13	15	1.11
30	-20.63	30	-16.15	20	0.83
40	-21.75	40	-17.53	25	0.22
45	-22.14	45	-18.51	30	-0.61
50	-22.37	50	-19.39	35	-1.63
55	-22.59	55	-19.91	40	-2.79
58	-22.65	58	-20.28	45	-4.03
64	-22.73	64	-20.79	50	-5.43
70	-22.73	70	-21.20	55	-6.87
80	-22.45	80	-21.61	60	-8.24
90	-21.93	90	-21.49	65	-9.75
100	-20.73	100	-20.73	70	-11.41
				75	-12.69
				80	-14.39
				85	-15.99
				90	-17.56
				95	-18.89
				100	-20.62

g-values of diglycerol/water, PEG200/water, acetone/water, DMSO/water, NMP/water and methanol/water at 298.2 K and compared with literature values for the binary mixtures of glycerol/water, and ethanol/water (¹ Stengele, 2002).

% (V_{wa}/V)	g-values diglycerol/water	% (V_{wa}/V)	¹g-values glycerol/water	% (V_{wa}/V)	g-values methanol/water
0	2.34	0	2.55	0	3.15
7	1.96	6	2.41	7	3.21
14	1.77	12	2.32	14	3.18
20	1.69	17	2.27	20	3.17
30	1.61	26	2.20	30	3.12
40	1.61	35	2.18	40	3.10
45	1.63	40	2.18	45	3.10
50	1.66	44	2.20	50	3.07
55	1.70	49	2.23	55	3.06
58	1.73	53	2.17	58	3.00
64	1.81	59	2.32	64	2.98
70	1.91	65	2.32	70	2.96
80	2.10	76	2.44	80	2.92
90	2.40	88	2.59	90	2.90
100	2.85	100	2.83	100	2.85
% (V_{wa}/V)	¹g-values ethanol/water	% (V_{wa}/V)	g-values PEG200/water	% (V_{wa}/V)	g-values acetone/water
0	3.20	0	1.78	0	1.20
7	3.14	7	1.56	7	1.25
14	3.05	14	1.44	14	1.29
20	2.99	20	1.38	20	1.34
30	2.90	25	1.37	30	1.43
40	2.89	30	1.47	40	1.55
45	2.91	35	1.38	45	1.62
50	2.91	40	1.31	50	1.68
55	2.91	45	1.42	55	1.76
58	2.92	50	1.49	58	1.81
64	2.92	55	1.55	64	1.91
70	2.91	58	1.59	70	2.02
80	2.90	64	1.68	80	2.24
90	2.86	70	1.79	90	2.51
100	2.83	80	2.03	100	2.85
		90	2.37		
		100	2.84		

% (V_{wa}/V)	g-values DMSO/water	% (V_{wa}/V)	g-values NMP/water
0	1.19	0	1.04
7	1.21	7	0.89
14	1.21	14	0.96
20	1.22	20	0.97
30	1.24	30	0.99
40	1.28	40	1.04
45	1.31	45	1.09
50	1.34	50	1.15
55	1.39	55	1.20
58	1.42	58	1.24
64	1.50	64	1.34
70	1.60	70	1.45
80	1.82	80	1.70
90	2.19	90	2.10
100	2.85	100	2.85

Appendix B (second paper)

E_i/E values of water/1,4-dioxane; methanol/1,4-dioxane and benzylalcohol/1,4-dioxane mixtures

% (V_{dx}/V)	E_i/E-values water- 1,4-dioxane	% (V_{dx}/V)	E_i/E-values methanol- 1,4-dioxane
0	-20.62	0	-5.26
5	-18.89	7	-4.42
10	-17.56	14	-3.45
15	-15.99	20	-2.80
20	-14.39	30	-1.78
25	-12.69	40	-0.90
30	-11.41	45	-0.52
35	-9.75	50	-0.19
40	-8.24	55	0.09
45	-6.87	58	0.24
50	-5.43	64	0.47
55	-4.03	70	0.59
60	-2.79	80	0.62
65	-1.63	85	0.50
70	-0.61	90	0.38
75	0.22	95	0.20
80	0.83	100	0.07
85	1.11		
90	1.18		
95	0.93		
100	0.22		

% (V_{dx}/V)	E_i/E-values benzylalcohol- 1,4-dioxane
0	-0.48
5	-0.42
7	-0.40
10	-0.36
14	-0.33
20	-0.27
25	-0.23
30	-0.20
40	-0.15
45	-0.13
50	-0.11
55	-0.09
58	-0.08
64	-0.07
70	-0.05
80	-0.036
90	-0.017
100	0.015

Water-1,4-dioxane binary mixtures

298.2K		Water-1,4-dioxane ONE DEBYE		Water-1,4-dioxane SUPERPOSITION OF DEBYE AND COLE-DAVIDSON				
% (V _{dx} /V)	% (V _{wa} /V)	τ [ns]	R ²	τ [ns]	l_2 parameter Cole- Davidson	l_1 parameter Debye	β - parameter	R ²
0	100	0.0085	0.9994	-	0.0000	1.0000	1.0000	-
5	95	0.0094	0.9989	0.0162	0.1595	0.8405	0.9555	0.9998
7	93	0.0098	0.9979	0.0157	0.2916	0.7084	0.9298	0.9996
10	90	0.0103	0.9979	0.0142	0.4803	0.5197	0.9441	0.9997
14	86	0.0109	0.9958	0.0145	0.6863	0.3137	0.9221	0.9995
20	80	0.0117	0.9912	0.0146	1.0000	0.0000	0.8688	0.9979
25	75	0.0124	0.9853	0.0163	1.0000	0.0000	0.8466	0.9971
30	70	0.0132	0.9785	0.0178	1.0000	0.0000	0.8348	0.9961
35	65	0.0141	0.9698	0.0192	1.0000	0.0000	0.8303	0.9922
40	60	0.0145	0.9617	0.0202	1.0000	0.0000	0.8210	0.9894
45	55	0.0157	0.9458	0.0220	1.0000	0.0000	0.8231	0.9785
50	50	0.0165	0.9382	0.0238	1.0000	0.0000	0.8141	0.9839
55	45	0.0175	0.8999	0.0274	1.0000	0.0000	0.7854	0.9885
58	42	0.0178	0.8861	0.0285	1.0000	0.0000	0.7781	0.9871
64	36	0.0181	0.8503	0.0305	1.0000	0.0000	0.7595	0.9847
70	30	0.0178	0.8105	0.0320	1.0000	0.0000	0.7358	0.9824
80	20	0.0160	0.7397	0.0333	1.0000	0.0000	0.6808	0.9777
90	10	0.0124	0.6637	0.0317	1.0000	0.0000	0.5931	0.9505
100	0	-	-	-	-	-	-	-

Methanol-1,4-dioxane binary mixtures

298.2K		Methanol-1,4-dioxane ONE DEBYE		Methanol-1,4-dioxane SUPERPOSITION OF DEBYE AND COLE- DAVIDSON	
% (V _{dx} /V)	% (V _{wa} /V)	τ [ns]	R ²	τ [ns]	R ²
0	100	0.0485	0.9898	0.0485	0.9898
5	95	0.0444	0.9934	0.0466	0.9918
7	93	0.0432	0.9891	0.0468	0.9910
10	90	0.0412	0.9737	0.0447	0.9910
14	86	0.0387	0.9626	0.0435	0.9828
20	80	0.0370	0.9872	0.0417	0.9833
25	75	-	0.9278	0.0401	0.9889
30	70	-	0.9162	0.0389	0.9844
35	65	-	0.9077	0.0372	0.9801
40	60	-	0.8620	0.0378	0.9811
45	55	-	0.8638	0.0359	0.9805
50	50	-	0.8689	0.0356	0.9803
55	45	-	0.8654	0.0333	0.9744
58	42	-	0.8858	0.0302	0.9654
64	36	-	0.9099	0.0272	0.9588
70	30	-	0.8972	0.0246	0.9514
80	20	-	0.8857	0.0181	0.9084
90	10	-	0.7279	0.0142	0.6446
100	0	-	-	-	-

Benzylalcohol-1,4-dioxane binary mixtures

298.2K		Benzylalcohol-1,4-dioxane ONE DEBYE		Benzylalcohol-1,4-dioxane SUPERPOSITION OF 2 DEBYE				
% (V _{dx} /V)	% (V _{wa} /V)	Tau [ns]	R ²	τ ₁ [ns]	τ ₂ [ns]	l ₂ parameter	l ₁ parameter	R ²
0	100	0.2120	0.9941	-	-	1.0000	0.0000	-
5	95	0.1595	0.9861	0.0610	0.1979	0.7825	0.2175	0.9966
7	93	-	-	-	-	-	-	-
10	90	0.1338	0.9824	0.0528	0.1729	0.7390	0.2610	0.9971
14	86	0.1201	0.9775	0.0408	0.1529	0.7691	0.2309	0.9985
20	80	0.0969	0.9713	0.0335	0.1267	0.7390	0.2610	0.9979
25	75	0.0821	0.9636	0.0290	0.1100	0.7139	0.2861	0.9969
30	70	0.0710	0.9411	0.0275	0.1028	0.6357	0.3643	0.9948
35	65	0.0611	0.9223	0.0238	0.0883	0.6226	0.3774	0.9920
40	60	0.0454	0.9079	0.0216	0.0692	0.5892	0.4108	0.9884
45	55	0.0399	0.8710	0.0182	0.0573	0.6229	0.3771	0.9862
50	50	0.0274	0.8557	0.0133	0.0439	0.7277	0.2723	0.9856
55	45	0.0242	0.8683	0.0083	0.0346	0.8309	0.1691	0.9871
58	42	0.0213	0.8855	0.0045	0.0286	0.8842	0.1158	0.9893
64	36	0.0196	0.8965	0.0051	0.0257	0.8730	0.1270	0.9689
70	30	0.0182	0.9433	0.0000	0.0219	0.9237	0.0763	0.9892
80	20	0.0151	0.9455	0.0028	0.0157	0.9821	0.0179	0.9523
90	10	0.0132	0.9252	0.0000	0.0161	0.9111	0.0889	0.9467
100	0	-	-	-	-	-	-	-

Appendix C (third paper)

E_i/E -parameter from the modified Clausius-Mossotti- Debye equation, g-values obtained from the Kirkwood-Fröhlich Eq., dielectric constant, density, refractive index and relaxation time τ in the investigated DMSO-water binary mixtures at 298.2 K.

% (V _{wa} /V)	% (V _{DMSO} /V)	E_i/E -values	g-values	Dielectric constant	Density [g/cm ³]	Refractive index	τ [ns] ONE DEBYE	R ²
0	100	-13.2556	1.1855	47.5082	1.09502	1.4765	0.0205	0.9953
7	93	-15.7428	1.2083	55.0777	1.09743	1.4754	0.0275	0.9910
14	86	-17.6865	1.2133	60.8573	1.09863	1.4741	0.0364	0.9911
20	80	-18.9587	1.2169	64.6058	1.09824	1.4710	0.0429	0.9916
30	70	-20.6325	1.2379	69.6113	1.09391	1.4648	0.0486	0.9939
40	60	-21.7469	1.2779	73.0585	1.08488	1.4525	0.0453	0.9883
45	55	-22.1430	1.3053	74.3564	1.07878	1.4460	0.0412	0.9950
50	50	-22.3712	1.3417	75.1956	1.07211	1.4385	0.0371	0.9953
55	45	-22.5932	1.3876	76.0882	1.06469	1.4308	0.0325	0.9951
58	42	-22.6538	1.4211	76.4481	1.06031	1.4232	0.0300	0.9945
64	36	-22.7337	1.4971	77.0945	1.05091	1.4075	0.0250	0.9936
70	30	-22.7340	1.5954	77.6537	1.04106	1.3911	0.0208	0.9933
80	20	-22.4498	1.8210	78.1455	1.02554	1.3757	0.0154	0.9946
90	10	-21.9251	2.1924	78.8808	1.01059	1.3607	0.0115	0.9974
100	0	-20.7271	2.8465	79.4399	0.99704	1.3461	0.0086	0.9999

g-values according to the Kirkwood-Fröhlich equation for diglycerol-water mixtures at 298.2 K.

% (V_{wa}/V)	% (V_{DG}/V)	g-values
0	100	2.3444
7	93	1.9647
14	86	1.7721
20	80	1.6936
30	70	1.6074
40	60	1.6096
45	55	1.6315
50	50	1.6618
55	45	1.7049
58	42	1.7340
64	36	1.8091
70	30	1.9064
0.80	20	2.1035
0.90	10	2.3957
1.00	0	2.8470

Curriculum Vitae

Personal information

Name, last name Hernandez-Perni, Maria Engracia
Date of birth 03.03.1973
Place of birth Valencia (Spain)

Education

2002 – 2004 PhD student under the supervision of Prof. Dr. Hans Leuenberger at the Institute of Pharmaceutical Technology, University of Basel, Switzerland
Tutorship in disperse dosage forms practical work

1996 - 2001 Working as a pharmacist in the Berta Morales pharmacy, Valencia, Spain

1991 - 1996 Pharmacy education at Valencia University
-Practical year in the Berta Morales pharmacy, Valencia, Spain
-Collaboration in physiology department, faculty of medicine, University of Valencia, Spain

1987 - 1991 Instituto Bachillerato Sorolla, Valencia, Spain

Publications

1. – Hernandez-Perni, G., Stengele, A., Leuenberger, H., 2004a. **Towards a better understanding of the parameter E_i/E in the characterization of polar liquids**, proceedings 5th European Symposium on Pharmaceutical Technology and Biotechnology. Ljubljana (Slovenia). International Journal of Pharmaceutics (accepted for publication)
2. – Hernandez-Perni, G., Stengele, A., Leuenberger, H., 2004b. **Detection of percolation phenomena in binary polar liquids by broadband dielectric spectroscopy**, proceedings 5th European Symposium on Pharmaceutical Technology and Biotechnology. Ljubljana (Slovenia). International Journal of Pharmaceutics (accepted for publication)
3. – Hernandez-Perni, G., Leuenberger, H., 2004. **The characterization of aprotic polar liquids and percolation phenomena in DMSO-water mixtures**. European Journal of Pharmaceutics and Biopharmaceutics (submitted: July 2004)

Symposium Communications

1. – **Poster presentation**: Study of the percolation effect and relaxation behavior of water-1,4dioxane, benzylalcohol-1,4dioxane and methanol-1,4dioxane binary mixtures. 5th Central European Symposium on Pharmaceutical Technology and Biotechnology. Special issue. Farm Vestn 2003; 54: 499-501
2. – **Oral presentation**: Percolation phenomena in DMSO-water binary mixtures. 3rd International conference on Broadband dielectric spectroscopy and its applications. August 23-26, 2004. Delft (The Netherlands)

Courses

1. – **Quality and GMP including case studies.** Parmacenter Basel-Zürich. March 2004
2. – **Pharmabusiness und –marketing.** Parmacenter Basel-Zürich. June 2004

Knowledge of Languages

Spanish and Catalan:	Mother tongue
English:	Excellent written and oral knowledge
German:	Good written and oral knowledge

During my PhD, I attended lectures and courses of:

Bandle E., Baumann P., Bettler B., Binder T., Boehm H.J., Brinkmann P., Dodds J., Eberte A., Glocker M., Ham L., Höfliger M., Hussain S., Iseli E., Jocham V.E., Kleinebudde P., Leuenberger H., Lückel., Ludwig G., Meier C., Meier T., Merkle H.P., Meissner K., Müller K., Pliska P., Pulham C., Schlegel H., Szucs T., Vestweber D., Waldmann H., Weitz G., Wild S., Zenobi R., Zeugin T., among others.